Cape Peninsula University of Technology

# The comparative analysis of adsorbents suitable for thermal desalination system

**By**

**Sindisiwe Ntsondwa**

**Thesis submitted in fulfilment of the requirements for the degree**

**Master of Engineering: Chemical Engineering**

In the faculty of

**Engineering and the Built Environment**

At the

**Cape Peninsula University of Technology**

**Supervisor: Dr V Msomi**

**Co-supervisor: Dr M Basitere**

**Bellville**

**May 2022**

# Declaration

I, Sindisiwe Ntsondwa declare that this work does not have any information which has been accepted for prize of any qualification. I declare that the content of this dissertation is my own unaided work and that the work produced has not been submitted before for academic examination towards any qualification. Furthermore, it represents my own opinions and not necessarily those of the Cape Peninsula University of Technology.

17 May 2022

**Signed** **Date**

# Abstract

Adsorption desalination is a new type of desalination that uses an adsorption-desorption cycle. The adsorbent and adsorbate are the two main components of this cycle. The adsorbent is a substance with both hydrophilic qualities and hydrophobic qualities that adsorb (attracts) and desorbs (releases) adsorbate that comes into contact with its surface area. When the adsorbent is exposed to low temperatures, the hydrophilic property is activated, whereas when the adsorbent is exposed to high temperatures, the hydrophobic property is stimulated. Hydrophilic happens during the adsorption process and hydrophobic takes place during desorption.

Each process is conducted for a period of time and that time is called the half cycle. By including the adsorption desalination (AD) cycle, the water vapour uptake rate is increased, resulting in more desalination water being produced in a shorter amount of time. Silica gel ($SiO_2$), activated alumina oxide ($Al_2O_3$), and molecular sieve zeolite are the three specific adsorbents used. These adsorbents used are determined by their natural sorption properties, such as porosity and surface area. These adsorbents were compared to find which one is suitable for the thermal desalination process.

To examine the performance of adsorbent material, the impact of cycle time, hot, cold and chilled water temperature, adsorption isotherms, cycle performance (COP) as well as adsorption energy are also required. Adsorption isotherms speak to the extreme measure of adsorbate adsorbed per unit mass of dry material at a particular pressure. A weighing apparatus capable of operating in the range of 5 g–10 kg of sample mass with an accuracy of 0.1 g and a time response less than 0.1 s used to directly monitor the dynamic development of the uptake during the isobaric adsorption and desorption stage.

The innovative lab work was performed on an AD-heat exchanger made up of granules of silica gel, zeolite and activated alumina using an aluminium designed heat exchanger. The process operated at different thermodynamic cycles ($T_h$ =70 °C, $T_{eva}$ =10 °C, $T_c$ = 30 and 35 °C), which are actually for the adsorption/desorption process. The half cycle time was found to be 1200s, because all three adsorbents were at equilibrium phase even though silica gel adsorbed 12% water vapour higher than zeolite, and 18% higher than activated alumina. The heat of adsorption of this process conducted using Origin software and it operates in the range of 12 kJ/mol – 15 kJ/mol.

# Acknowledgement

Firstly, I would like to thank the Lord, for his blessings and for guiding me toward my accomplishments. His love never ceases and his goodness is beyond our comprehension. Secondly, I would like to thank all the people and organisations whose support has been a milestone in completing this project and your invaluable assistance that you all provided during my study, more especially to acknowledge the contribution of the following individuals:

1. With much gratitude I would like to sincerely thank my academic supervisor, **Dr V. Msomi** for giving me the opportunity to work on this research under his guidance and support. It is very much appreciated that your great advice, encouragement and guidance for my thesis proved monumental towards this study's success. Thank you for being patient, kind and polite even when I am overwhelmed by the tough situations. Ndiyabonga Nyawose! Phingoshe! Mangamahle! Nomndayi!
2. To my co-superior **Dr M. Basitere,** I would like to express my sincere and heartfelt appreciation for persuasively guiding and encouraging me to be professional and to do the right thing even when the road got tough throughout your tireless support, discussions and invaluable guidance during my undergraduate and postgraduate studies. The target of this project wouldn't have been realized without his constant support.
3. To my mentor **Zamavangeli Mdletshe** who has the substance of a genius, to streamline my work patiently and effectively through constructive feedback.
4. To my best friend **Ntokozo Shangase**. Aah Shuku! Mkheshane! Thank you for such a wonderful contribution in installation and set-up of the apparatus used in this work. Not to forget the admin work you do when I am working under pressure. This work would not have been possible without his wealth of knowledge and dedication in assisting.
5. To **Cape Peninsula University of Technology's** physical and technical contribution is truly appreciated specifically to **Mr. Alwyn Bester** for assisting in building up the test rig. This project could not have achieved its target, without their support and funding.
6. Finally, and most particular, I would like to thank my family from the bottom of my heart, for their understanding during my study period, I am for ever grateful for your support. My friends more especially Yanga Mazule for suggesting Desalination.

The help and support from each of these individuals mentioned was, and will always be greatly appreciated.

# Research output

The following research outcomes represent the author's contributions to the knowledge of thermal adsorption desalination.

### Award:

The paper ID MSF#34 titled: The Mechanism of Adsorbents Adsorption Affinity in Relation to Geometric Parameters authored by Ms. S. Ntsondwa has been awarded as the best paper presentation during the 1st International Conference on Applied Research and Engineering organized by the Department of Mechanical Engineering, Cape Peninsula University of Technology, Cape Town, Western Cape on the 26-28 November 2021 in which participants from different countries registered and presented their papers.

### International conference papers:

- S. Ntsondwa, V. Msomi, M. Basitere and Z. Mdletshe. 2019. The Comparative Analysis of Adsorbents Suitable for Thermal Desalination System. 16 South Africa international conference on Agriculture, Chemical, Biological and Environmental Science (ACBES-19) Nov. 18-19, 2019, Johannesburg (South Africa) Pp 290-295, ISBN 978-81-943403-0-0, https://doi.org/10.17758/EARES8.EAP1119143.
- Sindisiwe Ntsondwa, Velaphi Msomi, and Moses Basitere. 2021. The Mechanism of Adsorbents Adsorption Affinity in Relation to Geometric Parameters. 2021 South Africa International Conference Applied Research and Engineering (ICARAE-2021) Nov. 26-28, 2021, Cape Town (South Africa). Pp 189-197.**https://doi.org/10.4028/p-j52rwy.**

### The following DHET-accredited research publications are under the review:

- Sindisiwe Ntsondwa, Velaphi Msomi, and Moses Basitere. 2022. Evaluation of the adsorptive process on adsorbents surface as a function of pressure in an isosteric system compared with adsorption isotherm. MDPI Journal. *ChemEngineering* 2022, *6*(4), 52; **https://doi.org/10.3390/chemengineering6040052**
- Sindisiwe Ntsondwa, Velaphi Msomi, and Ntokozo Shangase. 2022. Performance Evaluation of important parameters for a new designed small Scale Adsorption Chiller using Gravimetric Technique. Submitted to Ain Shams Engineering Journal. Manuscript number: ASEJ-S-22-00933.

# Table of content

Contents

## List of Figures

## Table of tables

## Nomenclature

| | |
|---|---|
| *x* | Maximal loading in kg/kg |
| y | Affinity constant (1/kPa). |
| z | Heterogeneity exponent. |
| Ce | Vapour uptake |
| Cp | Specific heat at pressure constant |
| $\Delta H_{ads}$ | Isosteric enthalpy of adsorption |
| I | Current |
| $m_a$ | Mass adsorbed (the loading) |
| m | Mass flowrate |
| m | Adsorption up-take |
| M | Mass of adsorbent |
| n | Adsorption desorption phase |
| P | Pressure |
| R | Ideal gas constant |
| $R_T$ | Resistance |
| T | Temperature |
| $T_{cond}$ | Temperature condenser |
| $T_{eva}$ | Temperature evaporator |
| $T_{reg}$ | Temperature regeneration |
| V | Voltage |
| $Q_{cond}$ | Condenser heat of adsorption |
| $Q_{eva}$ | Evaporator heat of adsorption |
| $Q_{des}$ | Desorption heat of adsorption |
| $q_e$ | Adsorbate amount |

## List of abbreviation

| Abbreviation | description |
|---|---|
| AD | Adsorption Desalination |
| COP | Coefficient of Performance |
| EDA | Electronic Design Automation |
| GPIO | General Purpose Input Pins |
| IDE | Integrated development environment |
| LED | Light Emitted Diode |
| RO | Reverse Osmosis |
| SDWP | Specific daily water production |

# Thesis overview

This thesis comprises of the following chapters:

- **Chapter one - Introduction**

Chapter 1 begins with the introduction of how water scarcity affects the world, to understand water availability, consumption, and water shortage. A comprehensive background of desalination theory is presented including the problem statement, research key questions, aim, and objectives.

- **Chapter two – Literature review**

This section comprises the reviewed literature related to the present work. It briefly describes major differences in the types of the desalination process. Adsorption fundamentals for their synthesis and its operation process, adsorption mechanism and provides a comprehensive source of knowledge for all commercial and adsorbents properties discussed.

- **Chapter three – The Mechanism of Adsorbents Adsorption Affinity in Relation to Geometric Parameters.**

This chapter describes the description of kinetic models of adsorption. It further optimizes the adsorption cycle by looking at different types of adsorbents used and compare the quantity of water uptake in each adsorbent

- **Chapter four - Performance Evaluation of important parameters for a new designed small Scale Adsorption Chiller using Gravimetric Technique**

The design of the operating principle of the proposed system is discussed in this chapter, which takes a broader view of the functioning of the mechatronics used in building gravimetric system. Introduction of the energy method based on the second thermodynamics rule. It also offers a brief comprehensive drawing and all phases and stages have been clearly illustrated.

- **Chapter five - Evaluation of the adsorptive process on adsorbents surface as a function of pressure in an isosteric system compared with adsorption isotherm**

This chapter provides a detailed summary of the experiments performed to test the adsorption properties of water vapour on adsorbents (silica gel, molecular sieve zeolite, and activated alumna) for an application of water desalination.

- **Chapter six – Conclusion and recommendations**

Chapter five discusses and summarizes the major findings of this research. Chapter six gives a comprehensive explanation of the findings and emphasizes the importance of the research.

# Chapter 1: Introduction

## 1.1. Background

For human development and the economic activities of a nation, access to potable water is important. Industry, ranches, and the general population all need safe and fresh water that is available. The limited freshwater resource is becoming increasingly scarce as the population of the earth continues to expand and evolve (Qasem & Zubair, 2019). The now-reported, on-going global water crises are guided by numerous variables. The factors making it impossible for water sources to meet water needs are climate change and population development (Mancosu et al., 2015).

Global energy demand, particularly in emerging market economies, is increasing rapidly due to population and economic growth, which also contributes to water crises. Increasing demand creates new challenges while accompanied by greater probabilities. Nevertheless, these forms of challenges build opportunities sometimes as the sustainable future energy in water production techniques requires a transformation of the way energy is produced, distributed, and consumed by society through new thinking and new technologies. Many people are brainstorming water process ideas that do not consume much energy (Alsaman et al., 2017).

The aim is to boost living standards, provide access to modern energy infrastructure and protect the global environment, because the same energy will be useful in water purification process. As an alternative way to solve water shortage, the manufacturing sector and academic institutions have embarked on exploring the ocean (Alsaman et al., 2017). Several variables such as water quality, type of energy source, position for feed consumption, and brine discharge are subject to the desire for desalination research. Nevertheless, the desalination business was dominated by only a few applied sciences (Thu et al., 2015).

Reverse osmosis (RO), and thermal desalination with a combined output of approximately 94% of total ability were the part of the few desalination process that were available then (Thu et al., 2015). The key indicator for determining a desalination technology is real electricity usage, irrespective of the power that may be in the high-standard structure i.e., energy, steam, or low-maintenance standard, such as low-temperature waste heat or renewable energy. Some crucial constraints, such as the right preparation for energy and water need, outweigh the energy efficiency factor when choosing a desalination technology (Thu et al., 2015).

In theory, a work-driven computer conducts the desalination very correctly, according to (Thu et al., 2015), resulting from much less irreversibility involved. However, to get the job done, it must be distinguished that high-standard strength in the form of electrical energy is needed. In the last

two decades, the advancement of adsorption cooling and heating systems have made major progress in comparison with the vapour compression considered to be a serious alternative (Thu et al., 2015).

Figure 1.1 is a pie chart of water distribution on earth. It shows that 97% of water is seawater (saline) and there is only 3% of freshwater (Rahimi & Chua, 2017). The 3% is divided into 4 factors: groundwater, icecaps and glaciers, surface water, and other stuff. Icecaps and glaciers are the main freshwater reservoirs, but this water is uncomfortably situated in certain areas. Shallow groundwater is the main source of fresh water, which is used. However, though rivers and lakes are the most highly used water resources, they contain just a limited amount of water in the world which is why it is needed to purify the saline (Distribution et al., 2020).

**Water distribution on earth**

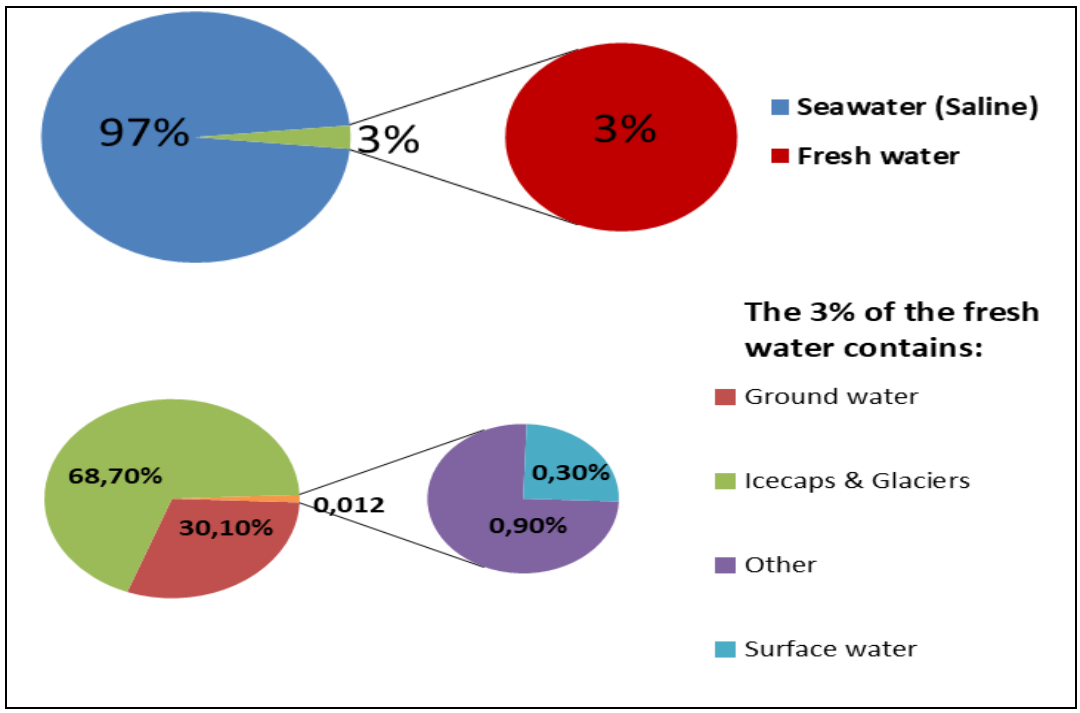


Figure 1.1: Water distribution on earth (Distribution et al., 2020)

The Figure 1.1 states that the highest percentage of water on the surface of the earth is seawater; therefore, the desalination process can be a solution to water scarcity. There are so many desalination techniques used. However, these processes generate high quality water and can provide drinking water in areas where there is no supply of natural drinking water. However, the major drawback of these systems is the fact that most of them are environmentally unfriendly. Its construction and maintenance are expensive because they require high energy for its operation (Youssef et al., 2017).

This prompted many researchers to work on a project of desalination (Youssef et al., 2017). Several studies are currently underway and are highly focusing on reducing the energy consumption that this device needs for its service. This includes the integration of the solar system and other mechanisms for enhancing efficiency against the system. One of the greatest problems facing society is seeking enough energy sources to meet the world's rising demand. As one of the technologies for energy conversion, more and more attention is paid to sorption cooling which is powered by a low degree of heat and provides cooling power (Wang et al., 2014).

Sorption phenomenon occurs by incorporating thermal desalination and adsorption desalination with an intention to shape adequate energy desalination devices. Sorption technology involves a technique of absorption process and adsorption process. Sorbents are the key differences between two forms of technology. Generally, the absorbents are based on liquid phase, and the adsorbents are granular or lightweight, the example is zeolite, silica gel and activated alumina. Adsorption/Desorption cycle is one of the performance enhancement mechanisms for the thermal desalination device (Wang et al., 2014).

It benefits from a wide spectrum of adsorbents for a wide range of temperatures applied to various heat sources, usually between 50 and 400oC. Furthermore, the features of strong adsorbents typically make it more possible under intense vibration circumstances (Wang et al., 2014). The main purpose of this research is to conduct a study analysing the isotherm affinity of adsorbents available from South African suppliers. A comparative analysis of these adsorbents suitable for the thermal adsorption desalination system premeditated to find adsorbents with a higher affinity to capture water vapour (Mitra et al., 2017)..

The adsorption desalination system is a newly developed desalination system that requires low-temperature input for desalination to take place. This system uses the adsorption-desorption cycle to increase the vapour uptake rate to its advantage. The study further describes a moderate desalination system that uses only reduced waste heat, which may be obtained in an infinite supply from either renewable energy sources or power plant exhaust (Ng et al., 2013). The Adsorption Desalination (AD) cycle produces two useful results, i.e., high-grade drinking water and cooling (Mitra et al., 2017).

The adsorption/desorption process works based on adsorbents and various adsorbents are available on the market. The operation of each adsorbent depends on the properties of the factory. This then indicates that the output of adsorbents varies with the manufacturer, which is why this study is being conducted. The content is primarily related to the promotion of adsorption cooling

growth in the field of working pairs of adsorptions, efficiency of heat and mass transfer, and cooling cycles of adsorption, etc. Because of the advancement of adsorption refrigeration technology (Gude, 2018).

Many chillers such as aqua low-grade adsorption heat have been successfully marketed in the research world. The progression of the adsorption cooling system has been summarized in more details as follows: working pairs of adsorptions and their mechanisms; adsorption cooling system structure; heat enhancement and mass transfer of the adsorption surface, and thermal characteristics of many advanced renewable cycles (Wang et al., 2014). A key item for the refrigeration adsorption and heat pump system is the working pair of adsorptions (Alnajdi et al., 2020).

Properties of the working pair have a significant effect on the efficiency coefficient of the system, rate increase in adsorbed temperature, and initial expenditure. For effective cooling efficiency, the correct adsorption working pairs are chosen based on the heat source temperatures, and the correct adsorption cooling cycles are also selected according to the authentic obligations. For different pairs used in adsorption cooling, the nature and properties of the technique are unique. The famous adsorption cooling working pairs mainly include activated alumina, molecular zeolite, silica gel, and many more (Alnajdi et al., 2020).

There are two working processes for refrigeration by adsorption. The first step is that of cooling and adsorption. The adsorption heat in this system discharges cooling water into the absorber plate, and the pressure within the adsorbed drops below the evaporation pressure. Under the pressure gap, the coolant evaporates and is absorbed by the adsorbent, and the evaporation process produces the cooling output. Secondly, is the mechanism of desorption and condensation. The low-grade heat in this cycle stimulates the endothermic desorption process. In the condenser, the desorbed refrigerant vapour condensate (Khalil et al., 2016).

## 1.2. Problem statement

The world is facing the scarcity of fresh water due to climate change and population growth. It is no secret that water is vital; it is one of life's basic absolutes and its impact extends far beyond other critical issues including issues that affect poverty. The highest percentage of water is seawater, and the desalination process is therefore the solution to this problem. This triggered the development of various systems used to purify seawater. However, the challenge with these systems, they require high energy for their operation. The adsorption/desorption cycle is known to be one of the energy-sufficient systems.

The adsorption/desorption mechanism operates based on adsorbents and the operation of each adsorbent depends on the properties of the factory. All adsorbents have their own geometric parameters (pore size, surface area and time regeneration). This then suggests that the performance of adsorbents varies with the manufacturer. This study will analyse the chemical properties of the three adsorbents (silica gel, molecular sieve zeolite, and activated alumina) with the aim of finding the one that may be suitable for thermal desalination operated by the South African solar intensity.

### 1.3. Aim and objectives

This study aims to make desalination more efficient using an affordable solid adsorbent. The Objectives are:

- Compare the quantity of water uptake in each adsorbent.
- Evaluation of adsorption isosteric enthalpy of adsorption in between the adsorbents and adsorption kinetics
- Optimize the adsorption cycle by looking at different types of adsorbents used.
- To determine the optimum cycle time for the given adsorption desalination (AD) system cycle under the given operational condition.
- Design and construct an adsorption chiller to assess the adsorption isotherm and kinetics, as well as investigate the efficiency of an adsorption cooling bed under adsorption cooling cycle conditions.

### 1.4. Research key questions

- Which adsorbent has a high adsorption capacity affinity in the shortest time?
- Which adsorbent produces high-quality potable water?
- What good changes do these adsorbents make in the desalination process?
- What is the reason for controlling the pressure/temperature of the adsorption-desorption cycle?

### 1.5. Hypothesis

There is currently no form of adsorbent that has been proven to be suitable for the new type of adsorption desalination. This can be a challenge in desalinating more water with high quality at a low energy without spending a lot of time. However, if various forms of adsorbents are evaluated, it will then be known which adsorbent is incredibly active for AD. The adsorption process will desalinate potable water at a high rate with low cost and the silica gel will be the adsorbent with the high thermal stability/affinity, high abrasion resistance, and high adsorption capacity.

# Chapter 2: Literature review

**Part of this Chapter Published as: Sindisiwe Ntsondwa,** V. Msomi, M. Basitere and Z. Mdletshe. 2019.The Comparative Analysis of Adsorbents Suitable for Thermal Desalination System. 16 South Africa international conference on Agriculture, Chemical, Biological and Environmental Science (ACBES-19) Nov. 18-19, 2019, Johannesburg (South Africa) Pp 290-295, ISBN 978-81-943403-0-0, https://doi.org/10.17758/EARES8.EAP1119143.

## 2.1. Introduction

This section comprises the reviewed literature related to the present work. It briefly describes major differences in the types of desalination process currently used in industry and it discusses the reasons of incorporating thermal desalination with adsorption desalination. In addition, it further discusses adsorption fundamentals, adsorption mechanism and it also provides a comprehensive source of knowledge for all commercial and properties of the adsorbents used in the study. The importance of adsorbents and the criteria of selecting the suitable adsorbents in terms of adsorption equilibrium, adsorption kinetics and adsorption dynamics is also summarised.

As mentioned in chapter 1, the water scarcity has increased worldwide into a point where the operating water system is a major responsibility that has implications for health standards, human safety, agriculture industry, energy industry, and human needs. Knowledge in regard to water scarcity sparked greater enthusiasm for the desalination of seawater as it is the oceans that have the highest water percentage on earth. This is then used as an alternative to take care of the problem of water deficiency. The abundant seawater is converted into freshwater throughout desalination process. Figure 2.1 shows desalination categories (Alsaman et al., 2017).

## 2.2. Desalination techniques

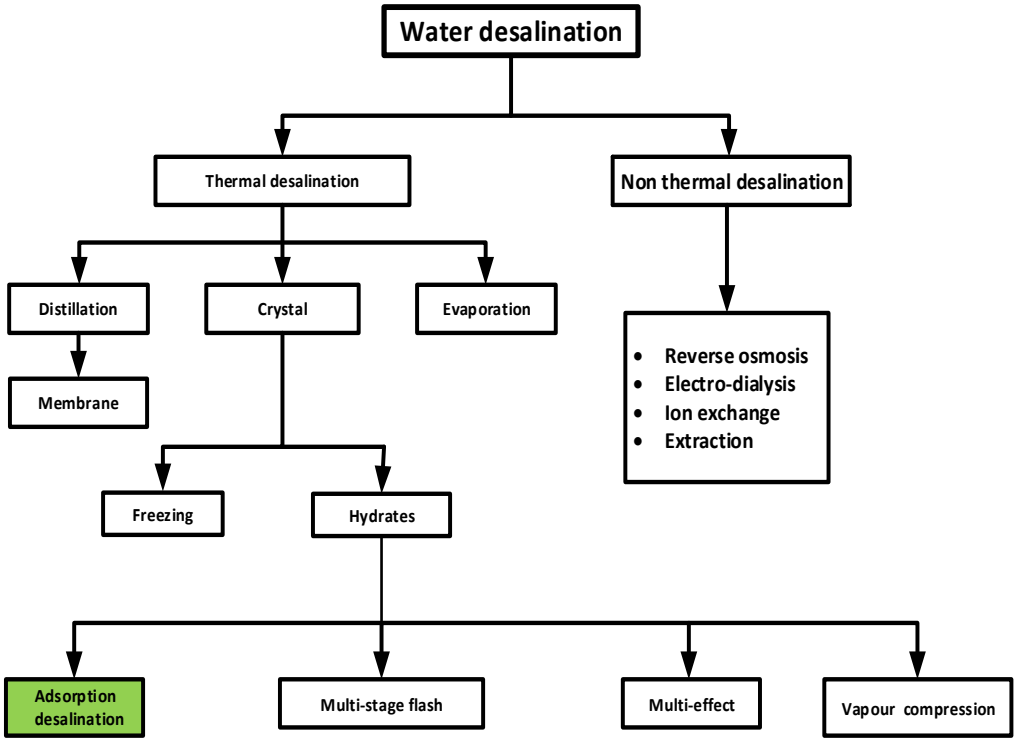


Figure 2.1: Desalination categories

Figure 2.1 depicts the market's current desalination technologies, which are classified into two categories: thermal and non-thermal desalination. Under the non-thermal desalination there is Reverse osmosis (RO), Electro-dialysis, Ion exchange, and Extraction desalination. Under thermal desalination there is distillation, crystal and evaporation. The most used system under non-thermal desalination is Reverse osmosis. RO is a technique for removing the large bulk of pollutants from water by forcing it through a semi-permeable membrane under pressure. The RO is separated into two portions; with the use of a semipermeable membrane (Barbosa et al., 2022).

In one compartment, saltwater is stored, while in the other, clean water is retained. The membrane will only allow pure water to travel through it and will not allow saltwater to get through. When pure water travels across a semipermeable membrane in osmosis, it moves from a dilute solution to a concentrated solution. Only tiny particles can pass through a semipermeable barrier, while all big particles are blocked. The RO depends on pressure and it obtain the better results through exerted high pressure. The amount of pressure needed is determined by the sodium content in the input water (Wenten & Khoiruddin, 2016).

When the inlet feed (seawater) is highly concentrated there is high pressure required to overcome osmotic pressure. Although reverse osmosis (RO) is a highly used approach, it is only effective for low-salinity seawater. High-salinity RO desalination requires high hydraulic pressure level, that will degrades membrane performance dramatically (Chen et al., 2020). RO still takes a significant amount of energy to overcome osmotic pressure, which rises with feed water salinity. After a while, the microscopic pores of a RO system become clogged, and the system need to be frequently maintained (Chen et al., 2020).

Even ordinary chlorine may harm a RO system. As a result, many RO owners invest in a pre-filter to prevent the RO unit from fouling or couple, and that lead to an additional cost on the maintenance of RO system. Another disadvantage is that once the filter replacement is placed, it can only generate a certain volume of water. However, the cost of frequent filter replacements and maintenance is ongoing (Rautenbach et al., 2000). Also designing acceptable high-strength membrane materials without sacrificing membrane transport qualities is anticipated to be a difficult issue (Rautenbach et el., 2020).

Furthermore, the introduction of mechanically resilient membrane components and transmission lines to high pressurizations would almost certainly necessitate a significant financial outlay. Though RO high-pressure can be constructed, classical in single-stage for highly saline desalination will have reduced power efficiency since the thermal efficiency rises with increasing

pressures. It also needs to be cleaned and disinfected once a year to keep it in a good condition. The issues mentioned above faced by reverse osmosis leads the water research industry into finding better ways of desalinating water (Chen et al., 2020).

There is also Electro-deionization, which incorporates electrodialysis with traditional ion-exchange, a mature technology that has been used commercially for the generation of deionised water for more than two decades (Wenten & Khoiruddin, 2016). According to Wenten & Khoirudde (2016) the ion exchange and electro-deionization are highly preferred as a polishing step of a RO plant to accomplish full removal of ions from high quality water, such as high-pressure boiler feed water or deionised water rather than working on its own (Wenten & Khoiruddin, 2016). The other non-thermal desalination is an extraction desalination, and it does not require a membrane.

Extraction desalination is a liquid–liquid technique used to separate preferentially absorb water from hypersaline water before separating the adsorbed potable water from the solvent through temperature variation (Barbosa et al., 2022). The finely balanced solubility qualities of directed solvents, which do not dissolve in water but may dissolve water and reject salt ions, enable extraction desalination (Guo et al., 2021). Extraction desalination has been offered as a potential option to the abovementioned technologies for hypersaline water desalination in the past (Choi et al., 2021).

The extraction desalination solvent, however, ought to be substantially non-polar to have low mixable compatible in the aqueous phase and have some advantageous locations for establishing hydrogen bonds in the aqueous phases to solubilize water (Choi et al., 2021). Furthermore, the solvent phase's water solubility must be temperature sensitive enough to allow for efficient water recovery (Barbosa et al., 2022). However, the jurisdiction directed solvent 's water yield severely restricts its performance and energy efficiency. As a result of that, a pool of information is gathered in literature in finding the better option of desalination.

Recently the use of thermal desalination incorporated with Adsorption desalination (AD) is highly recommended. This procedure allows salty water to be desalinated at a considerably high rate, lowering energy consumption dramatically (Ng et al., 2013). Thermal desalination breaks the bond between water and salt through evaporation. Because salts are non-volatile, thermally driven processes can reject nearly all the dissolved salt while still producing a high-quality distillate. Thermally powered adsorption processes on the other side do not use much energy but rather low- temperature heat and therefore they are more tempting than RO (Ng et al., 2009).

The thermal methods are also less susceptible to changes in feed salinity and can manage tough feed conditions. Another benefit is that they are not subjected to clogging/fouling than RO, because they do not require membranes. This system produces a high-quality potable water; however, on the other side, the thermal desalination consumes a lot of energy, and it has many stages to be operated before producing the final product; hence is incorporated with adsorption desalination in this study. The most important or most used thermal desalination is Multi-Effect Desalination (MED) and Multi-Stage Flash (MSF) (Raluy et al., 2006).

In these two plants, brine water enters the first effect and is warmed in tubes to reach the boiling point. Seawater is drenched on the surface of evaporator tubes to enhance efficient boiling and evaporation. Steam condensed on the opposing sides of the tubes from a boiler heats the tubes. The boiler's steam condensate is collected and reused in the boiler. The seawater then travels to the evaporator vessel, where the pressure is reduced, for the water to boil or flash. This procedure is done several times, with the pressure gradually dropped until flashing occurs at lower temperatures (Raluy et al., 2006).

The vapour that has condensed is distilled water. The high initial plant cost, which confines MED and MSF to large-scale operations, is a major key impediment to their widespread deployment. Due to high latent heat of vaporisation, energy consumption of MED and MSF is substantially high (Ng et al., 2013). According to Raluy et al., (2006), the MED and MSF is highly pollutant to the atmosphere. Therefore, this project bridges the gap by incorporating thermal desalination with adsorption to minimize high-energy usage and the number of stages used by a thermal desalination system (Israelachvili, 2011).

Adsorption is characterized as a sticking together or the adhesion of liquid, gas, or soluble solid molecules to the surface of a solid (Israelachvili, 2011). Adsorption process have long been recognised to humanity, and they are increasingly used to carry out desired bulk separation or purification purposes. A porous solid medium is typically the heart of an adsorption process. Porous solids are used because they have a large surface area or a large volume of micropores, and that large surface area or volume of micropore it is the one that allows the processes to achieve a high adsorption capacity (Rouquerol et al., 2014).

### 2.2.2. Advantages of AD

- Low expense of maintenance
- Low corrosion and fouling rate
- Environmentally sustainable, friendly

- ❖ No feed water pre-treatment needed
- ❖ Producing drinking water of a high quality
- ❖ Using waste thermal heating at low temperatures
- ❖ Cooling can be co-generated along with the potable water
- ❖ It produces pure distillate and minimizes contamination of (bio) genes.

There are various sorts of adsorption; physisorption and chemisorption. Physisorption works with Van de Waal connection and atoms keep up their actual structure, whereas chemisorption includes substance bonds, and its particles lose their character. Adsorption occurs whilst particles, or atoms connected to the outside of a substance without entering it. Just like the adsorption desalination process, the hydration circle encompasses external spherical interaction and not the internal sphere. Practically all adsorptive partition measures rely upon actual adsorption as opposed to chemisorption and this examination is hence organized through actual adsorption (Wang et al., 2014).

Physical adsorption alludes to the phenomenon of gas atoms sticking to the surface at a weight lower than the vapour weight and it includes just moderately weak intermolecular powers while chemisorption basically includes the arrangement of a synthetic connection between the adsorbate particle while examining the rudiments of adsorption (Alnajdi et al., 2020). The strong material that gives the surface to adsorption is alluded to as adsorbent; the species that will be adsorbed are named adsorbate (Mohammed et al., 2018). The adsorption process is depicted in **Error! Reference source not found.**.

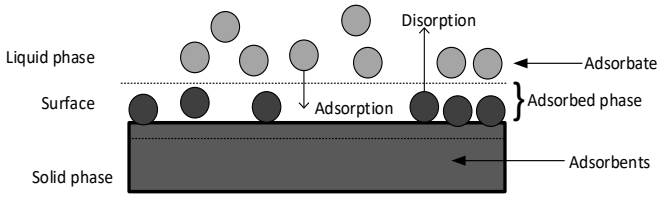


Figure 2.2: Adsorption fundamentals (Worch, 2012)

The optimal cycle rate of water produced rises directly with capacity, whereas the equivalent rate of energy utilised per kg of generated water drops from its level to the lower level in a decreasing rate. To achieve better results, the general overview of the adsorption isotherm, kinetics, and heat of adsorption using sorbent selection should be understood. The overwhelming logical reason for sorbent determination is the equilibrium isotherm. The adsorption equilibrium and its numerical representation are extremely important inside the adsorption structure. (Mohammed et al., 2018).

Awareness of adsorption equilibrium information provides the foundation for the assessment of the processes of adsorption and the design of adsorbers. For example, knowledge regarding the equilibrium in a specified adsorbate/adsorbent system is required to describe the adsorption capacity of water pollutants, pick an acceptable adsorbent, and build batch, flow-through, or fixed-bed adsorbers. In a given system, the equilibrium position is influenced by the strength of the adsorbate/adsorbent interface and is also seriously dependent on the adsorbate and adsorbent characteristics (Mohammed et al., 2018).

The comparison of adsorbents suitable for thermal adsorption can also be found through kinetics, adsorption isotherms, by the water solution properties including temperature, pH value, and the existence of competing adsorbate. The kinetics favour any adsorbent that regenerate the vapour at a low temperature and any adsorbent that adsorbed vapour at a temperature that does not require much of energy. The adsorption isotherm is more based on adsorbent geometric parameters. The correct selection of the adsorbents therefore results in the development of high quantities and high-quality water (Rahimi & Chua, 2017).

## 2.3. Selection of adsorbents

The choice of an appropriate adsorbent for a given separation is a perplexing issue. There are numerous physical and compound properties of adsorbent, anyway the most cycle of choice relies upon a distinction in either adsorption energy or adsorption equilibrium (Yang, 2003; Li et al., 2016). Dispersion rate is commonly an optional in significance. The equilibrium isotherm of all constituents in the gas blend, in the weight scope of activity, should be thought of. In view of the isotherm, the accompanying elements are imperative to the plan of the assessed detachment measure (Li et al., 2016).

- The product purities
- The method of sorbent regeneration
- Capacity of the adsorbent, in the operating temperature and pressure range

## 2.4. Standard separation

The adsorption mass separating compounds are adsorbent, and the adsorbent content is lawfully determined by the characteristics of the process of adsorption separation process or purification process. To apply adsorption in practice, it is necessary to analyse the conditions of the adsorbed sum on the parameters of the process characteristics and to express these circumstances theoretically. The equilibrium of adsorption, the kinetics of adsorption, and the dynamics of

adsorption are the three primary essential components of theoretically focused adsorption. (Mohammed et al., 2018).

The adsorption balance reveals the adsorbed sum's dependence on the adsorbate parameters and the temperature. The porous adsorbent solid has pores with dimensions in the steric separation process, allowing tiny molecules to join whilst prohibiting big molecules from entering. The equilibrium procedure is dependent on the solid's capacity to withstand various molecules, the stronger high adsorption species preferentially eliminated through solid. A key variable is the porous solid of the adsorption process. The success or failure of the phase is determined by the solid's equilibrium and kinetics (Mohammed et al., 2018).

The kinetic process is based on the varied diffusion rates of distinct species into the pore; hence, by adjusting the exposure period, the solid extracts the rapid diffusing species first. Solid having strong ability, but sluggish kinetics is not a suitable choice because adsorbate molecules take too long to penetrate the particle within. This indicates a prolonged period in a gas column and, as a result, a limited output. A solid with good kinetics, on the other hand, but a low capacity, is also not good because a large quantity of solid is needed for given pores. Therefore, the one that have high affinity and good kinetics is a strong solid (Worch, 2012).

The following should be considered to fulfil the separation conditions:

- The adsorbent need to have a sufficiently large surface area or volume or micro-pores
- To meet the first criteria, the adsorbent must have a reasonably large pore system to transport the molecules to the interior, and the porous solid must have a small pore size with an acceptable porosity. This means that a good solid must have a mixture of two pore ranges: micro-pores and macro-pores.

An adsorbent with sufficiently high selectivity, strength, and existence are the primary requirements for an economic separation process. Either adsorption kinetics or adsorption equilibrium differences may rely on selectivity. Thus, to properly understand an adsorption mechanism, it is a must to consider these two basic ingredients: equilibrium and kinetics. In current use most of the adsorption process depends on equilibrium selectivity (Condon, 2006b; Ramy et al., 2018). When considering such a method, it is useful to establish a separation factor:

$$\propto_{CD} = \frac{X_C / X_D}{Y_C / Y_D} \tag{2.1}$$

The $X_C$ and $Y_C$, in adsorbed and fluid phases at equilibrium, are the mole fractions of component C, respectively. The factor of separation thus defined is precisely identical to the relative volatility which quantifies the ability of distillation to separate the components. However, the similarity is essentially formal, and the separation factor and relative volatility have no quantitative relationship (Condon, 2006b; Mohammed et al., 2018).

## 2.5. Adsorption equilibrium

All adsorption systems are based on the adsorption equilibrium. The implementation of both kinetic and dynamic adsorption models requires knowledge of the adsorption equilibrium. Information regarding adsorption equilibrium as well as adsorption kinetics are required to forecast adsorption dynamics. These fundamental adsorption concepts apply not just to single-solute adsorption but also to multi-solute adsorption, which is defined as adsorbate competing for available adsorption sites and, most particularly, migration processes in fixed-bed adsorbers (Mohammed et al., 2018)

The state of equilibrium achieved after a protracted period while adsorbing molecules settled on adsorbent surfaces (Khanam et al., 2018). Equilibrium adsorption is the accumulation of adsorbents on the adsorbent surface at a constant rate. The adsorbed vapour measurements are based on the positive weight at the region in which vapour is adsorbed onto a largely empty constant exposure or pore space. In addition, the water vapour adsorbed relies on temperature (T) condition operated at, the pressure (P) balance, and the concept of the strength and vapour (Grande, 2012; Mohammed et al., 2018).

For a vapour adsorbed on a strong at a given temperature, the adsorbed total per unit mass of the strong adsorbent mass (Q) is then merely a fraction of P (Grande, 2012). The adsorption isotherm is the relationship between adsorbed mass and P at a particular temperature. Adsorbed mass frequently seen as a feature of the relative pressure, P/P°, in which pressure standardized to the adsorbate's immersion vapour pressure (P°) at temperature (T). The standardized isotherm is increasingly useful on a regular basis as it helps one to measure the net adsorption warms and various vapour attributes across a temperature range promptly (Worch, 2012).

Comparable isothermal frames are constructed for the adsorption of solutes from the arrangement by associating adsorbed mass with Ce (equilibrium concentration) or Ce/Cs, where Cs represent the solubility of the solvent (Worch, 2012). Considering the actual use of adsorption, it is necessary to compare the circumstances of the adsorbed quantity with the typical process

parameters and to describe these conditions on a theoretical basis. The three fundamental parts of the theory of practice-oriented adsorption are:

- Adsorption equilibrium
- Kinetics of adsorption
- Adsorption dynamics

The adsorption equilibrium explains the adsorbed amount's dependency on the concentration of adsorbate and the temperature (Ng et al., 2017). For the stated adsorbent and adsorbent pair, the equilibrium uptake mentioned is given:

$$q = f(P, T) \quad \ldots\ldots\ldots\ldots\ldots\ldots\ldots\ldots\ldots\ldots\ldots\ldots\ldots\ldots\ldots\ldots \quad (2.2)$$

**Equilibrium pressure vs. adsorbed mass**

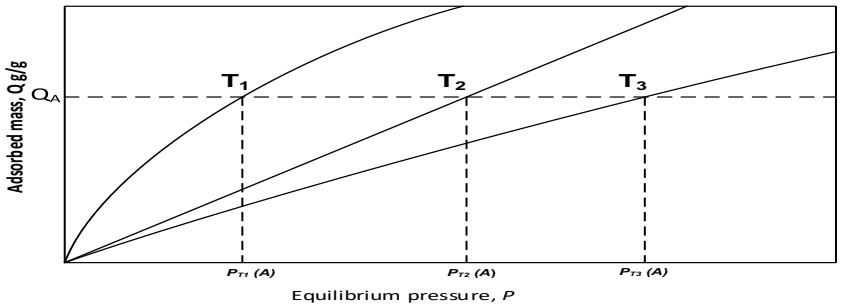


Figure 2.3: Schematic drawing showing the equilibrium pressure (P) of a vapour at three different temperatures (T1<T2<T3) with a fixed adsorbate mass (Q3) on an adsorbent (Chiou, 2002).

Adsorption equilibrium is expressed in three ways:

- **Adsorption isotherm:** is the adjustment in measure of adsorbate against the weight when the adsorbent temperature kept steady and the pressure fluctuates (Worch, 2012; Ng et al., 2017).

$$q = f(P) \text{ when } T \text{ is constant} \quad \ldots\ldots\ldots\ldots\ldots\ldots\ldots\ldots\ldots\ldots\ldots\ldots\ldots\ldots\ldots\ldots \quad (2.3)$$

- **Adsorption isobar:** the change in the volume of adsorbate vs. the temperature when the pressure is constant and the temperature of the adsorbent changes (Worch, 2012; Ng et al., 2017).

$$q = f(T) \text{ when } P \text{ is constant} \quad \ldots\ldots\ldots\ldots\ldots\ldots\ldots\ldots\ldots\ldots\ldots\ldots\ldots\ldots\ldots\ldots \quad (2.4)$$

- **Adsorption isostere:** the change in pressure against the temperature produced when the volume of adsorbate has remained constant (Worch, 2012; Ng et al., 2017).

$$P = f(T) \text{ when } q \text{ is constant} \quad \ldots\ldots (2.5)$$

The adsorption isotherm is frequently used to describe the aftereffects of adsorption in adsorption balance studies. Interestingly, isosteres and isobars are not really utilized in investigations of adsorption equilibrium (Chiou, 2002; Al-Jabari, 2016).

## 2.6. Adsorption kinetics

The adsorption energy portrays the time reliance of the adsorption cycle, which implies the expansion of the stacking with time, the decrease in liquid-phase concentration over time (Al-Jabari, 2016).

$$q = f(t), \text{ and } C = f(t) \quad \ldots\ldots (2.6)$$

## 2.7. Adsorption dynamics

The adsorption rate is generally determined by slow mass transfer processes from the liquid phase to the solid phase. Within the generally employed fixed-bed adsorbers, adsorption is not only a time-dependent but also a geometric-dependent mechanism. The time (t) and space (z) dependency is referred to as the dynamics of adsorption or column dynamics (Al-Jabari, 2016).

$$q = f(t, z), \text{and } C = f(t, z) \quad \ldots\ldots (2.7)$$

The combination of adsorbate and adsorbent thermodynamics process is intricate because the distributions of pore size, surface heterogeneity and distribution of site energy, as well as the properties of adsorbate, are affected. Overall, the characteristics represented adsorbate uptake, generating phase graphs known as adsorption isotherms where energy from the sorption site on the pore surfaces is favourable. To describe the vapour uptake or isotherms thus far, the existing adsorption models are individually and correlate to a given sort of isotherm pattern. In designing these isothermal models there is still a universal approach (Ng et al., 2017).

It is extremely valuable to comprehend the highlights of the adsorption isotherm of the adsorbent/adsorbate pair when building up any item configuration including the adsorption cycle. Estimation of adsorption isotherms for the silica gel-water, zeolite and activated alumina framework is hence significant for the investigation of the AD framework's particular everyday water creation limit (SDWP). Also, the process of choosing adsorbents for an objective adsorbate

particle dependent on the adsorption isotherm (Worch, 2012). With the accessibility of rapid processing, it is currently conceivable to ascertain the adsorption isotherms dependent on:

- Potential interactions
- Structure of adsorbents
- The adsorbent's geometry
- The nature of the adsorbed gas

**Adsorption isotherm at two different equilibrium temperatures**

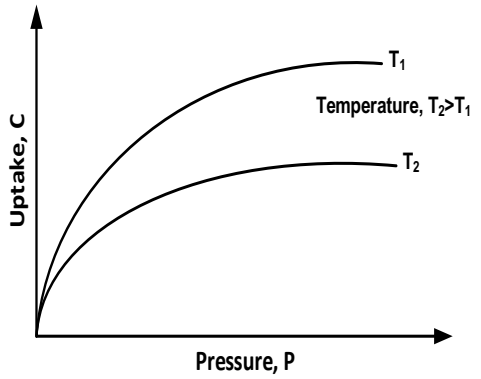


Figure 2. 4: Adsorption isotherm C=f(P) at T(Chiou, 2002)

### 2.7.1. Interaction potential

Adsorption happens when the effort required to bring the gas molecule to the adsorbed state is equal to the potential energy interaction. As a first approximation, the adsorbed state is assumed to be at saturated vapour pressure (Volmer et al., 2017).

$$-\emptyset = -\Delta G = \int_{P}^{P_0} VdP = RTln = RTln\frac{P_0}{P} \quad \text{..... (2.8)}$$

$P_0$ is the saturated pressure, and G is the free energy change. Between the adsorbent molecules and the adsorbent, the total adsorbate-adsorbate and adsorbate-adsorbent interface potential (Wu et al., 2014).

$$\emptyset_{total} = \emptyset_{adsorbate-adsorbate} + \emptyset_{adsorbate-adsobent} \quad \text{..... (2.9)}$$

### 2.7.2. Adsorbents

A substance called adsorbent is the material used in adsorption process for an interaction of adsorbents and adsorbate on the surface of the adsorbents. It is a solid material for collecting the molecules of the solute from a liquid or gas. The adsorbent determination for evacuation of water

contaminants relies upon concentration and type of pollution present in the water, effectiveness, and adsorption limit with respect to contamination. In addition, the adsorbents ought to be non-toxic, cost effectively accessible and they can be easily found in market. Adsorption often used to extract contaminants by allowing adsorbents like activated carbon or silica gel connected to them( Wu et al., 2014; Alnajdi et al., 2020).

Adsorbents are hygroscopic with a surface that may attract gaseous or liquid molecules (Wu et al., 2014).It is preferable for an adsorbent to have a wide specific surface area and a high polarity. There are more pores, or spaces to adsorb the adsorbate if the surface is big and that enhance the adsorbent to have the high affinity and strength to adsorb more. The size and distribution of adsorbent porosity determine the adsorbate molecule's diffusivity onto the surface of the adsorbent, making them essential properties of the adsorbent. However, if the adsorbent's polarity is strong, attracting adsorbent molecules to its surface is easy (Worch, 2012).

Part of the adsorption process requires what is referred to as a fixed bed adsorber, where a solid adsorbent bed moves through a material such as air. When the moisture evaporates, the adsorbent pulls the unwanted particles into the air. During the adsorption process, the heat of the adsorption is absorbed by the cooling water cycling through the adsorbent bed. The adsorption process continues until the adsorbents are saturated with water vapour and the valve between the adsorbent bed and the evaporator is closed. Using water bath to heat the water, the saturated adsorbents is regenerated, and that is called a desorption process (Wu et al., 2014).

The valve between the adsorbent bed and the condenser is in an open position and the hot water travels to the condenser from the regenerated water vapour. The heat of condensation in the condenser is rejected into the cooling water that circulates through the condenser and the condensate is gathered as pure water. Adsorbents in the shape of round pellets, or rods, with a radius of 0.25-5 mm are typically employed to improve performance by layering these beds. Abrasion affinity, good corrosion resistance, and small pore diameters all contribute to a larger exposed surface area and hence increased adsorption power (Qasem & Zubair, 2019).

### Factors affecting the adsorbents

- Porosity
- Adsorption isotherm
- Surface area of adsorbents
- Solubility of solute in a liquid
- Nature of adsorbents and adsorbate
- Experimental conditions e.g., temperature, pressure, etc.

In literature the factors stated above further explain that different substances adsorb different quantities of the same gas. Adsorbents like zeolite, activated alumina, and silica gel work well. Adsorbents with porous surfaces and hard surfaces are more effective. The surface area of the solid also influences the quantity of adsorption. The more adsorbent pore volume available, the more adsorption surface area available, and the stronger the adsorption. The particle size of a material determines its surface area. The nature of the gas also influences the quantity of adsorption.

Gases that are easier to liquefy or soluble in water are absorbed faster than others. The quantity of adsorption decreases with increasing temperature. According to the Le Chatelier principle, the forward process (adsorption) would be favoured at low temperatures because it is exothermic in nature. As a result, adsorption increases with lower temperatures and decreases with higher temperatures. As the gas pressure rises, the quantity of adsorption increases at a constant temperature. The Figure 2.5 graphically represents the factors affecting the adsorbent.

**The extent of adsorption versus pressure curve**

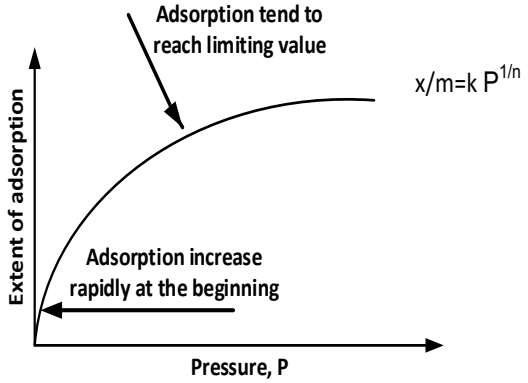


Figure 2.5: Graphical presentation of pressure effect on adsorbents

There are three types of adsorbents used in this study:

- Silica gel
- Activated alumina
- Molecular sieve zeolites

### 2.7.2.2. Silica gel

Silica gel is a porous type of silicon dioxide that is manufactured synthetically in the form of irregular hard granules or normal hard beads. Microporous cavity architecture offers a very prominent surface area (800 $m^2/g$). In a closed space, the relative humidity decreased to about

40 percent (D. Wang et al., 2014) . The gel can be regenerated (dried) in a thick-walled Pyrex dish after it has been saturated with water by heating it to 150 ° C (300 ° F) for a certain amount of time. A high-capacity silica gel desiccant permits this structure. Water molecules stick to the surface of Silica Gels because they have a lower vapour pressure than the surrounding air (D. Wang et al., 2014).

There is no additional adsorption after equal pressure is achieved. As a result, the higher the humidity of the surrounding air, the more water is adsorbed until equilibrium is attained (Li et al., 2016). The stored objects are vulnerable to harm in these higher humidity circumstances (over 50% relative humidity). The physical absorption of water vapour into the interior pores of silica gel makes it distinctive. There are no adverse effects, no chemical reaction, and no product reaction. Even when saturated with water vapour, the silica gel retains the appearance of a dry product, with the same structure (Ng et al., 2017).

Silica Gel is a popular and long-lasting desiccant and adsorbent utilized in a variety of industrial and consumer activities (Riffel et al., 2010). It is corrosive-resistant, odourless, tasteless, non-toxic, and chemically inert. It is a silica form with a large inner surface that is very porous. During adsorption, the silica gel undergoes no chemical reaction and no by-products are generated. Because it is generally pro, its size or form will not alter. Even when the silica gel is soaked with water, it remains dry and free flowing. If the gas stream is completely saturated, a 25% load of water-resistant silica gel is recommended as a protective bed (Ng et al., 2017).

**Chemical composition**

- White silica gel: $SiO_2$ x $H_2O$
- Blue silica gel: $SiO_2 + H_2O + CoCl_2$

### 2.7.2.3. Molecular sieve zeolite

Synthetic zeolite is a pale-yellow desiccant beaded 2.36 to 4.75 mm in diameter and are a substantial structure made up of a collection of aluminosilicates that have unusual industrial relevance. In a variety of chemical processes, zeolite molecular sieve is widely used as a catalyst and they are solids that are very stable and withstand the types of circumstances that challenge many other products. Because they have relatively, high melting points, high temperatures do not affect them, and they do not burn. In areas with high temperatures or low relative humidity, synthetic zeolite performs better in terms of adsorption (Moshoeshoe et al., 2017).

Zeolites can withstand high pressure and do not dissolve in water or other inorganic solvents or oxidize in the atmosphere. Though they may have carcinogenic (cancer-causing) impacts in

fibrous form, they not thought to cause health issues, such as skin contact or inhalation. Because they are non-reactive and made from naturally occurring minerals, no harmful environmental consequences are expected (Wang and Peng, 2010). Although zeolites may look extremely dull, what makes them helpful is not their stable and unreactive nature. The most intriguing aspect of zeolites is their permeable, cage-like, "framework" structure (Moshoeshoe et al., 2017).

In contrast to natural zeolites, usually exists in a variety of shapes and sizes, synthetic zeolites are manufactured in highly exact and consistent sizes (usually ranging from around 1m to 1 mm) to meet the needs of a certain application (Bundschuh et al., 2015). In other words, they are produced to trap inside molecules of a certain (lower) size. Zeolites are found in a wide variety in nature. Under high temperatures, synthetic zeolites are made from an alkaline aqueous solution of silicium and aluminum compounds (Moshoeshoe et al., 2017). There are several varieties of zeolites, and distinct classes may be identified based on the molar, ratio (modulus n).

**Example of the zeolites by classes is:**

- Type A have a module (n) value between 1.5 – 2.5
- Type X have a module (n) value between 2.2-3.0
- Type Y have a module (n) value between = 3.0 – 6.0

These traditional zeolites are hydrophilic, high silica zeolites are more hydrophobic with n> 10 and are also possible adsorbents for organic compounds (Bundschuh et al., 2015). Zeolite channels are sufficiently broad to allow the passage of foreign organisms. Dehydration occurs in the hydrated stages and is usually reversible at temperatures below 400 ° C. (OH, F) groups can disturb the structure because they comprise a tetrahedron apical that is not shared with the adjacent tetrahedron. Zeolites differ from other porous hydrates, because when water loss occurs, they maintain their structural integrity (Alsaman et al., 2017).

These zeolites used as efficient adsorbents after at least partial dehydration, retaining adsorbent molecules within the interstitial spaces. In the crystal lattice, the interstitial sizes of the openings restrict the size and shape of the adsorbable molecules (Wibowo et al., 2017). It is therefore feasible to separate a combination of different molecules, and that can be achieved through molecular sizes by letting certain molecules to be adsorbed by zeolite while others excluded from admission. Many crystalline zeolites characteristically designated as molecular sieves (Bundschuh et al., 2015).

### 2.7.2.4. Activated alumina ($Al_2O_3$)

A desiccant made of white beads with a diameter of 2 to 4 mm is known as activated alumina. It has a smaller surface area to weight ratio than silica gel, and the adsorbed amount fluctuates more in response to variations in relative humidity. (Mondal & George, 2015). Because of its adsorption properties, enabled alumina is typically employed in heatless regenerative dehumidifiers. It has a high rate of conversion and stability of crystals and low impurities. The outstanding performance of its products is high mechanical strength, strong electrical insulation, high wear resistance, and excellent corrosion resistance (Mondal & George, 2015).

In both gas and liquid applications, this type of adsorbent is an extremely efficient adsorbent and is used in a targeted manner by many sectors to extract elements from other media. For use in water filtration applications, activated alumina, known as an adsorbent, serves as a cost-effective adsorbent for the removal of fluoride from water. Removal of several other toxins, including arsenic, leads, and sulphur (Mondal & George, 2015). It is produced from aluminium hydroxide by dihydroxylation in a manner that creates a highly porous content; the surface area of this material can be significantly greater than 200 $m^2/g$ (Ambarita & Kawai, 2016).

Activated alumina is a compound used as a desiccant and as a drinking water source for fluoride, arsenic, and selenium (Yang, 2003; Ambarita & Kawai, 2016). Owing to the many tunnels it has, like pores, it has a very high surface-area-to-weight ratio. When the air moves through them the water in the air adheres to the alumina itself in between the tiny passages. The water molecules are trapped to dry up the air as it moves through the filter. This function is reversible. If heated to 200 °C, the alumina desiccant will release the trapped water. This approach is called desiccant regeneration (Mondal & George, 2015).

In conclusion, as Ng et al. (2013) point out, it is frequently possible to distribute compact water with adsorption without difficulty. However, creating an adsorption cycle on a commercial scale necessitates the availability of a suitable adsorbent in large quantities at a low cost. This has sparked substantial adsorption research and inspired the development of a new adsorbent. The prior adsorption measure utilized were either initiated carbon, or silica gel adsorbents yet the capability of adsorption as a detachment cycle enormously upgraded by the improvement of atomic strainer adsorbent, particularly the manufactured zeolite (Ng et al., 2013).

# Chapter 3: The Mechanism of Adsorbents Adsorption Affinity in Relation to Geometric Parameters

**Part of this Chapter is published as:** Sindisiwe Ntsondwa, Velaphi Msomi, and Moses Basitere. 2021. The Mechanism of Adsorbents Adsorption Affinity in Relation to Geometric Parameters. 2021 South Africa International Conference Applied Research and Engineering (ICARAE-2021) Nov. 26-28, 2021, Cape Town (South Africa). Pp 189-197. **https://doi.org/10.4028/p-j52rwy.**

## 3.1. Introduction

In the process of incorporating adsorption with thermal desalination, adsorbents are important because they increase the water vapour uptake rate, and this yield more desalinated water over a short period when adsorbents are chosen properly. The thermal properties, surface features, and water vapour absorption capacity are the most important factors to consider when choosing adsorbents for an AD cycle. Three types of adsorbents (Silica gel, zeolite and activated alumina) were compared to find which adsorbent can be used as the adsorbent-refrigerant pair, by looking at their adsorption affinity in relation to geometric parameters.

### 3.1.1. Chapter objectives

- To determine the optimum cycle time for a single adsorption desalination (AD) system cycle under certain operational conditions.
- Optimize the adsorption cycle by looking at different types of adsorbents used
- Compare the quantity of water uptake in each adsorbent

### 3.1.2. Sorption Phenomenon

Sorption technology is a method that combines adsorption and desorption. Sorbents are the fundamental distinctions between two types of technology. Generally, liquid phase absorbents, and granular or lightweight adsorbents are used. One of the performance enhancing strategies for the thermal desalination device is the adsorption/desorption cycle. It benefits from a wide spectrum of adsorbents for a wide range of temperatures applied to various heat sources, typically between 50°C and 400°C. Furthermore, the characteristics of strong adsorbents make it more viable under high vibration circumstances (R. Wang et al., 2014).

This method takes a use of the adsorption-desorption cycle to boost the vapour adsorption rate. It is a modest desalination technology that requires just reduced waste heat, which is abundantly accessible from renewable energy sources or power plant exhaust (Ng et al., 2013). The Adsorption Desalination (AD) cycle generates two beneficial outcomes with only one heat source: high-quality drinking water and cooling. Adsorbents are the most important part of the adsorption/desorption process, and there are many different types of them in the market. Each adsorbent's performance is determined by the factory's characteristics.

This suggests that the production of adsorbents varies depending on the producer, which is why this research is being carried out (Gude, 2018). The content is fundamentally related to the advancement of adsorption cooling development within the field of working pairs of adsorptions, productivity of heat and mass transfer, and cooling cycle of adsorption, etc. Many chillers, such

as silica gel-water adsorption, have been successfully marketed on the market because of advancements in adsorption refrigeration technology. The following are more detailed summaries of the adsorption cooling system progression:

- Working pairs of adsorptions and their processes
- Adsorption cooling system structure
- Heat enhancement and mass transfer of the adsorption surface and,
- Thermal characteristics of various advanced renewable cycles.

The working pair of adsorptions is a critical component of the refrigeration adsorption. Thermal characteristics of the working pair have a major impact on the system's efficiency coefficient, velocity rise in adsorbed temperature, and initial expenditure. For efficient cooling efficiency, the appropriate adsorption components are chosen based on the heat source temperatures, and the appropriate adsorption cooling cycles are chosen based on the real needs. The nature and characteristics of the method varies for various pairings employed in adsorption cooling (Alnajdi et al., 2020). There are two functioning methods for adsorption refrigeration.

The first process is adsorption and cooling. The heat from adsorption in this system cools the heat source by releasing cooling water or air, and the pressure within the adsorbed lowers below the evaporation pressure. Under the pressure gap, the coolant evaporates and is absorbed by the adsorbent, and the evaporation process produces the cooling yield. Secondly, consider the desorption and condensation mechanisms. This cycle's moderated heat drives the endothermal desorption process. The desorbed refrigerant vapour condensed and cooled through the heat sink in the condenser (Khalil et al., 2016).

Universally, the term adsorption refers to the enrichment of one or more elements in the area between two phases (interface layer or adsorption space). The terms adsorption and desorption frequently used to describe how was it approached the dynamic equilibrium. When the adsorbed quantity is not reduced to the same level by the approach of adsorption and desorption to the required equilibrium pressure or concentration, hysteresis of adsorption occurs. (Rouquerol et al., 2014). The adsorption isotherm is the response that occurs at a constant temperature between the quantity adsorbed and the equilibrium pressure, or concentration (Rouquerol et al., 2014).

### 3.1.3.Adsorption isotherms

The equilibrium of adsorption at a constant adsorbent temperature is known as the adsorption isotherm. (Alnajdi et al., 2020). Adsorption isotherms are one of the several useful methods for understanding the process of adsorption and for quantitative evaluation of the partition or

distribution of interest solutes at equilibrium between the solid and fluid phases involved. Adsorption isotherms refer to a set of measurements of adsorption performed at a given temperature and whose effects are plotted as a relationship between adsorbed and non-adsorbed quantities (Israelachvili, 2011; Alnajdi et al., 2020). The table below shows the mathematical adsorption isotherm models.

Table 3-1: Mathematical adsorption model used to calculate geometric parameters and the equations are taken from (Alnajdi et al., 2020).

| **Isotherm** | **Nonlinear form** | **Linear form** |
|---|---|---|
| **Langmuir** | $q_e = \frac{Q_o b C_e}{1 + bC_e}$ | $\frac{C_e}{q_e} = \frac{1}{bQ_o} + \frac{C_e}{q_o}$ |
| **Toth** | $q_e = \frac{K_T C_e}{(a + C_e)^{\frac{1}{t}}}$ | $logq_e = logC_e - \frac{1}{t} ln(a_T + C_e)$ |
| **Dubinin-Astakhov(D-A)** | $q^* = q^o \times exp\left\{-\left[\frac{RT}{E} \times in\frac{P_o}{P}\right]^n\right\}$ | |
| **BET** | $q_e = \frac{q_s C_{BET} C_e}{(C_s - C_e)\left[1 + (C_{BET} - 1)\frac{C_e}{C_s}\right]}$ | $\frac{C_e}{q_e(C_s - C_e)} = \frac{1}{q_s C_{BET}} + \frac{C_{BET} - 1}{q_s C_{BET}} \frac{C_e}{C_s}$ |
| **Freundlich** | $q_e = K_f \times C_e^{\frac{1}{n}}$ | $logq_e = logK_f - \frac{1}{n} logC_e$ |

Adsorption isotherms are utilized in the assessment of surface characteristics such as adsorbent affinity and adsorption capacity to develop effective adsorption systems. This aids in the development of effective adsorption systems. The structure of these isotherms retains much knowledge about the essence of the phase of adsorption. Adsorption is often used to extract contaminants by allowing adsorbents like activated alumina, molecular sieve zeolite or silica gel connected to them. Adsorbents are porous solids that bind to the molecules on their surface, which might be liquid or gaseous (Moshoeshoe et al., 2017; Youssef et al., 2015).

The adsorption process primarily employs what is known as a fixed bed adsorber, in which a material such as air travels through a solid adsorbent bed. Adsorbents are often

employed to attract unwanted particles in the air when moisture evaporates. But in this case are used as an intermediate phase in adsorption desalination to reduce the energy consumption and speed up the process. Placing several levels of these beds helps to enhance efficiency. In addition, the adsorbents are used in desalting, and they can continue adsorbing until they get into saturation phase (Alnajdi et al., 2020). The saturation phase of each adsorbent differs from one to another.

This means that some other adsorbents have a high adsorption affinity than the other and that is explained more in (Alnajdi et al., 2020). In the process of adsorption desalination, it is important to use an adsorbent that has a higher affinity to adsorb, hence the selection of geometric parameters is import(Condon, 2006b). One of the essential jobs for adsorption technology users is choosing an adsorbent for a certain application. In theory, an adsorbent may be chosen based on a variety of variables such as adsorption capacity and selectivity, adsorbate uptake kinetics, compatibility with operating conditions, and, of course, cost (Tien, 2019).

Adsorption is influenced by the properties of the solid surface and the liquid media. Gases and vapours adsorb on highly developed solid surfaces. The adsorption isotherm is used to select or synthesize adsorbents for a specific adsorbate molecule. Geometric parameters that are of interest are the pore size diameter, surface area, the affinity to adsorb the vapour, distance between the fin and the material of the fin and the pipe. These geometric parameters will be compared using three different types of adsorbents in a gravimetric method to see which adsorbent that has the higher affinity.

The adsorbents used; activated alumina, silica gel and molecular sieve zeolites. Surface features of adsorbents, including surface chemistry and pore size distribution (PSD), have been demonstrated to play a key impact in the adsorption process, therefore the research. The adsorbent pore size distribution (PSD) specifies the fraction of its structure which a molecule of a given size and shape can access. The size of the adsorbents relative to the pore size of the adsorbents is important in controlling the adsorptive mechanism of competition for a given size pore. Table 3.2 is showing the adsorbents granule’s dimensions.

Table 3-2: Adsorbent granules dimensions

| *Properties* | *Zeolite (3A)* | *Silica gel* | *Activated alumna* |
|---|---|---|---|
| **Size** | 3-5 mm | 3-5 mm | 2-5 mm |
| **Shape** | Spherical | Beads | Spherical |
| **Qualified Ratio of Particle size (%)** | 94 | 97 | 92 |
| **Bulk density G/L** | 760 | 767 | 750 |
| **Moisture (%)** | <2 | 1.43 | 1.5 |

The overarching goal in designing adsorption chillers that use different types of adsorbents as the adsorbent-adsorbate pair is to leverage low-temperature waste-heat sources from industry. This research aims to find the adsorbent with good geometric parameters that can adsorb and desorb using desorption conditions. The three adsorbents used (silica gel, zeolite, and molecular sieve zeolite) compared through adsorption cycle and the one that extract more adsorbate means it has high affinity to adsorb. Adsorption isotherms are utilized in the assessment of surface characteristics such as the adsorbent's affinity and adsorption capacity to build effective adsorption systems.

## 3.2. Material and system design

The gravimetric method used in the process of finding the geometric parameters by capturing the efficient water vapour uptake, and it was used to determine the optimum cycle time for the given AD cycle under the given operational conditions. The system consists primarily of three chambers, an experimental setup designed and built: adsorbents chamber, feed inlet chamber and evaporator. A series of valves and tubes connected in the chamber for heat transfer purposes. The evaporator is attached to the feed input chamber and serves as a vapour source. Each chamber is situated within an independent water flow and is connected to a water circulator to manage the temperature of the chamber.

There are two working processes for refrigeration by adsorption. The first step is that of cooling and adsorption. The adsorption heat in this system releases cooling water into the heating element, and the pressure within the adsorber falls below the evaporation pressure. Under the pressure difference, the coolant evaporates and is absorbed by the adsorbent, and the evaporation process produces the cooling results. Second, the mechanism of desorption and

condensation. The low-grade heat triggers the endothermic process of desorption during this period. In the condenser, the desorbed refrigerant vapour condensed and cooled through the heat sink.

Vacuum pump utilized for departure reason. A warming tape wrapped around the associating cylinders to control the solid shapes temperature. A reading rag pressure sensor is used. A variety of thermocouple sensors are connected to the temperature determined at various positions in the test ring. Every second, data is recorded by temperature sensors and pressure transmitters coupled to a data recorder. In a certain temperature range, the isotherms and kinetics of the various adsorbents were measured over a specific temperature range. The test-rig kinetics of sorption design shown in Figure 3.1 with dotted line on the schematic lay out, and it is the important part of the system.

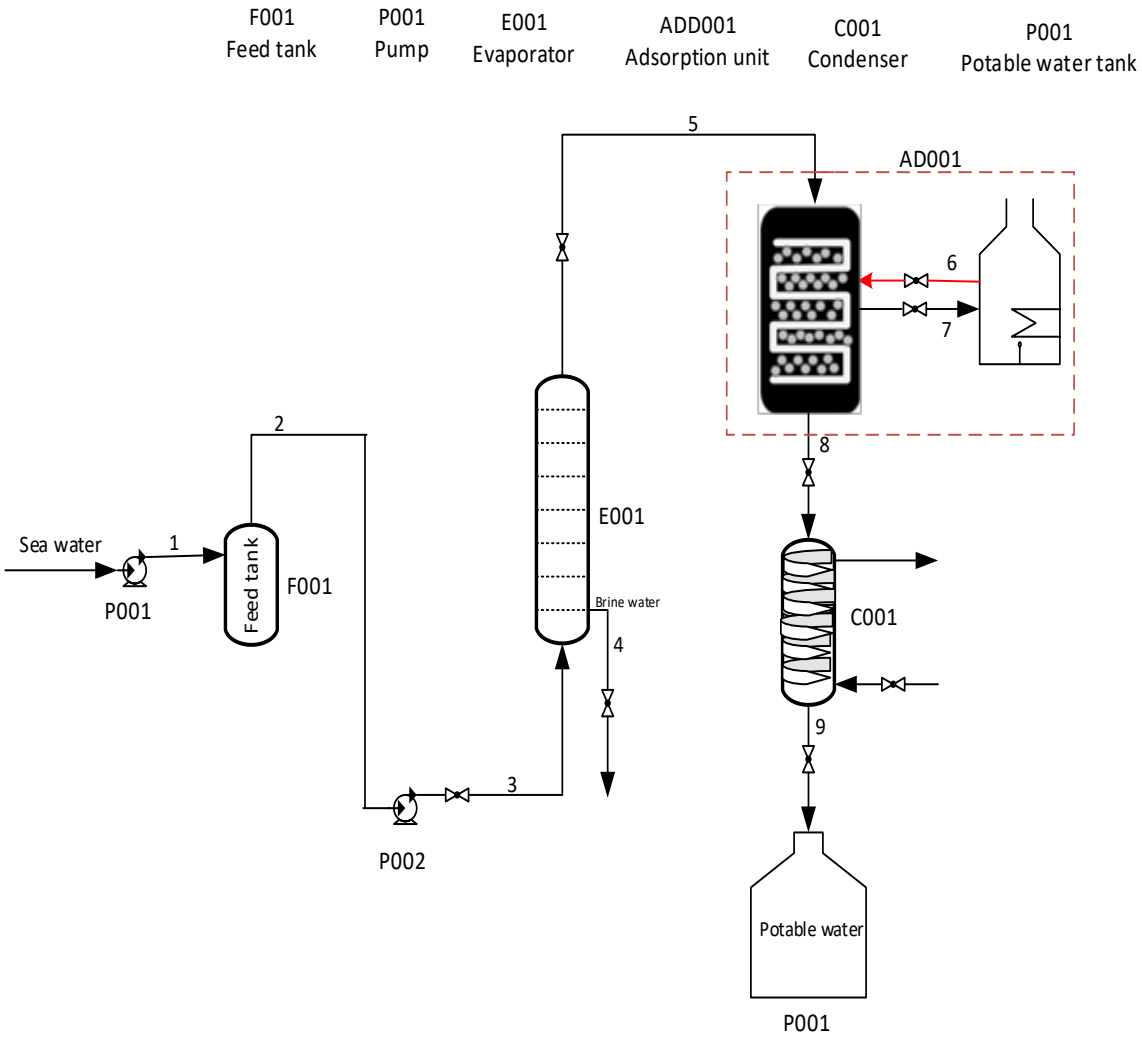


Figure 3.1: Schematic diagram representing experimental set-up

## 3.3. Procedure

The adsorbent dried up in an oven, cooled to the isobaric adsorption and then weighed. The evaporator is filled with water and heated up until the seawater start boiling. The adsorbents placed on the vacuumed heat exchanger column. The coil connected to the heat exchanger is from the cooling refrigerator cools the adsorbent until they reach the saturation stage and become hydrophilic. The scale weighs each step and records to the data logger. Once the adsorbents are saturated, the steam released from the evaporator and adsorbed by adsorbents for a certain amount of time. The regenerated water release from the water bath to the heat exchanger and adsorbents become hydrophobic and reject the steam. After desorption the vapour moves to the condenser and the condensate (Fresh water) is collected from the condenser chamber.

## 3.4. Results and Discussion

The three distinct adsorbents, activated alumna, silica gel and molecular sieve zeolite, were examined in a single bed adsorption system. The system has been thermodynamically simulated for three adsorbents using adsorption equilibrium isotherms to test which adsorbent has a high affinity to adsorb the vapour (Aristov, 2012; Ng et al., 2001). The difference in weight of the silica gel between its saturated condition and the final desorbed state regarding temperature and time is measured using a moisture balancing approach. Adsorption, as is well known, is dependent on the solid surface properties and the kinetics (Ng et al., 2001).

Gases and vapours adsorb on solids with a highly developed surface (silica gel in this case). Moisture balancing studies and representative plots for the three types of adsorbents, namely silica gel, activated alumina, and zeolite, are presented in Figure 3.2. The behaviour of water vapour desorption rates has been discovered to be time and temperature dependent. The graph of the percentage desorption obtained over time is shown in Figure 3.2 it further shows the mass adsorbed as a function of time for three distinct adsorbents. Silica gel has the highest moisture adsorption capability from 300s to 1200s as shown in Figure 3.2.

The results reveal that the silica gel-water pair has greater adsorption properties suitable for this adsorption chiller. The molecular sieve zeolite, on the other hand, requires a higher temperature heat source for a steady desorption process, which consumes more energy. The activated alumina has a smaller surface area to weight ratio and displays more variation in the amount adsorbed as a function of relative humidity variations (Ng et al., 2017). Activated alumina is mostly utilized in heat rejection regeneration dehumidifiers because of its adsorption properties. According to the results on Figure 3.3 the silica gel outperforms the zeolite and activated alumina during adsorption cycle.

In Figure 3.3 it is observed that the cycle of 1200 s is sufficient to achieve 90% regeneration for all three investigated adsorbents. All adsorbents in Figure 3.2 rapidly increase until they reach 1200 s that is where they start to move slowly as they are approaching the equilibrium phase. It is stated in literature that in high-temperature regeneration and in less than 20°C evaporation temperature, the synthetic zeolite has a superior adsorption performance (Youssef et al., 2015). The silica gel has shown to be more successful due to its ability to be regenerated at temperatures as high as 82°C, whereas molecular sieves can be regenerated at 550°C.

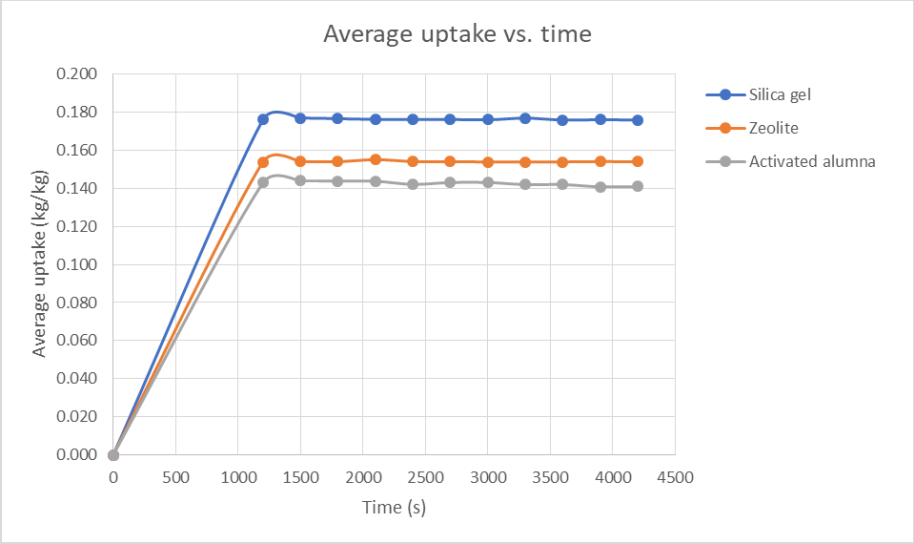


Figure 3.2:Comparison of adsorbent in adsorption cycle

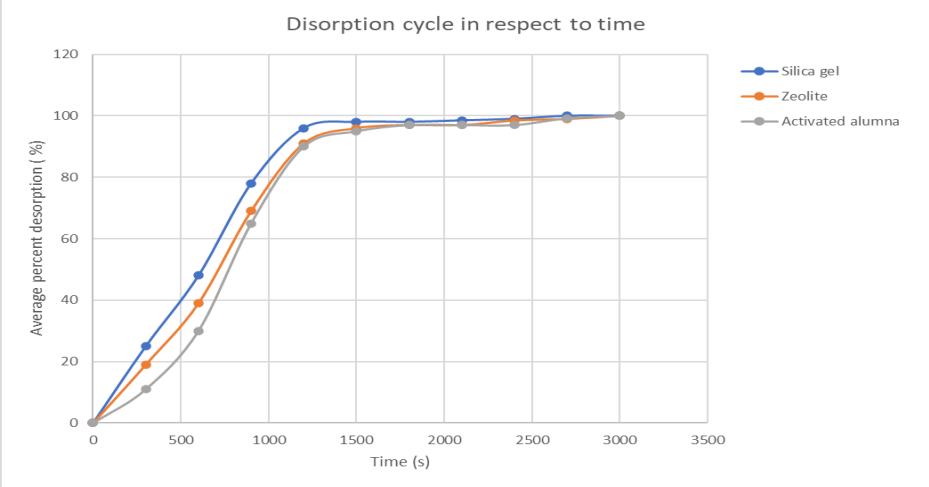


Figure 3.3: The graph of average description cycle with respect to time

As it has been stated on the procedure that for adsorbent to be able to adsorb water vapour, it needs to be saturated with hot water. Figure 3.4 represent the kinetics needed to operate the system. It is shown that when the chiller runs cold water at 30℃ the steam is highly regenerated

at 70℃ and when the adsorption run at 35℃ it regenerates at most at 65℃. The 65℃ can be seen as the right temperature to use because it requires less energy as compared to 70℃. However, the water is produced more at 70℃. It is, therefore, safe to say the optimum temperature is 30℃ for adsorption process and 70℃ for regeneration temperature.

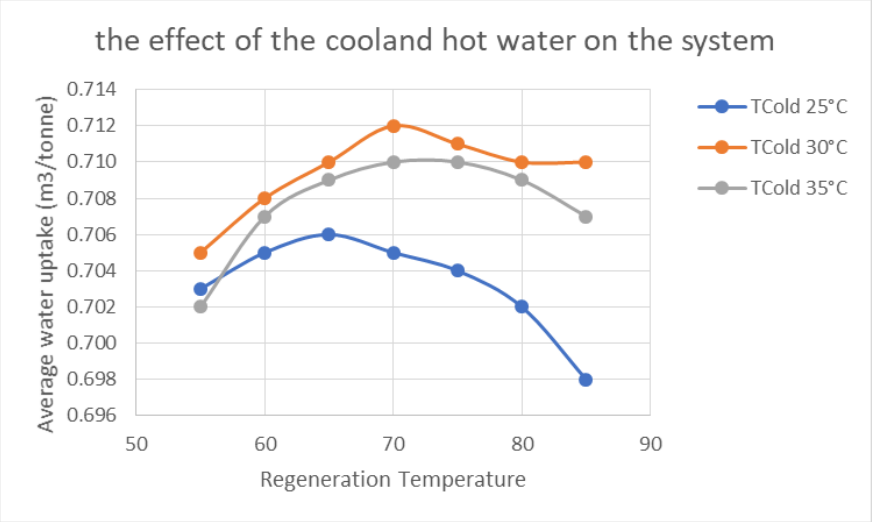


Figure 3.4: Regeneration temperature in relation with average water uptake

## 3.5. Conclusion

The adsorption desalination system is a newly developed thermal desalination system that requires low-temperature input for desalination to take place. For this system to remain utilizing the low energy, an adsorbent that can easily desorb vapour at a low temperature is needed (Sah et al., 2015). The main purpose of this research is to conduct a study that use the geometric parameters of adsorbents to find the adsorbent with the high affinity while operating with low regeneration temperature. A gravimetric analysis is used to conduct this study and premeditated under the following kinetics conditions evaporator; $T_{eva}$= 10°C, condenser $T_c$= 30°C, and desorption at $T_h$= 75°C.

To study each adsorbent's adsorption affinity, the regeneration temperature and desorption rate were monitored concurrently using gravimetric method. The tested adsorbent range between 2-5 mm for activated alumina and 3-5 mm for silica gel and zeolite. The volume intake of water vapour cycle explored in relation to time. The silica gel adsorbs 12% vapour higher than zeolite and 18.9% vapour to $Al_2O_3$ at equilibrium (1200s). Through the results provided in this study, it can be concluded that the silica gel is the suitable adsorbent for adsorption chiller as it outperformed the other two adsorbents when they were compared based on adsorption chiller's conditions.

## 3.6. References


Abdulsalam, J., Mulopo, J., Bada, S.O. & Oboirien, B. 2020. Equilibria and Isosteric Heat of Adsorption of Methane on Activated Carbons Derived from South African Coal Discards. *ACS Omega*, 5(50): 32530–32539.

Al-Jabari, M. 2016. Kinetic models for adsorption on mineral particles comparison between Langmuir kinetics and mass transfer. *Environmental Technology and Innovation*, 6: 27–37. http://dx.doi.org/10.1016/j.eti.2016.04.005.

Alnajdi, O., Wu, Y. & Calautit, J.K. 2020. Toward a Sustainable Decentralized Water Supply : Review of Adsorption Desorption Desalination ( ADD ) and Current Technologies : Saudi Arabia ( SA ). : 1–30.

Alsaman, A.S., Askalany, A.A., Harby, K. & Ahmed, M.S. 2017. Performance evaluation of a solar-driven adsorption desalination-cooling system. *Energy*, 128: 196–207. http://dx.doi.org/10.1016/j.energy.2017.04.010.

Ambarita, H. & Kawai, H. 2016. Experimental study on solar-powered adsorption refrigeration cycle with activated alumina and activated carbon as adsorbent. *Case Studies in Thermal Engineering*, 7: 36–46. http://dx.doi.org/10.1016/j.csite.2016.01.006.

Aristov, Y.I. 2012. Adsorptive transformation of heat: Principles of construction of adsorbents database. *Applied Thermal Engineering*, 42: 18–24.

Bakhtyari, A. & Mofarahi, M. 2019. A New Approach in Predicting Gas Adsorption Isotherms and Isosteric Heats Based on Two-Dimensional Equations of State. *Arabian Journal for Science and Engineering*, 44(6): 5513–5526. https://doi.org/10.1007/s13369-019-03838-2.

Barbosa, G.D., Bara, J.E., Weinman, S.T. & Turner, C.H. 2022. Molecular aspects of temperature swing solvent extraction for brine desalination using imidazole-based solvents. *Chemical Engineering Science*, 247: 116866. https://doi.org/10.1016/j.ces.2021.116866.

Bindu, B. 2019. Getting Started with EasyEDA an Online PCB Design Software | StudentCompanion.

Builes, S., Sandler, S.I. & Xiong, R. 2013. Isosteric heats of gas and liquid adsorption. *Langmuir*, 29(33): 10416–10422.

Bundschuh, J., Ghaffour, N., Mahmoudi, H., Goosen, M., Mushtaq, S. & Hoinkis, J. 2015. Low-cost low-enthalpy geothermal heat for freshwater production: Innovative applications using thermal desalination processes. *Renewable and Sustainable Energy Reviews*, 43: 196–206. http://dx.doi.org/10.1016/j.rser.2014.10.102.

Cameron, N. 2019. *Arduino Applied:Comprehensive Projects for Everyday Electronics*.

Chakraborty, A., Saha, B.B., Koyama, S. & Ng, K.C. 2006. On the thermodynamic modeling of the isosteric heat of adsorption and comparison with experiments. *Applied Physics Letters*, 89(17): 2004–2007.

Chen, X., Boo, C. & Yip, N.Y. 2020. Transport and structural properties of osmotic membranes in high-salinity desalination using cascading osmotically mediated reverse osmosis. *Desalination*, 479(January): 114335. https://doi.org/10.1016/j.desal.2020.114335.

Chiou, C.T. 2002. *Partition and adsorption of organic contaminants*. John Wiley & Sons, Inc., Hoboken, New jersey.

Choi, O.K., Seo, J.H., Kim, G.S., Hendren, Z., Kim, G.D., Kim, D. & Lee, J.W. 2021. Non-membrane solvent extraction desalination (SED) technology using solubility-switchable

amine. *Journal of Hazardous Materials*, 403(April 2020): 123636. https://doi.org/10.1016/j.jhazmat.2020.123636.

Condon, J.B. 2006a. Heat of Adsorption - an overview | ScienceDirect Topics. *Elsevier*. https://www.sciencedirect.com/topics/chemistry/heat-of-adsorption 22 October 2021.

Condon, J.B. 2020. *Measuring the physisorption isotherm*.

Condon, J.B. 2006b. *Surface Area and Porosity Determinations by Physisorption Measurements and Theory*. 1st ed. Elsevier B.V.

Distribution, W., Moisture, S. & Ice, G. 2020. What is the big deal? *SPC Water, Sanitation and Hygen: Water distribution*, 2: 2–3.

Gabelman, A. 2017. Adsorption basics: Part 2. *Chemical Engineering Progress*, 113(8): 1–6.

Gediz Ilis, G., Demir, H., Mobedi, M. & Baran Saha, B. 2019. A new adsorbent bed design: Optimization of geometric parameters and metal additive for the performance improvement. *Applied Thermal Engineering*, 162(July): 114270. https://doi.org/10.1016/j.applthermaleng.2019.114270.

Giraldo, L., Rodriguez-Estupiñán, P. & Moreno-Piraján, J.C. 2019. Isosteric heat: Comparative study between Clausius-Clapeyron, CSK and adsorption calorimetry methods. *Processes*, 7(4).

Grande, C.A. 2012. Advances in Pressure Swing Adsorption for Gas Separation. , 2012: 100–102.

Gude, V.G. 2018. Exergy Evaluation of Desalination Processes.

Guo, J., Tucker, Z.D., Wang, Y., Ashfeld, B.L. & Luo, T. 2021. Ionic liquid enables highly efficient low temperature desalination by directional solvent extraction. *Nature Communications*, 12(1): 1–7. http://dx.doi.org/10.1038/s41467-020-20706-y.

Halvorsen, H.-P. 2018. *Programming With Arduino*. 978-82-691106.

Israelachvili, J.N. 2011. *Intermolecular and surface forces*. 3rd ed. Elisvier.

Kaiser, R. 1970. *Carbon molecular sieve*.

Khalil, A., El-Agouz, E.S.A., El-Samadony, Y.A.F. & Sharaf, M.A. 2016. Experimental study of silica gel/water adsorption cooling system using a modified adsorption bed. *Science and Technology for the Built Environment*, 22(1): 41–49.

Khanam, M., Jribi, S., Miyazaki, T., Saha, B.B. & Koyama, S. 2018. Numerical investigation of small-scale adsorption cooling system performance employing activated carbon-ethanol pair. *Energies*, 11(6).

Li, A., Thu, K., Ismail, A. Bin, Shahzad, M.W. & Ng, K.C. 2016. Performance of adsorbent-embedded heat exchangers using binder-coating method. *International Journal of Heat and Mass Transfer*, 92: 149–157. http://dx.doi.org/10.1016/j.ijheatmasstransfer.2015.08.097.

Loh, W.S., Rahman, K.A., Chakraborty, A., Saha, B.B., Choo, Y.S., Khoo, B.C. & Ng, K.C. 2010. Improved isotherm data for adsorption of methane on activated carbons. *Journal of Chemical and Engineering Data*, 55(8): 2840–2847.

Mancosu, N., Snyder, R.L., Kyriakakis, G. & Spano, D. 2015. Water scarcity and future challenges for food production. *Water (Switzerland)*, 7(3): 975–992.

Mitra, S., Kumar, P., Srinivasan, K. & Dutta, P. 2015. Performance evaluation of a two-stage silica gel + water adsorption based cooling-cum-desalination system. *International Journal*

*of Refrigeration*, 58: 186–198.

Mitra, S., Thu, K., Saha, B.B., Srinivasan, K. & Dutta, P. 2017. Modeling study of two-stage, multi-bed air cooled silica gel + water adsorption cooling cum desalination system. *Applied Thermal Engineering*, 114: 704–712. http://dx.doi.org/10.1016/j.applthermaleng.2016.12.011.

Mohammed, R.H., Mesalhy, O., Elsayed, M.L. & Chow, L.C. 2019. Assessment of numerical models in the evaluation of adsorption cooling system performance. *International Journal of Refrigeration*, 99: 166–175. https://doi.org/10.1016/j.ijrefrig.2018.12.017.

Mohammed, Ramy H., Mesalhy, O., Elsayed, M.L., Hou, S., Su, M. & Chow, L.C. 2018. Physical properties and adsorption kinetics of silica-gel/water for adsorption chillers. *Applied Thermal Engineering*, 137(March): 368–376. https://doi.org/10.1016/j.applthermaleng.2018.03.088.

Mohammed, Ramy H, Mesalhy, O., Elsayed, M.L., Su, M. & Chow, L.C. 2018. Revisiting the adsorption equilibrium equations of silica-gel/water for adsorption cooling applications. *International Journal of Refrigeration*, 86: 40–47. https://doi.org/10.1016/j.ijrefrig.2017.10.038.

Mondal, P. & George, S. 2015. A review on adsorbents used for defluoridation of drinking water. *Reviews in Environmental Science and Biotechnology*, 14(2): 195–210. http://dx.doi.org/10.1007/s11157-014-9356-0.

Moshoeshoe, M., Silas Nadiye-Tabbiruka, M. & Obuseng, V. 2017. A Review of the Chemistry, Structure, Properties and Applications of Zeolites. *American Journal of Materials Science*, 2017(5): 196–221. http://journal.sapub.org/materials.

Nasir, S.Z. 2020. Introduction to Proteus - The Engineering Projects. *TheEngineeringProjects*.

Ng, K.C., Burhan, M., Shahzad, M.W. & Ismail, A. Bin. 2017. A Universal Isotherm Model to Capture Adsorption Uptake and Energy Distribution of Porous Heterogeneous Surface. *Scientific Reports*, 7(1): 1–11. http://dx.doi.org/10.1038/s41598-017-11156-6.

Ng, K.C., Chua, H.T., Chung, C.Y., Loke, C.H., Kashiwagi, T., Akisawa, A. & Saha, B.B. 2001. Experimental investigation of the silica gel-water adsorption isotherm characteristics. *Applied Thermal Engineering*, 21: 1631–1642. www.elsevier.com/locate/apthermeng.

Ng, K.C., Thu, K., Chakraborty, A., Saha, B.B. & Chun, W.G. 2009. Solar-assisted dual-effect adsorption cycle for the production of cooling effect and potable water. *International Journal of Low-Carbon Technologies*, 4(2): 61–67.

Ng, K.C., Thu, K., Kim, Y., Chakraborty, A. & Amy, G. 2013. Adsorption desalination: An emerging low-cost thermal desalination method. *Desalination*, 308: 161–179. http://dx.doi.org/10.1016/j.desal.2012.07.030.

Nuhnen, A. & Janiak, C. 2020. A practical guide to calculate the isosteric heat/enthalpy of adsorption: Via adsorption isotherms in metal-organic frameworks, MOFs. *Dalton Transactions*, 49(30): 10295–10307.

Olkis, C., Brandani, S. & Santori, G. 2019a. A small-scale adsorption desalinator. *Energy Procedia*, 158: 1425–1430. https://doi.org/10.1016/j.egypro.2019.01.345.

Olkis, C., Brandani, S. & Santori, G. 2019b. Cycle and performance analysis of a small-scale adsorption heat transformer for desalination and cooling applications. *Chemical Engineering Journal*, 378(April): 122104. https://doi.org/10.1016/j.cej.2019.122104.

Osman, S.M., Hasan, E.H., El-Hakeem, H.M., Rashad, R.M. & Kouta, F. 2013. Conceptual

design of multi-capacity load cell. , 03002: 03002.

Qasem, N.A.A. & Zubair, S.M. 2019. Performance evaluation of a novel hybrid humidification-dehumidification (air-heated) system with an adsorption desalination system. *Desalination*, 461(March): 37–54. https://doi.org/10.1016/j.desal.2019.03.011.

Rahimi, B. & Chua, H.T. 2017. *Low Grade Heat Driven Multi-Effect Distillation and Desalination*. 1st ed. Elsivier Inc.

Raj, R. & Baiju, V. 2019. Thermodynamic analysis of a solar powered adsorption cooling and desalination system. *Energy Procedia*, 158: 885–891. https://doi.org/10.1016/j.egypro.2019.01.226.

Raluy, G., Serra, L. & Uche, J. 2006. Life cycle assessment of MSF, MED and RO desalination technologies. *Energy*, 31(13): 2361–2372.

Rautenbach, R., Linn, T. & Eilers, L. 2000. Treatment of severely contaminated waste water by a combination of RO, high-pressure RO and NF - Potential and limits of the process. *Journal of Membrane Science*, 174(2): 231–241.

Rezk, A. 2012. Theoretical and experimental investigation of silica gel/water adsorption refrigeration systems. *Doctor of Philosophy*, 1: 2017.

Riffel, D.B., Wittstadt, U., Schmidt, F.P., Núñez, T., Belo, F.A., Leite, A.P.F. & Ziegler, F. 2010. Transient modeling of an adsorber using finned-tube heat exchanger. *International Journal of Heat and Mass Transfer*, 53(7–8): 1473–1482. http://dx.doi.org/10.1016/j.ijheatmasstransfer.2009.12.001.

Rouquerol, F., Rouquerol, J., Sing, K.S.W., Llewellyn, P. & Maurin, G. 2014. *Adsorption by Powders and Porous Solids Principles, Methodology and Applications*. 2nd ed.

Sah, R.P., Choudhury, B. & Das, R.K. 2015. A review on adsorption cooling systems with silica gel and carbon as adsorbents. *Renewable and Sustainable Energy Reviews*, 45: 123–134. http://dx.doi.org/10.1016/j.rser.2015.01.039.

Santamaria, S., Sapienza, A., Frazzica, A., Freni, A., Girnik, I.S. & Aristov, Y.I. 2014. Water adsorption dynamics on representative pieces of real adsorbers for adsorptive chillers. *Applied Energy*, 134: 11–19.

Sapienza, A., Santamaria, S., Frazzica, A., Freni, A. & Aristov, Y.I. 2014. Dynamic study of adsorbers by a new gravimetric version of the Large Temperature Jump method. *Applied Energy*, 113: 1244–1251. http://dx.doi.org/10.1016/j.apenergy.2013.09.005.

Seol, S.H., Nagano, K. & Togawa, J. 2020. Modeling of adsorption heat pump system based on experimental estimation of heat and mass transfer coefficients. *Applied Thermal Engineering*, 171(February): 115089. https://doi.org/10.1016/j.applthermaleng.2020.115089.

Shen, C.H., Kee, T.S., Lee, B.C.T. & Albert, F.Y.C. 2017. Development and Implementation of Load Cell in Weight Measurement Application for Shear Force. *International Journal of Electronics and Electrical Engineering*, 5(3): 240–244.

Shen, D., Bülow, M., Siperstein, F., Engelhard, M. & Myers, A.L. 2000. Comparison of experimental techniques for measuring isosteric heat of adsorption. *Adsorption*, 6(4): 275–286.

Thu, K., Kim, Y.D., Shahzad, M.W., Saththasivam, J. & Ng, K.C. 2015. Performance investigation of an advanced multi-effect adsorption desalination (MEAD) cycle. *Applied Energy*, 159: 469–477. http://dx.doi.org/10.1016/j.apenergy.2015.09.035.

Thu, K., Yanagi, H., Saha, B.B. & Ng, K.C. 2013. Performance analysis of a low-temperature waste heat-driven adsorption desalination prototype. *International Journal of Heat and Mass Transfer*, 65: 662–669. http://dx.doi.org/10.1016/j.ijheatmasstransfer.2013.06.053.

Tien, C. 2019. *Introduction to Adsorption, Basics, Analysis, and Applications*. Elsevier.

Tun, H. & Chen, C.C. 2021. Isosteric heat of adsorption from thermodynamic Langmuir isotherm. *Adsorption*, 27(6): 979–989. https://doi.org/10.1007/s10450-020-00296-3.

Volmer, R., Eckert, J., Füldner, G. & Schnabel, L. 2017. Evaporator development for adsorption heat transformation devices – Influencing factors on non-stationary evaporation with tube-fin heat exchangers at sub-atmospheric pressure. *Renewable Energy*, 110: 141–153. http://dx.doi.org/10.1016/j.renene.2016.08.030.

Vordos, N., Gkika, D.A. & Bandekas, D. V. 2020. Wheatstone Bridge and Bioengineering. *Journal of Engineering Science and Technology Review*, 13(5): 4–6.

Wang, D., Zhang, J., Yang, Q., Li, N. & Sumathy, K. 2014. Study of adsorption characteristics in silica gel-water adsorption refrigeration. *Applied Energy*, 113: 734–741.

Wang, R., Wang, L. & Wu, J. 2014. ADSORPTION REFRIGERATION TECHNOLOGY THEORY AND APPLICATION. *John Wiley & sons*: 526.

Wenten, I.G. & Khoiruddin. 2016. Reverse osmosis applications: Prospect and challenges. *Desalination*, 391: 112–125. http://dx.doi.org/10.1016/j.desal.2015.12.011.

Wibowo, E., Sutisna, Rokhmat, M., Murniati, R., Khairurrijal & Abdullah, M. 2017. Utilization of Natural Zeolite as Sorbent Material for Seawater Desalination. In *Procedia Engineering*. Elsevier Ltd: 8–13.

Worch, E. 2012. *Adsorption Technology in Water Treatment*.

Wu, J.W., Biggs, M.J. & Hu, E.J. 2014. Dynamic model for the optimisation of adsorption-based desalination processes. *Applied Thermal Engineering*, 66(1–2): 464–473. http://dx.doi.org/10.1016/j.applthermaleng.2014.02.045.

Wyma, B.D. 2020a. *Measuring Pilot Control Force in General Aviation Subtitle: Strain gauges and Load Cell*.

Wyma, B.D. 2020b. *Measuring Pilot Control Force in General Aviation Subtitle: Strain gauges and Load Cell*. Florida Institute of Technology.

Yan, S., Cao, Z., Guo, Z., Zheng, Z., Cao, A., Qi, Y., Leng, Q. & Zhao, W. 2018. Design and fabrication of full wheatstone- bridge-based angular GMR sensors. *Sensors (Switzerland)*, 18(6): 1–8.

Yang, R.T. 2003. *Adsrbents: Fundamentals and Applications*. 1st ed. http://elib.tu-darmstadt.de/tocs/95069577.pdf.

Youssef, P.G., Dakkama, H., Mahmoud, S.M. & AL-Dadah, R.K. 2017. Experimental investigation of adsorption water desalination/cooling system using CPO-27Ni MOF. *Desalination*, 404: 192–199.

Youssef, P.G., Mahmoud, S.M. & AL-Dadah, R.K. 2015. Performance analysis of four bed adsorption water desalination/refrigeration system, comparison of AQSOA-Z02 to silica-gel. *Desalination*, 375: 100–107.

# Chapter 4: Performance Evaluation of important parameters for a new designed Adsorption Chiller using Gravimetric Technique

**Part of this Chapter is under the review as: Sindisiwe Ntsondwa,** Velaphi Msomi, and Ntokozo Shangase. 2021. Performance Evaluation of important parameters for a new designed small Scale Adsorption Chiller using Gravimetric Technique. Ain Shams Engineering Journal. Manuscript number: ASEJ-S-22-00933.

## 4.1. Introduction

The demand for and interest in developing energy efficient desalination methods with a cooling energy based on renewable energies or low-grade heat sources is significant. Many researchers and academic institutions believe that adsorption systems can help solve global issues like global warming and water scarcity issues (Mancosu et al., 2015). Adsorption chillers have piqued the interest of academics in recent decades because of its thermal compression, environmentally acceptable refrigerants, non-corrosive fluids, and lack of crystallization issues. The adsorption method has been regarded as a feasible water cleaning solution (Qasem & Zubair, 2019).

Adsorption procedures are widely utilized for wastewater, groundwater, and industrial effluent treatment, as well as the creation of drinking water (Rahimi & Chua, 2017). Apart from its ease of use, flexibility, adaptable design, low energy needs, and cost-effectiveness trade-off, this treatment technique may offer various advantages for water purification. Overall, the economic and technological feasibility of adsorption processes is determined by a variety of criteria such as; adsorbent type, fluid characteristics (molecular spacing), pollutants to be removed, operating conditions, process setup, regeneration, and waste disposal (Ng et al., 2017).

Adsorption tests in packed columns are necessary to compute important scale-up characteristics such as regeneration temperature, adsorption temperature, saturation periods, bed adsorption capacity, and mass transfer parameters. This process configuration also allows for the determination of the adsorbent's maximal performance and the identification of the ideal dynamic operating situation. It should be noted that the operating circumstances of dynamic adsorption systems indicate residence durations shorter than the equilibrium time, and as a result, mass transfer resistances play a significant role in pollutant removal (Ng et al., 2017).

Most of the adsorption experimental and numerical data available in the literature focused on traditional chillers with huge bed sizes of up to 38 kg (Olkis et al., 2019a). However, as compared to traditional cooling systems, the major disadvantage of adsorption chillers are the adsorbents restricted heat and mass transfer characteristics, which results in low specific cooling power (SCP) and, as a result, the high system sizes. In addition, these large-scale systems are resulting into inflexibility in operation and component replacement. This paper proposes a unique, small-scale adsorption desalination method to address this research gap (Mohammed et al., 2019).

The equipment used to build the-current used chiller is expensive and not all academic institutions can afford to build them. That alone can limit researchers' work in finding the better ways of improving the adsorption desalination process. Because of the limited small experimental measurements, an experimental configuration has been devised and built to evaluate sorption

kinetics and the water production of the system. The gravimetric small lab scale adsorption chiller designed using the Load cell, HX711 Amplifier, LCD, Switches/Buttons, and Arduino. This small lab scale was designed according to gravimetric method standard.

### 4.1.1.Chapter objectives

- Design and construct an adsorption chiller to assess the adsorption isotherm and kinetics, as well as investigate the efficiency of an adsorption cooling bed under adsorption cooling cycle conditions.

### 4.1.2. The comparison of techniques to design adsorption chiller

There are several techniques to be used in building an adsorption chiller, however, each process has its own advantages and disadvantages. This section of the study has endeavoured to give a summary of the adsorption concepts, methods, and implementation of adsorption chillers. Throughout the research it has been found that it is possible to divide methods for adsorption measurements narrowly into dynamic and static methods. The static measurements are performed by volumetric or gravimetric methods, and dynamic methods demonstrated by chromatographic isotherm determination (Condon, 2006a; Ramy H. Mohammed et al., 2018).

This design is specifically built using statistic measurements. For volumetric and gravimetric, the general purpose is the same. As a function of the gas's pressure, one wishes to calculate the amount of a gas adsorbed on the surface. One ends with a series of paired data from which the amount adsorbed versus the pressure is extracted from certain physical parameters (Condon, 2006a). Such parameters include a number assuming the surface area and a quantity that is in some way related to the adsorbent's adsorption affinity. Other parameters occasionally found in terms of pore size and volume are porosity (Condon, 2020).

To get both data sets, the volumetric technique uses one measurement form, and is the most low-costly method. However, the price naturally goes up as one wishes to do more sophisticated work. The cost benefit starts to vanish to use it in this mode, and the amount of effort needed to do careful work becomes very high, with several possible pitfalls. The key downside of the volumetric approach is that it is not as suited as the gravimetric technique for careful analysis work (Santamaria et al., 2014). For the pressure change to be minor, the tested adsorbent should be in a tiny amount, therefore the process might be presumed to be isobaric.

The primary disadvantage of this approach is that the testing settings are not representative of the adsorption cooling unit's actual operating conditions (Santamaria et al., 2014). The gravimetric approach, on the other hand, uses mass balances to directly evaluate adsorbent capacity under

precise operating circumstances. The essential advantage of the gravimetric methodology is extremely high exactness and accuracy. As a result, this approach is more suited to determining the adsorption isotherms and the kinetics of working pairs. The theory of the gravimetric approach is more reliable than the volumetric methods (Condon, 2006b; Ramy H. Mohammed et al., 2018).

In the gravimetric perceptive one essentially brings in the pressure of the adsorbate for the gravimetric technique and tests the mass gain of the sample. In relation to the strain, the isotherm is then simply mass gain. The essential advantage of the gravimetric methodology is extremely high exactness and accuracy. A similar benefit is seen in normal gravimetric analytical chemistry (Sapienza et al., 2014). With this strategy, great research centre work and pore investigation can be completed. The technique does not have numerous blunders related with it. The alignment is moderately simple and is minor for routine examination (Condon, 2020; Sapienza et al., 2014).

#### 4.1.2.1. Gravimetric method

Gravimetric techniques include all laboratory tests in which the analysed data is a measurement of weight or a change in mass. Gravimetric analysis is without a doubt the earliest quantitative analytical approach, as mass is the most essential of all quantitative measures. It is still a relatively modern tool for investigating sorption phenomena of gases in porous substances. The method of volatilization gravimetric is used when chemical energy is used to eliminate a volatile species. In determining the moisture content of bread, for example, in this study the thermal energy is used to vaporize the water in the sample (Condon, 2020).

A similar benefit is seen in normal gravimetric analytical chemistry(Sapienza et al., 2014). With this strategy, great research centre work and pore investigation can be completed. The technique does not have numerous blunders related with it. The alignment is moderately simple and is minor for routine examination. In routine mode, the gravimetric technique is commonly quicker than the volumetric strategy, because of less alignments that are required. Test arrangement, degassing, response, and adjustment are simpler, and the mass changes can be continued in a suitable direct way (Condon, 2020; Sapienza et al., 2014).

#### 4.1.2.2.The key distinctions of gravimetric and volumetric method:

- Expense. The gravimetric approach is usually expensive as compared to the volumetric method. Only high precision pressure transducers and high precision volume measurements are required for the volumetric approach. The gravimetric method, on the

other hand, necessitates a high-precision vacuum balance and maybe a significant amount of setup time (Condon, 2020).

- Ability. In general, the gravimetric method is more efficient and precise as compared to volumetric analysis because temperature variations, and calibration mistakes are avoided when using gravimetric analysis (Condon, 2020).

A mathematical model used to assess system performance by solving the capable set of equations from the thermodynamic model. As the literature state that there are many methods to be used to determine the adsorption isotherm, this study is performed using the gravimetric method. One of the reasons for choosing this model over the volumetric, is because in routine mode, the gravimetric method is typically faster than the volumetric method, as it needs less calibration (Condon, 2006). Sample preparation, degassing, reacting, and adjusting are easier and can be done with the mass adjustments in a straightforward manner (Condon, 2006).

It is a very significant benefit, which the volumetric approach does not naturally deliver. The theory of the gravimetric approach is more reliable than the volumetric methods (Mitra et al., 2015), (Ramy H. Mohammed et al., 2018). In the gravimetric perceptive one essentially brings in the pressure of the adsorbate for the gravimetric technique and tests the mass gain of the sample. In relation to the strain, the isotherm is then simply mass gain. However, things are not so easy in the engineering of machinery. Typically, the vacuum system is a traditional metal system, but the balance is a model of very high precision (Condon, 2006).

The essential advantage of the gravimetric methodology is extremely high exactness and accuracy. Out of all the testing methods mentioned here, the literature state that the gravimetric method is the most efficient and superior to the volumetric method. That knowledge alone influenced this study's decision to use the gravimetric approach to develop a tiny adsorption chiller. A chiller that is not only limited in using vacuum-swing adsorption (VSA) like the large plant. With this method, high-quality laboratory work and pore analysis can be carried out. The method does not have many errors associated with it (Kaiser, 1970).

## 4.2. Material and system design

The small and easy to operate adsorption chillers are very limited, a simple but precise experimental apparatus is designed and built to assess the equilibrium uptake of each working pair under all operating conditions. This lab scale is intended for testing advanced, non-commercial adsorption materials that are currently unavailable in large numbers on a small scale. The operating concept of this small single bed desalination is to assess the adsorption isotherm,

kinetics of any working pairs, investigating the performance of an adsorption cooling bed under distinctive adsorption cooling cycle circumstances.

A heat resisting tape is wrapped around the cylinders to control the heat transfer. Variety of thermocouple sensors are connected to the temperature determined at various positions in the test rig. The adsorber/adsorbent bed is the most particular significance from the three columns (adsorber, evaporator, and condenser) utilized in adsorption cooling/heating systems, whereas the others are identical to typical adsorption systems. At the bottom of the built heat exchanger, there is a load cell transducer mounted. It transforms a force to an observable and standardized electrical signal, such as friction, compression, strain, or torque.

The key innovation of this system is to test the adsorbents' ability to adsorb and control the adsorption cycle by means of dynamic weight measurements rather than volumetric ones. A clear view of a pictorial structure in Figure 4.1 shows the adsorption/desorption process operated in the lab. The chamber 2 in Figure 4.1 is the main focus of the system, that is where the adsorbents are placed at. The steam produced by the evaporator get to be adsorbed by the adsorbent and the adsorbed quantity is measured by the calibrated load cell, before it goes to the condensation stage.

The vapour mixture obtained by adsorbents in reactor bed leaves at the top of the evaporator into a heat exchanger. When the gas reaches the heat exchanger, the adsorbents readily adsorb the vapour, depending on their affinity strength. The adsorbents are packed well in between the tube fins that circulate hot and cold water. The main function of the refrigeration coolant was to cool the adsorbent until they reach the saturation point. The cool water from the refrigerant actually stimulate the adsorbent to be more hydrophilic. Once the adsorbent reach the saturation point, start to adsorb the vapour from the evaporator.

The steam is adsorbed for a certain period and that process is called adsorption process. The hot water from water bath released to circulate around the adsorbents. The hot water assists the adsorbents to regenerate the steam adsorb after adsorption. The adsorption affinity of the adsorbent used is shown on the data logger represented on the testing rig in Figure 4.1. The low-grade heat triggers the endothermic process of desorption during this period. In the condenser, the desorbed refrigerant vapour condensed and cooled through the heat sink. Vacuum pump utilized for vapour departure reason.

A reading rag (0-100 KPa) pressure sensor is used. A variety of thermocouple sensors are connected to the temperature determined at various positions in the test ring. Every second,

temperature sensors and pressure transmitters coupled to a data logger capture the data. The isotherms and kinetics of the various adsorbents utilized were measured throughout a temperature range. Figure 4.2 shows the Carnot cycle explaining more about reactor bed. The heat exchanger adsorption is located and connected to the hydraulic heating/cooling system and the supporting gravimetric weighing unit.

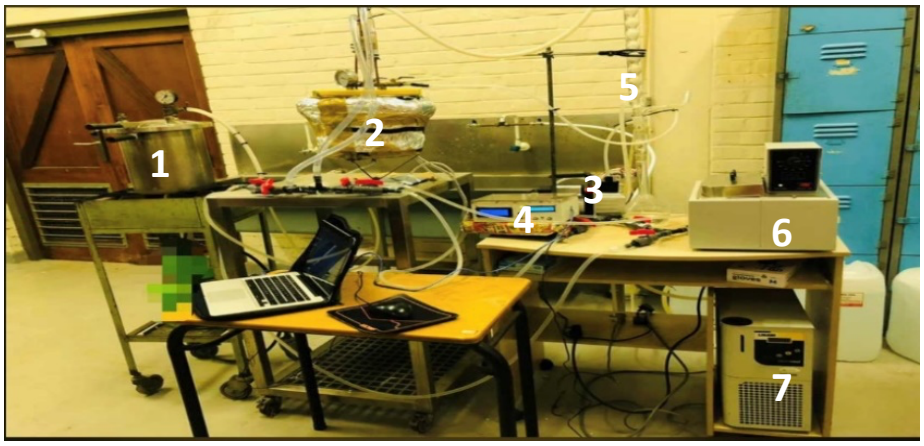


Figure 4.1: Pictorial diagram of the system

The numerical values on Figure 4.1 represent the following:

1) Evaporator
2) Adsorber
3) Vacuum pump
4) Data logger
5) Condenser
6) Water bath
7) Cooling refrigerant

**Carnot cycle**

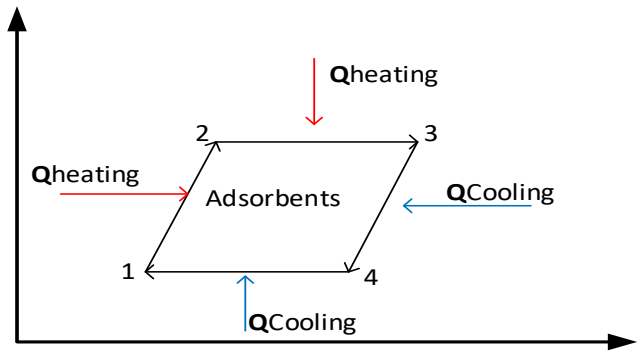


Figure 4.2: Carnot cycle based on a reactor bed

**Pre-heating process (1-2**): The valves between the adsorbent bed and the condenser and evaporator (V1 and V2) are shut during this heating and saturation time, and the adsorbent bed is managed as a closed framework subject to heat source at $T_H$ temperature using heat transfer fluid heating methods. Meanwhile, the bed temperature has expanded delicately, which additionally builds the vapour pressure inside the bed. Although at the most elevated concentration, the aggregate sum of refrigerant in the adsorbed cycle stays consistent. This cycle proceeds until the condenser pressure at point 2 surpasses the vapour pressure.

**Desorption Process (2-3):** The heating of the adsorbent bed proceeded after the first stage, and the valve (V2) linking the bed to the condenser was opened. The temperature of the bed is gradually raised, allowing a part of the adsorbed refrigerant to leave the solid surface of the adsorbent in a process known as 'desorption.' The desorbed vapour then goes into the condenser, where it condenses. When the adsorbed amount reaches the lowest concentration limit, the vapour pressure in the treated bed equals the condenser pressure.

**Pre-cooling process (3-4):** The refrigeration and depressurization time for the bed is monitored once the bed achieves the maximum temperature in the procedure at point 3, and the two valves (V1 and V2) are closed. The temperature was then reduced, enabling the pressure within the adsorber to drop to evaporator pressure at the end of the procedure.

**Adsorption process (4-1):** In the last cycle of successful cooling, the valve between the adsorber and the evaporator is opened, and the adsorber is continuously cooled by the fluid flow cooling, causing an adsorptive vapor to collect on the adsorbent surface and converted into a new phase called 'adsorbed phase' in a process called adsorption. Instead, the adsorber is directed through the adsorptive vapor by the evaporator's evaporated vapor, which provides the cooling effect. The adsorbent bed in this process must be cooled in order to remove the heat generated by both the heating cycle and the adsorption process.

### 4.3. Designed electronic weighing scale control part

As stated in the introduction, there are a variety of ways for assessing adsorbent absorption in the adsorption process. However, there are principally two methods (Volumetric and Gravimetric method) widely used to determine surface area by physisorption. This study is specifically conducted using the gravimetric system, which gives results through weighing pressure of the adsorbate and measures the mass gain of the sample. Therefore, a weighing scale, temperature reading, and the pressure reading were a need in the designed system, because the measurements are mostly conducted inside the reactor bed.

The scale is built and placed inside the vacuumed adsorber (reactor bed) chamber. This electronic weighing scale system is divided into two parts of development; hardware, and software. The block diagram in Figure 4.3 shows the stages followed when designing the electronic weighing scale, and how the components were interface. The Arduino is programmed according to the flowchart of the system shown in Figure 4.4. When the electronic weighing scale switched on, it firstly initialize the load cell values and that takes about 45 seconds as shown in Figure 4.4 the HX711 receive signals from the load cell and amplified it.

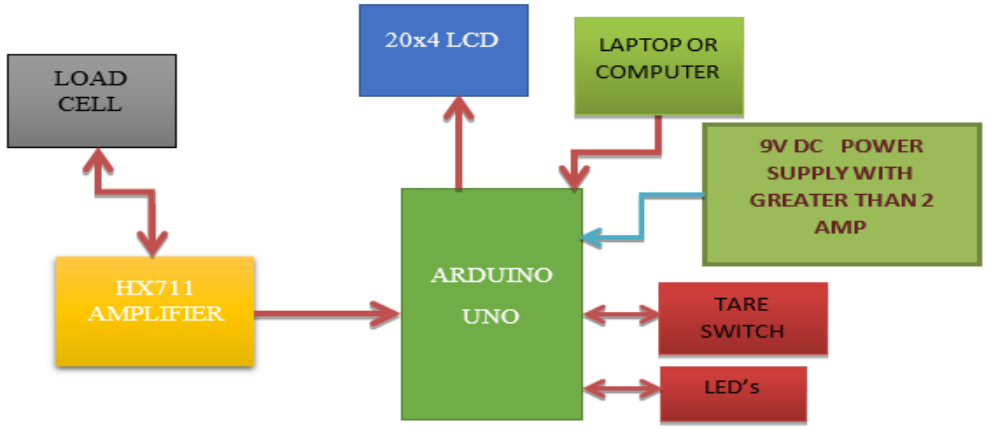


Figure 4.3: Block diagram of the electronic weighing scale

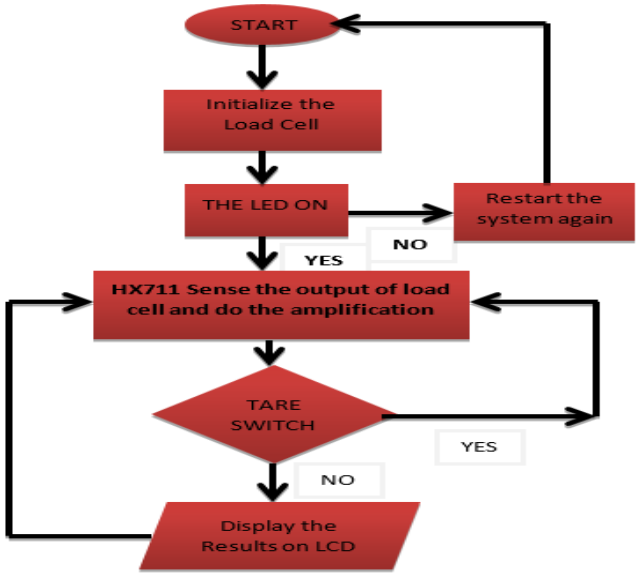


Figure 4.4: Flowchart of software for electronic weighing scale

## 4.4. Hardware development modules

The mechatronics hardware component used in building the rig to desalinate the water; load cell, Wheatstone bridge, microcontroller, HX711 amplifier, Arduino Uno, and light-emitting diode LED. A "load cell" is the main component of an electronic weighing scale system (Osman et al., 2013). The millivolts output of the load cell processed when the weight placed on top of it. The HX711 amplifier, it amplifies the millivolts' output and connect it to the microcontroller's input. The Arduino Uno runs the program according to the code, and the results of the microcontroller's output. It then displayed on the LCD as results of what has been weighed. Figure 4.5 shows the process.

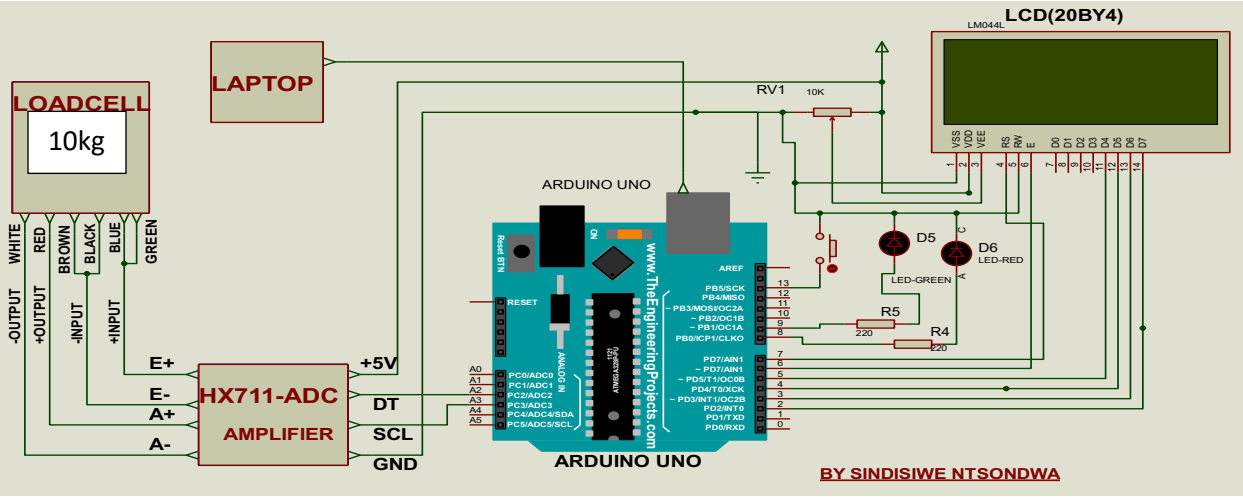


Figure 4.5: Simulation of all components using proteus

### 4.4.1. Load cell

A load cell converts a quantifiable and standardized electrical signal from a force such as tension, compression, pressure, or torque. The electrical signal varies in response to the strain on the load cell. The most often used load cells are strain gauges, pneumatic load cells, and hydraulic load cells. This load cell is installed at the bottom of the heat exchanger as designed. The load cell used utilizes a set of four strain gauges, the combination of which results in a Wheatstone bridge circuit application. A strain gauge is a device that measures the amount of strain on an object (Osman et al., 2013; Shen et al., 2017).

### 4.4.2. Microcontroller and Arduino Uno

A microcontroller is a single-chip computer with programmable input/output peripherals, memory, and a CPU core. It is important because a microcontroller contains the processor and memory, as well as some controllable input/output pins. These output/input pins are called GPIO (General Purpose Input Output Pins). An open-source Arduino board with 14 GPIO is used in this setup.

There are several types of Arduino boards in the market, and each has its own advantageous features in it. However, this system used Arduino Uno. The Arduino Uno is the central unit of the electronic weighing scale system.

The entire components are interfaced on the board and programmed as per their functionality to operate in synchronization, monitor, and control the other functional parts of the system. The ATmega328-based Arduino Uno is a microcontroller board. ATmega has a 20 MHz speed, a power supply range of 1.8-5.5, an operational temperature range of -40°C to 85°C, 32KB Flash, 1KB EEPROM, and 2KB RAM. The Arduino contains 14 digital I/O pins (six of which are PWM outputs), 6 analog inputs, a 16 MHz crystal oscillator, a USB connection, a power connector, an ICSP header, and a reset button.

It comes with everything needed to get started with the microcontroller; the only thing needs to be done is plugging it into a computer through USB or power it with an AC-to-DC converter or battery. The Uno is different from prior boards in that it does not use the FTDI USB-to-serial driver chip. Instead, an Atmega8U2 has been programmed to function as a USB-to-serial converter. (Cameron, 2019).The Arduino Uno features a voltage regulator (LM7805) which is built-in that converts 9V/12V DC to 5V DC. A Wheatstone bridge used in this system, to determine the unknown resistance value of the resistors instead of a voltage divider.

### 4.4.3. Wheatstone bridge

5.4.3. In other terms, a Wheatstone bridge is a design of four balanced resistors with a known excitation voltage applied, as shown in Figure 4.6 (Vordos et al., 2020). Although the excitation voltage Vex is constant, the output voltage Vout varies based on the strain gauge shape. If all resistors in Equation 4.1 are balanced, Vout is zero. Vout will vary if the resistance of any of the resistors changes. The change in Vout may be measured and interpreted using Ohm's law. Vout is completely reliant on resistance.

$$R_1/R_2 = R_4/R_3 \quad (4.1)$$

The current measured in amperes flowing through a wire between two places is proportional to the voltage across the two points, according to Ohm's law (Cameron, 2019). In this connection, resistance (measured in ohms) is added as an independent constant. Equation 2 expresses Ohm's law, but when applied to the four legs of the Wheatstone bridge circuit, Equation 3 results (Vordos et al., 2020; Shen et al., 2017). When force is applied to the load cell and $V_{OUT}$ is measured, the structure and resistance of the strain gauges change. $V_{OUT}$ may be simply determined from the collected data using equation 3 (Yan et al., 2018).

$$I = V/R \tag{4.2}$$

$$V_{out} = (R_3/R_3 + R_4 - R_2/R_1 + R_2)V_{EX} \tag{4.3}$$

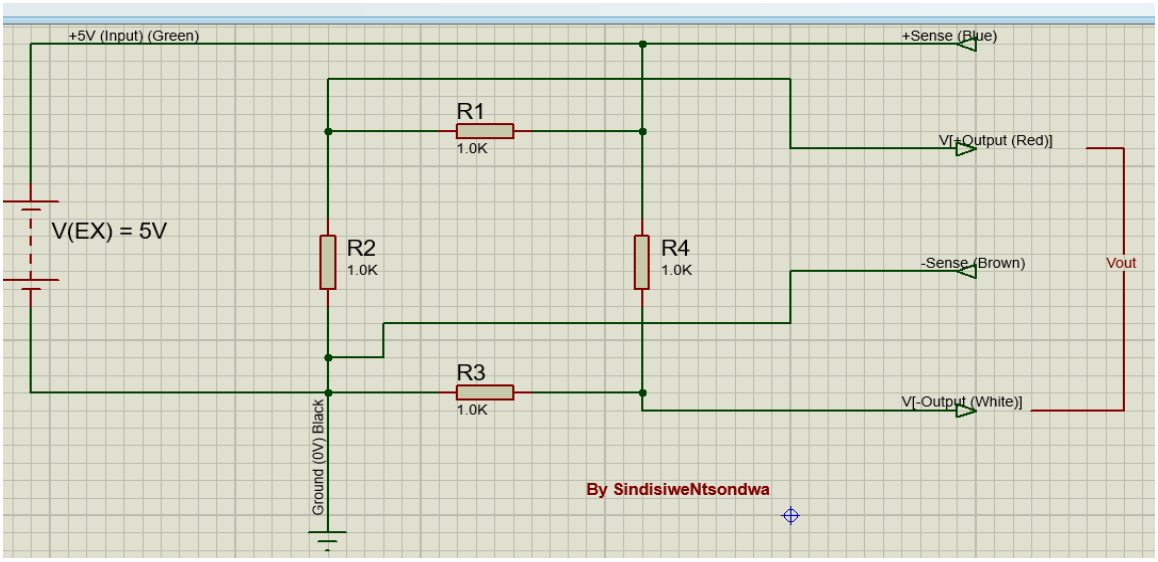


Figure 4.6: Load cell bridge

### 4.4.4. HX711 Amplifier

The HX711 amplifier is an electronic scale module that converts measured changes in resistance value changes into electrical output via a conversion circuit (Wyma, 2020a). The load cell Amplifier is a tiny breakout board for the HX711 IC that allows load cells weight measurement readable. Calibration assists in finding an accurate weight measurement by connecting the amplifier to an Arduino Uno and reading the changes in the resistance output of the scale. Load cells connect to the HX711 via a four-wire Wheatstone bridge configuration, and the HX711 communicates with the Arduino Uno via a two-wire (Clock and Data) interface (Wyma, 2020b).

### 4.4.5. Laptop and LCD

The LCD is used to indicate how much is the weight adsorbed by adsorbents during adsorption and the results detected by the load cell. Figure 4.7 portrays a 20x4 LCD, which is a 20 character by 4-line display with white text on a blue background and two registers, Command and Data. It is also fully compatible with the Arduino Liquid Crystal library, as it has a 16-pin to be an interface to the Arduino Uno (Cameron, 2019). It is open-source software, and once the software has been successfully installed, you can program the code according to the project specifications (Cameron, 2019).

The communication between the Laptop and the Arduino Uno is accomplished via a USB cable, as shown in Figure 4.1. The C++ programming language is used to program the Arduino. C++ provides programmers with extensive control over system resources and memory. It is not always necessary to connect the laptop more especially if the process of uploading the code to the Arduino Uno is completed, the external power supply can be used (Halvorsen, 2018). This process powered by a 230V AC power source converted to a 9 Volt/12 Volt DC power source supplied by a current of at least 2A.

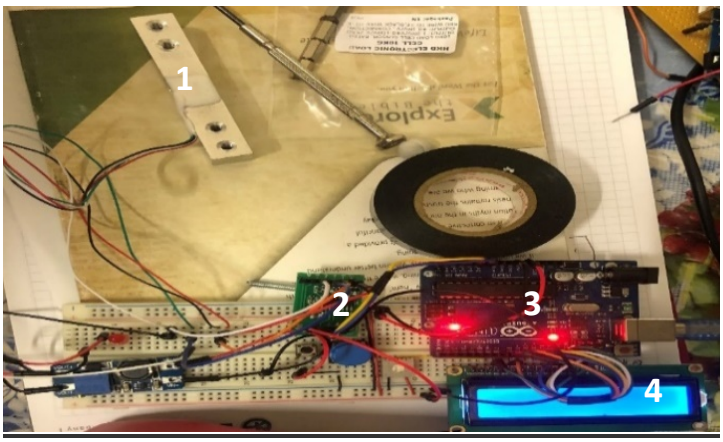


Figure 4.7: Pictorial structure of the mechatronics used

The indicated numbers on the on Figure 4.7 represent the following:

1. Load cell
2. Hx711
3. Arduino and
4. LCD

## 4.5. Designing and simulating in a computer

At the beginning of building the circuit on the software, the necessary calculation were conducted according to the design specifications. Equation 4 calculates the expected maximum power in watts for the entire project. A light-emitting diode (LED) is a two-lead semiconductor light source. When a sufficient current is delivered to the leads, electrons within the device can recombine with electron holes, emitting energy in the form of photons, as illustrated in Figure 4.3. Figure 4.8 shows the schematic of the LED circuit (Halvorsen, 2018). The datasheet of a light-emitting diode LED current used is:

$I_{R(LED)} = 0.02A$

Measured voltage across the LED $V_{F(LED)} = 1.91\ V.$

Therefore, the value of the current limiting resistor used to protect LED is calculated using the KVL law as shown in equation 4.5.

$$P = V \times I \tag{4.4}$$

$$R_{\Omega} = \left(V_{CC} - V_{F(LED)}\right)/I_R \tag{4.5}$$

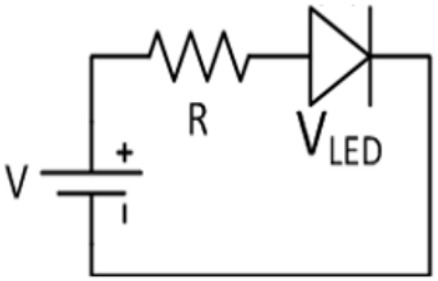


Figure 4. 8: schematic diagram of the LED

### 4.5.1. EasyEDA and Proteus Software

The values of the components have been selected. The simulation performed before the prototype of this was built on the breadboard so that it can carry on interfacing it with the power plant process. Simulation of this project conducted using the following electronic software on the computer Arduino Software (IDE), EasyEDA, and Proteus software. Tools that were also used are the multimeter and logic probe. Figure 4.5 shows the complete simulated circuit.The Proteus design package is a proprietary software tool suitable for open-source offline software and that is mostly used for electronic design automation.

The program is used by electronic design specialists and technicians to create schematics and electronic prints for printed circuit board manufacturing. EasyEDA is a web-based EDA tool suite that allows hardware engineers to create, simulate, trade, and discuss schematics, simulations, and printed circuit boards in a public or private environment. EasyEDA is likewise free and open-source, however, it is online software (Nasir, 2020; Bindu, 2019). The designed scale will be able to test sophisticated, non-commercial adsorption materials that are not currently accessible in the big quantities on a modest scale.

### 4.5.2. Arduino software (IDE)

The produced code for this system was created using an open-source Arduino software integrated development environment (IDE) to code the gravimetric method's parameters. The code created uploaded into the board and is simplified to be compatible with Windows, Mac OS X, and Linux. The Arduino code is written in C++ and includes several unique methods and functions. C++ is an easy-to-understand programming language. This Arduino software integrated development

environment (IDE) code is used for a precision scale with a 10 kg load cell, HX711 ADC and mode selector to write and run the code on a computer.

Due to the limited amount of small lab adsorption desalination chiller, a small suitable testing rig built in a manner that will be able to conform with the objectives of this study. All the components mentioned above are related to a major goal of building an adsorbent chiller that will be able to read the amount of adsorbate adsorbed by the hydrophilic adsorbent inside the adsorption chiller. A chiller that will not condensate during the regeneration process. Hopefully this idea of small scale will assist other upcoming researchers who are interested in the adsorption desalination study but do not afford the fancy equipment to conduct the results.

## 4.6. Results and discussion

This section gives a full account of the experimental results carried out to determine the feasibility of the designed adsorption desalination chiller. The experiment performed using silica gel as an adsorbent. To examine the performance of adsorbent material, the impact of cycle time, hot, cold, and chilled water temperature considered as well as adsorption isotherms, cycle performance, coefficient of performance (COP) and adsorption energy are also required. Adsorption isotherms speak to the extreme measure of adsorbate adsorbed per unit mass of dry material at a particular pressure.

An adsorption chiller that runs hot water for desorption process under the temperature lower than 90°C using the mass recovery technique is designed, and experimentally examined. The major goal was to design a lab small chiller to produce desalinated water without condensing during the regenerating process. All column serves a vital purpose, which is why it is critical to verify each one to ensure that it is appropriate for use, and it performs at its best. The key benefit of this process is the ability to evaluate the adsorption dynamics of various adsorber configurations by simulating operating conditions and finding the water production.

Like any other system designed, it is a must to test its performance before it can be used. The first test made in this chiller was to check if the adsorbents can adsorb steam for a period without the steam changing phase during adsorption phase. Figure 4.9 demonstrates the results found in the first attempt using adsorption as a function of time. The results revealed that the rate of vapour adsorbed on silica gel was rapidly moving at first, then steadily increased until equilibrium was reached, and then the predicted equilibrium was achieved at 1200 s. The most important point is that there was a volume produced and there was a successful adsorption attempt.

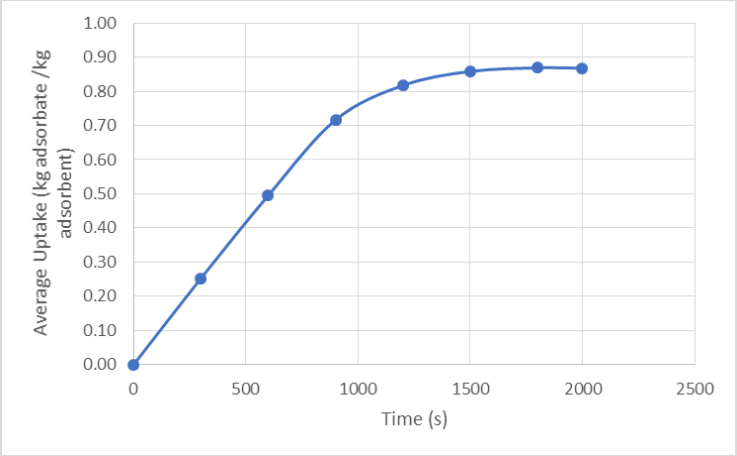


Figure 4.9: Vapour average uptake vs. time

The increase in the average uptake in Figure 4.9 shows that the system can produce the condensate and, therefore, can be used on adsorption chiller purposes. The equilibrium state for this test was found to be at 1200 s. To avoid inaccuracies, each test is performed several times to ensure that the experimental set-up is repeatable and that repeated measurements for the same operating circumstances are accurate. Throughout several runs of experiments conducted. It has been observed that the amount or the quantity of adsorbents used contributes to the effects of the adsorption chiller.

In the process of testing the designed testing rig, the performance of coefficient (COP) was analysed as well. The COP is the ratio of provided energy to energy input to the cycle during the desorption stage. The undermentioned assumptions were utilized in this model: The adsorbent bed has no inert material, the adsorbed refrigerant is considered as a liquid for detailed heat capacity calculations, and the refrigerant leaves the condenser and evaporator saturated. A mathematical model for measuring system performance by solving the thermodynamic model's feasible formula.

The mathematical modelling was built on the following assumptions (Raj & Baiju, 2019) (Seol et al., 2020):

- A vapour is an ideal gas.
- Radiation heat transport is not taken into account.
- In all operations, evaporators and condensers are excellent.
- The adsorbent particles are all uniformly sized and porosity spherical particles.
- Thermal equilibrium is postulated between the adsorption bed and the vapor.
- For calculations of specific heat capacity, the adsorbed refrigerant is regarded as a liquid.

The energy required to remove the vapour from adsorbents (Thu et al., 2013):

$$Q_{des} = M_{hw} C_{phw} T_{hw} \left(T_{h,in} - T_{hw,out}\right) \quad (4.6)$$

$$Q_{eva} = m_{ev} C_{p,eva} T_{eva} \left(T_{chilled,in} - T_{chilled,out}\right) \quad (4.7)$$

$$Q_{cond} = m_{cond} C_{pcw} T_{cond} \left(T_{cond,in} - T_{cond,out}\right) \quad (4.8)$$

$$COP = 1/t_{cycle} \int_0^{t_{cycle}} (Q_{evaLP} + Q_{evaHP})/Q_{des} \quad (4.9)$$

$$SDWP = n \int_0^{t_{cycle}} \left(m_{water}/M_{sg}\right) dt \quad (4.10)$$

- Where m is the flow rate for (hot water, condenser and cool water)
- $C_p$ is a specific capacity
- Temperature of water, respectively
- LP and HP is low pressure and high pressure
- $M_{sg}$ is the total mass of adsorbent in the reactor bed
- n is the total number of cycle per day
- t is the period of a cycle

The AD cycle's performance is shown in Figure 4.10 and Figure 4.11 in terms of important metrics such as specific daily water production (SDWP) and performance coefficient (COP) for various heat source inlet temperatures. It should be mentioned that all of the results were obtained under cyclic-steady state settings. The SDWP and COP were computed from experimental data under steady state settings as a function of cycle time and driving heat source temperature, as illustrated in equations 4.9 and 4.10. The stepwise-linear fin height resulted in significant gains in COP and SDWP. The graph also shows that the COP increases with pressure.

In Figure 4.10, the COP with 2 kPa pressure is 20% higher than 1.6 kPa pressure, and 1.6 kPa pressure is 31% higher than the 1.3 kPa pressure. Multi-module integration is always necessary from a system standpoint to match the cooling capacity. By simply implementing varied fin heights for each module based on its location in the module integration, COP and SDWP were significantly improved. Figure 4.10 of SDWP shows that 2kPa pressure is 55% higher than 1.6 kPa pressure, and 1.6 kPa pressure is 68% higher than the 1.3 kPa. This research provided a system-level technique and demonstrated a measurable amount of improvement. According to the graph, the COP grows steadily over time with half cycle time.

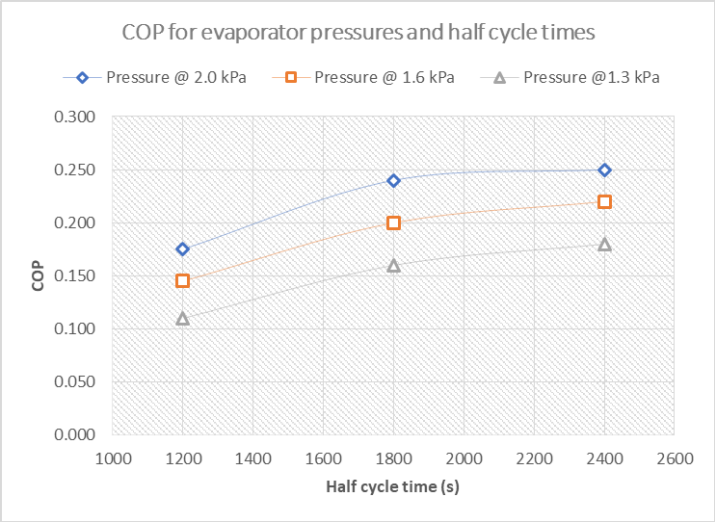


Figure 4.10: COP for evaporator pressure half cycle time

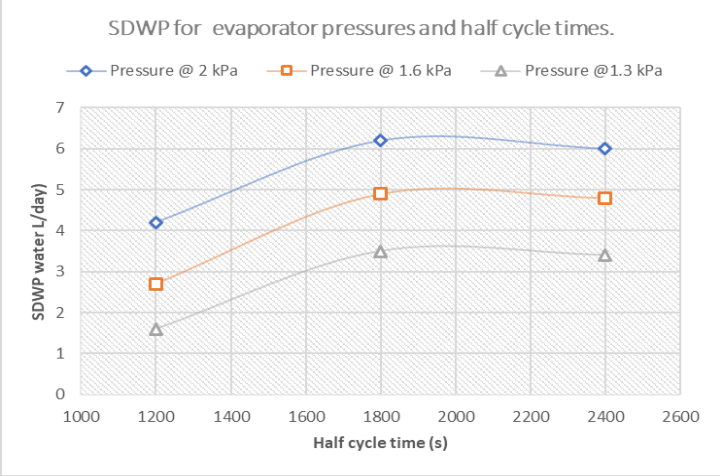


Figure 4.11: COP for evaporator pressure half cycle time

## 4.7. Conclusion

The goal of this work is to create a compact, inexpensive adsorption chiller for the academic institution labs that cannot currently afford the gravimetric method. A small lab scale is designed to improve the adsorption desalination study. Its performance tested and it works so well. The coefficient of performance (COP) and specific daily water (SDWP) output are used to evaluate the cycle's performance. The design operated using the following parameters: pressure at 2 kPa, half cycle for adsorption at 1800 s and adsorbents mass as low as 2.5 kg. It has been noticed that the mass has a major role on the adsorption results. When there is a high quantity of mass, the half cycle increases as well.

## 4.8. References


Abdulsalam, J., Mulopo, J., Bada, S.O. & Oboirien, B. 2020. Equilibria and Isosteric Heat of Adsorption of Methane on Activated Carbons Derived from South African Coal Discards. *ACS Omega*, 5(50): 32530–32539.

Al-Jabari, M. 2016. Kinetic models for adsorption on mineral particles comparison between Langmuir kinetics and mass transfer. *Environmental Technology and Innovation*, 6: 27–37. http://dx.doi.org/10.1016/j.eti.2016.04.005.

Alnajdi, O., Wu, Y. & Calautit, J.K. 2020. Toward a Sustainable Decentralized Water Supply : Review of Adsorption Desorption Desalination ( ADD ) and Current Technologies : Saudi Arabia ( SA ). : 1–30.

Alsaman, A.S., Askalany, A.A., Harby, K. & Ahmed, M.S. 2017. Performance evaluation of a solar-driven adsorption desalination-cooling system. *Energy*, 128: 196–207. http://dx.doi.org/10.1016/j.energy.2017.04.010.

Ambarita, H. & Kawai, H. 2016. Experimental study on solar-powered adsorption refrigeration cycle with activated alumina and activated carbon as adsorbent. *Case Studies in Thermal Engineering*, 7: 36–46. http://dx.doi.org/10.1016/j.csite.2016.01.006.

Aristov, Y.I. 2012. Adsorptive transformation of heat: Principles of construction of adsorbents database. *Applied Thermal Engineering*, 42: 18–24.

Bakhtyari, A. & Mofarahi, M. 2019. A New Approach in Predicting Gas Adsorption Isotherms and Isosteric Heats Based on Two-Dimensional Equations of State. *Arabian Journal for Science and Engineering*, 44(6): 5513–5526. https://doi.org/10.1007/s13369-019-03838-2.

Barbosa, G.D., Bara, J.E., Weinman, S.T. & Turner, C.H. 2022. Molecular aspects of temperature swing solvent extraction for brine desalination using imidazole-based solvents. *Chemical Engineering Science*, 247: 116866. https://doi.org/10.1016/j.ces.2021.116866.

Bindu, B. 2019. Getting Started with EasyEDA an Online PCB Design Software | StudentCompanion.

Builes, S., Sandler, S.I. & Xiong, R. 2013. Isosteric heats of gas and liquid adsorption. *Langmuir*, 29(33): 10416–10422.

Bundschuh, J., Ghaffour, N., Mahmoudi, H., Goosen, M., Mushtaq, S. & Hoinkis, J. 2015. Low-cost low-enthalpy geothermal heat for freshwater production: Innovative applications using thermal desalination processes. *Renewable and Sustainable Energy Reviews*, 43: 196–

206. http://dx.doi.org/10.1016/j.rser.2014.10.102.

Cameron, N. 2019. *Arduino Applied:Comprehensive Projects for Everyday Electronics*.

Chakraborty, A., Saha, B.B., Koyama, S. & Ng, K.C. 2006. On the thermodynamic modeling of the isosteric heat of adsorption and comparison with experiments. *Applied Physics Letters*, 89(17): 2004–2007.

Chen, X., Boo, C. & Yip, N.Y. 2020. Transport and structural properties of osmotic membranes in high-salinity desalination using cascading osmotically mediated reverse osmosis. *Desalination*, 479(January): 114335. https://doi.org/10.1016/j.desal.2020.114335.

Chiou, C.T. 2002. *OF ORGANIC CONTAMINANTS IN ENVIRONMENTAL SYSTEMS PARTITION AND ADSORPTION OF ORGANIC CONTAMINANTS*. John Wiley & Sons, Inc.

Choi, O.K., Seo, J.H., Kim, G.S., Hendren, Z., Kim, G.D., Kim, D. & Lee, J.W. 2021. Non-membrane solvent extraction desalination (SED) technology using solubility-switchable amine. *Journal of Hazardous Materials*, 403(April 2020): 123636. https://doi.org/10.1016/j.jhazmat.2020.123636.

Condon, J.B. 2006a. Heat of Adsorption - an overview | ScienceDirect Topics. *Elsevier*. https://www.sciencedirect.com/topics/chemistry/heat-of-adsorption 22 October 2021.

Condon, J.B. 2020. *Measuring the physisorption isotherm*.

Condon, J.B. 2006b. *Surface Area and Porosity Determinations by Physisorption Measurements and Theory*. 1st ed. Elsevier B.V.

Distribution, W., Moisture, S. & Ice, G. 2020. What is the big deal? *SPC Water, Sanitation and Hygen: Water distribution*, 2: 2–3.

Gabelman, A. 2017. Adsorption basics: Part 2. *Chemical Engineering Progress*, 113(8): 1–6.

Gediz Ilis, G., Demir, H., Mobedi, M. & Baran Saha, B. 2019. A new adsorbent bed design: Optimization of geometric parameters and metal additive for the performance improvement. *Applied Thermal Engineering*, 162(July): 114270. https://doi.org/10.1016/j.applthermaleng.2019.114270.

Giraldo, L., Rodriguez-Estupiñán, P. & Moreno-Piraján, J.C. 2019. Isosteric heat: Comparative study between Clausius-Clapeyron, CSK and adsorption calorimetry methods. *Processes*, 7(4).

Grande, C.A. 2012. Advances in Pressure Swing Adsorption for Gas Separation. , 2012: 100–102.

Gude, V.G. 2018. Exergy Evaluation of Desalination Processes.

Guo, J., Tucker, Z.D., Wang, Y., Ashfeld, B.L. & Luo, T. 2021. Ionic liquid enables highly efficient low temperature desalination by directional solvent extraction. *Nature Communications*, 12(1): 1–7. http://dx.doi.org/10.1038/s41467-020-20706-y.

Halvorsen, H.-P. 2018. *Programming With Arduino*. 978-82-691106.

Israelachvili, J.N. 2011. *Intermolecular and surface forces*. 3rd ed. Elisvier.

Kaiser, R. 1970. *Carbon molecular sieve*.

Khalil, A., El-Agouz, E.S.A., El-Samadony, Y.A.F. & Sharaf, M.A. 2016. Experimental study of silica gel/water adsorption cooling system using a modified adsorption bed. *Science and Technology for the Built Environment*, 22(1): 41–49.

Khanam, M., Jribi, S., Miyazaki, T., Saha, B.B. & Koyama, S. 2018. Numerical investigation of small-scale adsorption cooling system performance employing activated carbon-ethanol pair. *Energies*, 11(6).

Li, A., Thu, K., Ismail, A. Bin, Shahzad, M.W. & Ng, K.C. 2016. Performance of adsorbent-embedded heat exchangers using binder-coating method. *International Journal of Heat and Mass Transfer*, 92: 149–157. http://dx.doi.org/10.1016/j.ijheatmasstransfer.2015.08.097.

Loh, W.S., Rahman, K.A., Chakraborty, A., Saha, B.B., Choo, Y.S., Khoo, B.C. & Ng, K.C. 2010. Improved isotherm data for adsorption of methane on activated carbons. *Journal of Chemical and Engineering Data*, 55(8): 2840–2847.

Mancosu, N., Snyder, R.L., Kyriakakis, G. & Spano, D. 2015. Water scarcity and future challenges for food production. *Water (Switzerland)*, 7(3): 975–992.

Mitra, S., Kumar, P., Srinivasan, K. & Dutta, P. 2015. Performance evaluation of a two-stage silica gel + water adsorption based cooling-cum-desalination system. *International Journal of Refrigeration*, 58: 186–198.

Mitra, S., Thu, K., Saha, B.B., Srinivasan, K. & Dutta, P. 2017. Modeling study of two-stage, multi-bed air cooled silica gel + water adsorption cooling cum desalination system. *Applied Thermal Engineering*, 114: 704–712. http://dx.doi.org/10.1016/j.applthermaleng.2016.12.011.

Mohammed, R.H., Mesalhy, O., Elsayed, M.L. & Chow, L.C. 2019. Assessment of numerical models in the evaluation of adsorption cooling system performance. *International Journal of Refrigeration*, 99: 166–175. https://doi.org/10.1016/j.ijrefrig.2018.12.017.

Mohammed, Ramy H., Mesalhy, O., Elsayed, M.L., Hou, S., Su, M. & Chow, L.C. 2018. Physical properties and adsorption kinetics of silica-gel/water for adsorption chillers. *Applied Thermal Engineering*, 137(March): 368–376. https://doi.org/10.1016/j.applthermaleng.2018.03.088.

Mohammed, Ramy H, Mesalhy, O., Elsayed, M.L., Su, M. & Chow, L.C. 2018. Revisiting the adsorption equilibrium equations of silica-gel/water for adsorption cooling applications. *International Journal of Refrigeration*, 86: 40–47. https://doi.org/10.1016/j.ijrefrig.2017.10.038.

Mondal, P. & George, S. 2015. A review on adsorbents used for defluoridation of drinking water. *Reviews in Environmental Science and Biotechnology*, 14(2): 195–210. http://dx.doi.org/10.1007/s11157-014-9356-0.

Moshoeshoe, M., Silas Nadiye-Tabbiruka, M. & Obuseng, V. 2017. A Review of the Chemistry, Structure, Properties and Applications of Zeolites. *American Journal of Materials Science*, 2017(5): 196–221. http://journal.sapub.org/materials.

Nasir, S.Z. 2020. Introduction to Proteus - The Engineering Projects. *TheEngineeringProjects*.

Ng, K.C., Burhan, M., Shahzad, M.W. & Ismail, A. Bin. 2017. A Universal Isotherm Model to Capture Adsorption Uptake and Energy Distribution of Porous Heterogeneous Surface. *Scientific Reports*, 7(1): 1–11. http://dx.doi.org/10.1038/s41598-017-11156-6.

Ng, K.C., Chua, H.T., Chung, C.Y., Loke, C.H., Kashiwagi, T., Akisawa, A. & Saha, B.B. 2001. Experimental investigation of the silica gel-water adsorption isotherm characteristics. *Applied Thermal Engineering*, 21: 1631–1642. www.elsevier.com/locate/apthermeng.

Ng, K.C., Thu, K., Kim, Y., Chakraborty, A. & Amy, G. 2013. Adsorption desalination: An emerging low-cost thermal desalination method. *Desalination*, 308: 161–179. http://dx.doi.org/10.1016/j.desal.2012.07.030.

Nuhnen, A. & Janiak, C. 2020. A practical guide to calculate the isosteric heat/enthalpy of adsorption: Via adsorption isotherms in metal-organic frameworks, MOFs. *Dalton Transactions*, 49(30): 10295–10307.

Olkis, C., Brandani, S. & Santori, G. 2019a. A small-scale adsorption desalinator. *Energy*

*Procedia*, 158: 1425–1430. https://doi.org/10.1016/j.egypro.2019.01.345.

Olkis, C., Brandani, S. & Santori, G. 2019b. Cycle and performance analysis of a small-scale adsorption heat transformer for desalination and cooling applications. *Chemical Engineering Journal*, 378(April): 122104. https://doi.org/10.1016/j.cej.2019.122104.

Osman, S.M., Hasan, E.H., El-Hakeem, H.M., Rashad, R.M. & Kouta, F. 2013. Conceptual design of multi-capacity load cell. , 03002: 03002.

Qasem, N.A.A. & Zubair, S.M. 2019. Performance evaluation of a novel hybrid humidification-dehumidification (air-heated) system with an adsorption desalination system. *Desalination*, 461(March): 37–54. https://doi.org/10.1016/j.desal.2019.03.011.

Rahimi, B. & Chua, H.T. 2017. *Low Grade Heat Driven Multi-Effect Distillation and Desalination*. 1st ed. Elsivier Inc.

Raj, R. & Baiju, V. 2019. Thermodynamic analysis of a solar powered adsorption cooling and desalination system. *Energy Procedia*, 158: 885–891. https://doi.org/10.1016/j.egypro.2019.01.226.

Raluy, G., Serra, L. & Uche, J. 2006. Life cycle assessment of MSF, MED and RO desalination technologies. *Energy*, 31(13): 2361–2372.

Rautenbach, R., Linn, T. & Eilers, L. 2000. Treatment of severely contaminated waste water by a combination of RO, high-pressure RO and NF - Potential and limits of the process. *Journal of Membrane Science*, 174(2): 231–241.

Rezk, A. 2012. Theoretical and experimental investigation of silica gel/water adsorption refrigeration systems. *Doctor of Philosophy*, 1: 2017.

Riffel, D.B., Wittstadt, U., Schmidt, F.P., Núñez, T., Belo, F.A., Leite, A.P.F. & Ziegler, F. 2010. Transient modeling of an adsorber using finned-tube heat exchanger. *International Journal of Heat and Mass Transfer*, 53(7–8): 1473–1482. http://dx.doi.org/10.1016/j.ijheatmasstransfer.2009.12.001.

Rouquerol, F., Rouquerol, J., Sing, K.S.W., Llewellyn, P. & Maurin, G. 2014. *Adsorption by Powders and Porous Solids Principles, Methodology and Applications*. 2nd ed.

Sah, R.P., Choudhury, B. & Das, R.K. 2015. A review on adsorption cooling systems with silica gel and carbon as adsorbents. *Renewable and Sustainable Energy Reviews*, 45: 123–134. http://dx.doi.org/10.1016/j.rser.2015.01.039.

Santamaria, S., Sapienza, A., Frazzica, A., Freni, A., Girnik, I.S. & Aristov, Y.I. 2014. Water adsorption dynamics on representative pieces of real adsorbers for adsorptive chillers. *Applied Energy*, 134: 11–19.

Sapienza, A., Santamaria, S., Frazzica, A., Freni, A. & Aristov, Y.I. 2014. Dynamic study of adsorbers by a new gravimetric version of the Large Temperature Jump method. *Applied Energy*, 113: 1244–1251. http://dx.doi.org/10.1016/j.apenergy.2013.09.005.

Seol, S.H., Nagano, K. & Togawa, J. 2020. Modeling of adsorption heat pump system based on experimental estimation of heat and mass transfer coefficients. *Applied Thermal Engineering*, 171(February): 115089. https://doi.org/10.1016/j.applthermaleng.2020.115089.

Shen, C.H., Kee, T.S., Lee, B.C.T. & Albert, F.Y.C. 2017. Development and Implementation of Load Cell in Weight Measurement Application for Shear Force. *International Journal of Electronics and Electrical Engineering*, 5(3): 240–244.

Shen, D., Bülow, M., Siperstein, F., Engelhard, M. & Myers, A.L. 2000. Comparison of experimental techniques for measuring isosteric heat of adsorption. *Adsorption*, 6(4): 275–286.

Thu, K., Kim, Y.D., Shahzad, M.W., Saththasivam, J. & Ng, K.C. 2015. Performance investigation of an advanced multi-effect adsorption desalination (MEAD) cycle. *Applied Energy*, 159: 469–477. http://dx.doi.org/10.1016/j.apenergy.2015.09.035.

Thu, K., Yanagi, H., Saha, B.B. & Ng, K.C. 2013. Performance analysis of a low-temperature waste heat-driven adsorption desalination prototype. *International Journal of Heat and Mass Transfer*, 65: 662–669. http://dx.doi.org/10.1016/j.ijheatmasstransfer.2013.06.053.

Tien, C. 2019. *Introduction to Adsorption, Basics, Analysis, and Applications*. Elsevier.

Tun, H. & Chen, C.C. 2021. Isosteric heat of adsorption from thermodynamic Langmuir isotherm. *Adsorption*, 27(6): 979–989. https://doi.org/10.1007/s10450-020-00296-3.

Volmer, R., Eckert, J., Füldner, G. & Schnabel, L. 2017. Evaporator development for adsorption heat transformation devices – Influencing factors on non-stationary evaporation with tube-fin heat exchangers at sub-atmospheric pressure. *Renewable Energy*, 110: 141–153. http://dx.doi.org/10.1016/j.renene.2016.08.030.

Vordos, N., Gkika, D.A. & Bandekas, D. V. 2020. Wheatstone Bridge and Bioengineering. *Journal of Engineering Science and Technology Review*, 13(5): 4–6.

Wang, D., Zhang, J., Yang, Q., Li, N. & Sumathy, K. 2014. Study of adsorption characteristics in silica gel-water adsorption refrigeration. *Applied Energy*, 113: 734–741.

Wang, R., Wang, L. & Wu, J. 2014. ADSORPTION REFRIGERATION TECHNOLOGY THEORY AND APPLICATION. *John Wiley & sons*: 526.

Wenten, I.G. & Khoiruddin. 2016. Reverse osmosis applications: Prospect and challenges. *Desalination*, 391: 112–125. http://dx.doi.org/10.1016/j.desal.2015.12.011.

Wibowo, E., Sutisna, Rokhmat, M., Murniati, R., Khairurrijal & Abdullah, M. 2017. Utilization of Natural Zeolite as Sorbent Material for Seawater Desalination. In *Procedia Engineering*. Elsevier Ltd: 8–13.

Worch, E. 2012. *Adsorption Technology in Water Treatment*.

Wu, J.W., Biggs, M.J. & Hu, E.J. 2014. Dynamic model for the optimisation of adsorption-based desalination processes. *Applied Thermal Engineering*, 66(1–2): 464–473. http://dx.doi.org/10.1016/j.applthermaleng.2014.02.045.

Wyma, B.D. 2020a. *Measuring Pilot Control Force in General Aviation Subtitle: Strain gauges and Load Cell*.

Wyma, B.D. 2020b. *Measuring Pilot Control Force in General Aviation Subtitle: Strain gauges and Load Cell*. Florida Institute of Technology.

Yan, S., Cao, Z., Guo, Z., Zheng, Z., Cao, A., Qi, Y., Leng, Q. & Zhao, W. 2018. Design and fabrication of full wheatstone- bridge-based angular GMR sensors. *Sensors (Switzerland)*, 18(6): 1–8.

Yang, R.T. 2003. *Adsrbents: Fundamentals and Applications*. 1st ed. http://elib.tu-darmstadt.de/tocs/95069577.pdf.

Youssef, P.G., Dakkama, H., Mahmoud, S.M. & AL-Dadah, R.K. 2017. Experimental investigation of adsorption water desalination/cooling system using CPO-27Ni MOF. *Desalination*, 404: 192–199.

Youssef, P.G., Mahmoud, S.M. & AL-Dadah, R.K. 2015. Performance analysis of four bed adsorption water desalination/refrigeration system, comparison of AQSOA-Z02 to silica-gel. *Desalination*, 375: 100–107.

# Chapter 5: Evaluation of adsorptive process on the adsorbents surface as a function of pressure in isosteric system compared with adsorption isotherm

**Part of this Chapter is Published as:** Sindisiwe Ntsondwa, Velaphi Msomi, and Moses Basitere. 2022. Evaluation of the adsorptive process on adsorbents surface as a function of pressure in an isosteric system compared with adsorption isotherm. *ChemEngineering* 2022, *6*(4), 52; **https://doi.org/10.3390/chemengineering6040052**

## 5.1. Introduction

Adsorption desalination is a novel kind of desalination that uses an adsorption–desorption process to operate. Adsorbents and adsorbate are the two main components of the adsorption and desorption process with porous material. The surface area of the adsorbents adsorbs and desorbs the adsorbate. In the process of adsorption cycle, the adsorbents adsorb the adsorbate for a certain amount of time. While in the desorption cycle, the adsorbents reject the adsorbate. The ability to adsorb is highly functioning when the adsorbent is subjected to low temperature circumstances, whereas the desorption takes place when the adsorbent is exposed to hot temperature conditions (Bakhtyari & Mofarahi, 2019).

In contrast, desorption takes place when the adsorbent is exposed to hot temperature conditions. A chiller's ability to perform well is therefore directly proportional to the adsorbent's capacity to absorb vapour and how rapidly the bed can adsorb or desorb liquid refrigerant (Bakhtyari & Mofarahi, 2019). To offer a high adsorption capacity, a solid adsorbent with a large surface area is preferred, because it assist in producing a large amount of water to determine a change in the heat of adsorption ($\Delta H_{ads}$). It is therefore important to understand the amount of vapour adsorbed, as this knowledge is utilized to calculate the energy used by an adsorption chiller (Gediz Ilis et al., 2019).

Calculating isosteric heat is equivalent to determining the change in heat of adsorption $\Delta H_{ads}$ using molecular simulations and observational calculations. They are both approaches to determine the change in heat of adsorption ($\Delta H_{ads}$) (Chakraborty et al., 2006; Nuhnen & Janiak, 2020). New strategies have been presented during recent years for the understanding of adsorption information, particularly for the examination of micropore and mesopore sizes. Determining $\Delta H_{ads}$ for an adsorption chiller built into a small lab single unit is a perplexing process with no clear underlying notion. There is a need to take desalination into consideration, fueled by water scarcity in the world as whole (Rouquerol et al., 2014; Chakraborty et al., 2006).

It is not surprising that, when viewed in the context of more traditional theories of surface coverage and pore filling, it is difficult to obtain a balanced picture of the significance of recent advances in areas such as energy adsorption and density functional theory for a small lab-scale adsorption chiller. This study intends to bridge the gap in literature on the adsorptive process on a small lab scale by the intensity of the linkage between the adsorbate and adsorbent. The goal of this work is not only to discuss these methodologies, but also to provide a computational method for researchers to utilize with data from gas sorption isotherms (Rouquerol et al., 2014).

This extensive overview of the numerous ways for determining the isotherm graph procedure using methods such as Freundlich–Langmuir, isotherm enthalpy, and intensity may be useful for researchers transitioning to adsorption porous studies (Nuhnen & Janiak, 2020; Tun & Chen, 2021). According to the current review, the Langmuir adsorption model is the most widely utilized. However, it, like other existing models, fails to fully reflect sorption phenomena in shale formations, which are characterized by surface heterogeneity and the presence of many components. As a result, efforts have been made to develop and improve the model for use in shale formations (Babatunde et al., 2022).

The Freundlich model, on the other hand, describes a multi-layer adsorption process, while advances in molecular simulation offer the possibility of a more accurate representation of the sorption mechanism. However, independent of governing factors, both the Langmuir and Freundlich models have frequently been used to determine the maximum adsorption capacity of adsorbents. Hence, since both models have their own shortcomings, the Freundlich and the Langmuir models were combined to form a Freundlich–Langmuir model. This combination is suitable for predicting adsorption on heterogeneous surfaces and avoids the Freundlich model's limitation of increased adsorbate concentration (Babatunde et al., 2022).

As a result, at low adsorbate concentrations, this model reduces to the Freundlich model, while it predicts using the Langmuir model at high adsorbate concentrations. It also evaluates the adsorption isosteric enthalpy of adsorption between the adsorbent with Clausius–Clapeyron equation to quantify the intensity of contact between an adsorbate and a solid adsorbent. In conclusion, this isotherm combination is a practical and useful model for studying adsorption equilibrium. For the reasons stated above, this article uses the Clausius–Clapeyron relationship and Freundlich–Langmuir theory to simulate the isosteric adsorption of the used adsorbents (Tun & Chen, 2021; Babatunde et al., 2022).

The testing method can be categorized as either direct operation or indirect operation. Due to the high cost of these technologies, the indirect technique is by far the most popular method of determining isosteric enthalpy. This study uses the indirect method because is affordable as compared to the direct process. However, this study also introduces computed steps using Origin software. The bulk of research in the literature related to isosteric adsorption using the Clausius–Clapeyron model explains only the fundamental formula. It is very rare to find clear details based on the fundamental formulas or graphs of the isotherms with step-by-step explanations of how the process is conducted (Mohammed et al., 2018).

Linear regression analysis has become one of the most widely used tools for defining the best fitting adsorption models in recent years. The use of nonlinear isotherm modelling has grown in popularity in tandem with the advancement of computer technology. In the process of adsorption desalination, the adsorption materials should, in general, fulfil the criteria of acceptability for sorption applications, which include an excellent detection limit, low energy usage, and high operating endurance (Nuhnen & Janiak, 2020). If the adsorbents used do not meet these criteria, then they are not suitable for the adsorption desalination process (Nuhnen & Janiak, 2020).

Two criteria commonly used to analyze an adsorptive process are the adsorption isotherm and the isosteric heat. The isotherm represents the adsorption capacity, whereas the isosteric heat represents the intensity of contacts on adsorbate and the adsorbents used (Builes et al., 2013). A common approach for determining surface qualities is the adsorption process of gasses on porous adsorbents, as well as separating and capturing gases and vapours (Abdulsalam et al., 2020). Adsorption isosteric heat is defined as the enthalpy change obtained from adsorption isotherms at two or more temperatures for a fixed number of adsorbed molecules (Shen et al., 2000).

The adsorbed vapour measurements are made in relation to the strong mass at the point where a vapour is adsorbed onto a pore space (Abdulsalam et al., 2020). The pore structure of the solid adsorbent determines the adsorption isotherm (Olkis et al., 2019). Surface area, pore volume, and pore size distribution are all retrieved from gas adsorption isotherms to form the pore structure (Loh et al., 2010). All adsorption models are based on the adsorption equilibrium. The implementation of both kinetic and dynamic adsorption models requires knowledge of the adsorption equilibrium (Giraldo et al., 2019; Khanam et al., 2018).

### 5.1.1. Adsorption equilibrium

The adsorption equilibrium is the accumulation of adsorbents on the adsorbent surface at a constant rate. The adsorbed vapour measurements are made in relation to the strong mass at the point where a vapour is adsorbed onto a previously empty strong surface or pore space. Van der Waals forces and hydrophobic interactions produce the attraction (not covalent bonding) (Nuhnen & Janiak, 2020). The state of equilibrium is achieved after a protracted period during which adsorbing molecules settle on the adsorbent surfaces (Khanam et al., 2018). Working pairs for adsorption are typically chosen depending on the temperature of the available heat source and the cooling load (Rahimi & Chua, 2017).

The thermo-physical characteristics, kinetics, and equilibrium isotherms of an adsorption working pair are important parameters that affect the effectiveness of an adsorption chiller. Furthermore,

the vapour uptake is dependent on the temperature (T), the partial weight of the pressure (P) balance, and the adsorbate–solid interaction strength. The effect in the listed parameters does affect the vapour production. For a vapour adsorbed on a strong mass at a constant temperature, the adsorbed sum per unit mass of the strong mass (Q) is then merely a fraction of P (Rezk, 2012). The adsorption isotherm is the relationship between Q and P at a particular temperature.

Because the adsorption process is exothermic, temperature has a large influence on the quantity of adsorbate adsorbed. Exothermic processes that operate at greater temperatures, according to Le Chatelier's principle, prefer circumstances that produce less heat (Gabelman, 2017). As a result, at a given pressure, the amount of adsorbate adsorbed at equilibrium decreases as temperature rises (Gabelman, 2017). Q is often exhibited as a detail of the relative pressure where P is standardized to the immersion vapour pressure of the adsorbate at temperature T. Adsorption equilibrium is expressed in three ways:

- Adsorption isotherm
- Adsorption isobar
- Adsorption isostere

### 5.1.2. Adsorption isostere

The effect of isosteric heat ($\Delta H_{ads}$) on the combination of adsorbent and adsorbate is among the most important thermodynamic factors for the development of realistic gas classification, gas storage, and adsorption cooling systems (Chakraborty et al., 2006). Isosteric heat is a degree of the power of an adsorbate's interaction with a solid adsorbent. Understanding isosteric heat is an essential and relevant criterion for adsorption system heat control, as it assists in building a better adsorption chiller (Abdulsalam et al., 2020). The adsorption isostere is calculated using origin software and the Clausius–Clapeyron model equation. The study further graphically shows the enthalpy change that occurs in vapour extracted from the primary phase until it reaches the adsorbed gas phase.

The adsorbent's ability to absorb water vapour is a direct function of cycle performance. As a result, the adsorbent employed in the cycle should have strong adsorbate (water vapour) absorption, as well as the capacity to regenerate at a low temperature. The adsorbent material is usually a hydrophilic porous substance with a large surface area that forms transient hydrogen bonds with water molecules. Adsorbate molecules on the adsorbent surface have a lower activation energy than during the main gas phase; hence, heat is released during adsorption. The

heat emitted when an adsorptive adheres to a surface is known as the isosteric enthalpy of adsorption, or $\Delta H_{ads}$ (Abdulsalam et al., 2020).

The isosteric enthalpy of adsorption is the opposite of the isosteric enthalpy of desorption and is emitted during the adsorption process ($H_{ads}$ = 0 kJ/mol). $\Delta H_{des}$ is essential for the reverse desorption procedure ($\Delta H_{ads} = -\Delta H_{des}$) in the case of physisorption (Nuhnen & Janiak, 2020). As a result, adsorption enthalpy is a crucial measure in adsorption processes and is used to gain a better understanding of adsorbate–adsorbent interactions. Because $H_{ads}$ classifies interactions between adsorbed species and adsorbents based on the intensity of contact, interactions between adsorbed species and adsorbents can be categorized, for example, as weak physisorption (Builes et al., 2013).

Similarly, $\Delta H_{ads\ is}$ used to calculate the regeneration energy for adsorbate desorption. Regeneration energies are particularly significant in pressure swing studies, since the energy needed in desorption is proportional to the ultimate tensile strength (Nuhnen & Janiak, 2020). Calculations based on experiments and adsorption isotherm models are two sorts approaches to determining $\Delta H_{ads}$. The experimental method is made up of direct and indirect processes. There has been little research employing the direct technique to identify $\Delta H_{ads}$, since it is sophisticated and expensive to conduct. This study used the indirect technique of adsorption isotherms to derive the isosteric heat as a function of adsorption.

This method of isotherm commonly estimates the adsorbate–adsorbent interaction energy with at least two adsorption isotherms collected using at least six different temperatures near to each other. Because the isosteric adsorption fluctuates with temperature, it is recommended to use more than one adsorption isotherm with $\Delta T$ = 10 °C (Nuhnen & Janiak, 2020). Utilizing a large temperature difference among adsorption isotherms will cause artificial mistakes in the computed result (Giraldo et al., 2019). Isosteric enthalpy is computed using Equation (1):

$$\Delta H_{ads}(m_a) = -R \times \ln(P_2/P_1)((T_1 \times T_2)/(T_2 - T_1)) \quad (5.1)$$

- R= Ideal gas constant (J/mol K)
- m= adsorption up-take (kg/kg)
- P= Pressure (kPa)
- T= Temperature (K)
- $\Delta H_{ads}$ = KJ/mol

$\Delta H_{ads}(m_a)$ is usually expressed as $\Delta H_{ads}$ without ($m_a$). It is, however, the result of gas uptake. m represents the adsorption's isosteric heat. This work introduces $\Delta H_{ads}(m_a)$ because to compute the isosteric enthalpy of adsorption as the result of vapour uptake. $\Delta H_{ads}(m_a)$ is determined

utilizing information from more than one test of adsorption isotherms at six unique temperatures: $T_1$ up to $T_6$. The temperatures $T_1$-$T_6$ have distinct values but are near to each other. According to the literature, the temperature differential should be between 10 and 20 degrees Celsius. All the adsorption isotherms have ($m_a$) vs. ($P1/P_2$) data points.

### 5.1.3. The Clausius-Clapeyron formuls

The Clausius–Clapeyron formula links the adsorption isotherm's temperature dependence with the adsorption heat effects. The Clausius–Clapeyron equation is derived from the use of two approximations: an adsorbed phase with a small molar volume and a gaseous phase that possesses perfect gas behavior. Researchers from several fields of study are now investigating adsorbent materials to improve the performance of adsorption chillers. Understanding the isosteric heat of adsorption provides for a better calculation of the vapour uptake duration by determining the capacity of the integrated material to swiftly disperse the heat generated in the framework (Tun & Chen, 2021; Ng et al., 2009).

### 5.1.4. Chapter objectives

This study aims to evaluate the adsorption isosteric enthalpy of adsorption in between the adsorbent by using the Clausius–Clapeyron equation to quantify the intensity of contact between an adsorbate and a solid adsorbent by comparing the combination of two computed isotherms (Freundlich–Longmuir) with experimental data for a laboratory scale.

## 5.2. Adsorption experimental approach

The isosteric heat is the difference in enthalpy derived using the adsorption isotherm at a minimum of two temperatures (Tun & Chen, 2021; Gabelman, 2017). Under constant temperature and pressure, a discrete volume of gas transitions itself from the large gaseous state to its adsorbed phase, with the heat dispersed to the surrounding environment. The purpose of this study is to discuss the approach used in determining the adsorbate interaction strength and to provide useful graphs with equations used to calculate the isosteric enthalpy of adsorption. The research carried out with the use of two isotherms and six temperatures (283 K, 293 K, 303 K, 313 K, 323 K, and 333 K) using the gravimetric method (Mohammed et al., 2018).

The adsorbents were dried in an oven, cooled to the isobaric adsorption temperature, and then weighed. Seawater was poured into the evaporator, which heated the seawater until it boiled. The adsorbents were placed on top of the adsorption-chiller reactor bed, vacuumed, and sealed. From there, the adsorbents were cooled by the coil linked to the heat exchanger from the cooling refrigerator until it reached saturation and became hydrophilic. During saturation, the vapour was

discharged from the evaporator to be absorbed by the saturated adsorbents for a period. Each step of vapour up-take was recorded with operational conditions using the data logger.

The Clausius–Clapeyron formula was used to determine the isosteric enthalpy of adsorption from two adsorption isotherms at various but close temperatures, with ΔT of 10 °C. For the given experimental data, a full computational explanation of the Clausius–Clapeyron model equation for determining $\Delta H_{ads}$ is provided (Nuhnen & Janiak, 2020; Loh et al., 2010). A logarithmic scale of the amount of vapour adsorbed ($m_a$) in relation to the pressure isotherm graph at a low control pressure area was used to assess and confirm the quality of the crucial and underlying isotherm (Shen et al., 2000). The vapour up-take weight was recorded using the data logger.

The Freundlich–Langmuir isotherm was utilized, which corresponds to the Freundlich–Langmuir Equation (2). This is the formula for calculating the isosteric heat of gas-phase adsorption using experimental data. It is vital to recognize that temperature and pressure are separate factors; thus, if the temperature changes, the pressure may be adjusted to maintain the same $\Delta H_{ads}$ (Nuhnen & Janiak, 2020).

$$m_a = (x.b.P^z/1 + y) \qquad (5.2)$$

Where:

- P is the pressure in kPa
- y is the affinity constant (1/kPa).
- *x* is the maximal loading in kg/kg
- z is the heterogeneity exponent.
- $m_a$ is the mass adsorbed (vapour uptake) in kg/kg

After that, the formula rearranged to form the Freundlich-Langmuir equation to look like this:

$$P(m_a) = \sqrt[z]{m_a/(x.y - n.y)} \qquad (5.3)$$

Then, using the resulting pressures ($P_1$ to $P_6$) under equal vapour adsorbed (loadings), the $H_{ads}$ ($m_a$) is determined (m). The isosteric heat of adsorption determined through graphing $\ln P_{1\text{-}6}$ vs $1/T_{1\text{-}6}$ for the isosteric adsorptions, that is, designed for equivalent uptake at the six temperatures, utilizing m vs. $P_{1\text{-}6}$ data triples from the Freundlich-Langmuir and straight-line fits. With uniform uptake, the gradient m of a linear-regression with six data points at $\ln P_{1\text{-}6}$ vs. $T_{1\text{-}6}$ provides $\Delta H_{ads}$ (ma). There are $m_{ai}$ in relation to $p_i$ data points in each adsorption isotherm. The data triple $m_a$ in relation to $P_1/P_2$ utilized for a uniform vapour uptake of $m_a$.

The data pair's $\ln P_2$ vs. $1/T_2$ and $\ln P_1$ vs. $1/T_1$ define a straight line with a negative slope for a given value of $m_a$.

$$(\Delta H_{ads}(m_a)/R) = \left(\ln P_2 - \ln P_1/\left((1/T_2) - (1/T_1)\right)\right) < 0 \qquad (5.4)$$

This method yields a heat of adsorption $\Delta H_{ads}(m_a)$ for all the empirically observed and interpolated loading $m_a$. This enables the plotting of $\Delta H_{ads}(m_a)$ as a function of Fractional loading (Figure 5.4) by specifying:

$$\Delta H_{ads} = R \times m < 0 \text{ (m is the gradient from the straight-line graph)} \qquad (5.5)$$

## 5.3. Results and discussion

Vapour data from silica gel were extrapolated using the nonlinear prediction model with the Langmuir–Freundlich model for comparing the experimental data to the simulation, using computer software called Origin. Data from the test versus data from the isotherm model were used to demonstrate the suitability of the model equations in Figure 5.1 with subfigure 1A and 1B. The regression error among experiment and simulation data were calculated with Origin software as well. The graph in Figure 5.2–5.3 demonstrates the final findings. The adsorbate–adsorbent interaction energy was calculated indirectly using adsorption isotherms obtained at similar but different temperatures ($T_{283K\,-\,333K}$).

The Freundlich-Langmuir fit of uptake vs. p isotherm

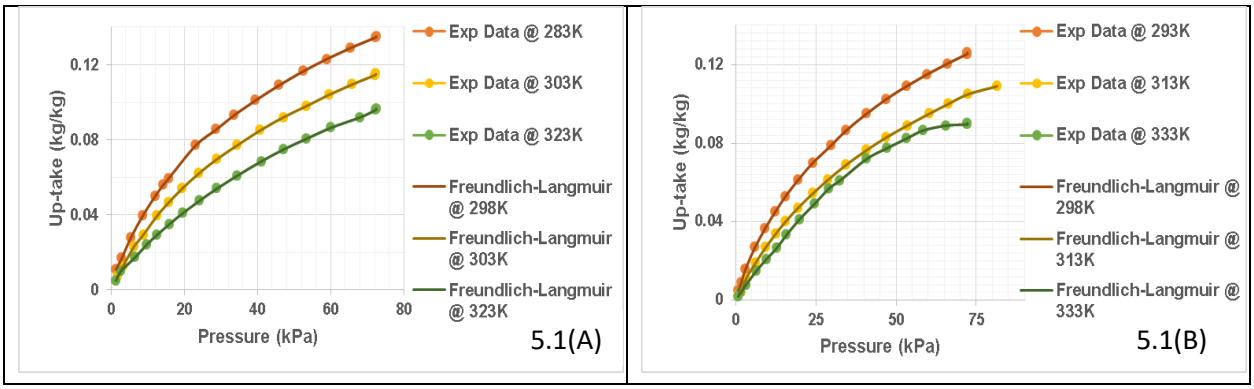


Figure 5.1: The Freundlich-Langmuir fit for vapour adsorbed at six different types of temperatures (283 K, 293 k, 303 K, 313 K, 323 K, 333 K). Subfigure 1(A) represent the vapour uptake of 283 K, 303 K and 323 K. Subfigure 1(B) represent the vapour uptake of 293 K, 313 K and 333 K.

Data for the six temperatures were extrapolated utilizing Langmuir and the Freundlich nonlinear equation. These six adsorption isotherms were used to calculate the isosteric heat of adsorption ($\Delta H_{ads}$) using the Clausius–Clapeyron model equation. Adsorption equilibrium data were

measured at 283 K, 293 K, 303 K, 313 K, 323 K, and 333 K on silica gel in the pressure range of 0.08 kPa to 73 kPa (Figure 5.1). The Langmuir–Freundlich model was used to fit the collected data (Equation (2)) using the Origin program. Figure 5.1 shows the quantity of vapour adsorbed on the silica gel, and the results show that as the pressure increased, the vapour uptake increased.

Figure 5.1 shows the simulation-projected values and experiment results for all models. The vapour uptake adsorbed on the silica gel appears to decrease as the temperature rises. This is because, at greater temperatures, the adsorbed molecules absorb more energy, leading to evaporation (Bénard & Chahine, 2007). The models (Langmuir and Freundlich) were also found to be sufficiently accurate in estimating the adsorbed vapour uptake on silica gel, with a regression error of less than 4% at all temperatures used. According to the literature, an advantageous isotherm has a convex shape and reflects a significant amount of adsorbate at a lower pressure (Gabelman, 2017).

An unreliable isotherm, on the other hand, has a concave form and high pressure is needed to accomplish cost-effective adsorption. Irreversible adsorption is the pinnacle of the preferred model, with maximal adsorption occurring at very low partial pressures. Figure 5.1 presents the recommended curve as stated in the literature. These results for vapour adsorption on silica gel are close to the Langmuir isotherm. After the fit-on Figure 5.1 was generated from Origin using a nonlinear fit with code relating to Equation (2), the new computed values were generated to form an exponential graph.

From an exponential graph, Origin software was used to form linear regression using the values of lnp vs. uptake as shown in Figure 5.2. The linear regression at six temperatures offers a continuous uptake vs. lnp2 data triples, but only within a narrow uptake area, as demonstrated in the adsorption model of lnp against the uptake plot. Only a few parts of lnp versus uptake can be estimated using a linear regression, as seen in Figure 5.2. When compared to the Freundlich–Langmuir fit, the approximation linear regression at six temperatures provides a continuum of uptake in relation to calculated lnp data, but only over a limited uptake region.

The relationship of lnp versus uptake becomes linear throughout a larger uptake range, just for gases operating under adsorbents with low affinity. Because of the enhanced contact among the adsorbents and vapour uptake, a linear regression of lnp against uptake is not practicable for adsorbents with high regeneration; hence, the isotherm fits using the Freundlich-Langmuir model as indicated above. It is also noted in Figure 5.2 that the straight line lies only in a certain region,

hence the 10-loading uptake were introduced in Figure 5.3. The six isotherms were fitted by a linear function as a first approximation, and then utilized to produce $H_{ads}$ (m).

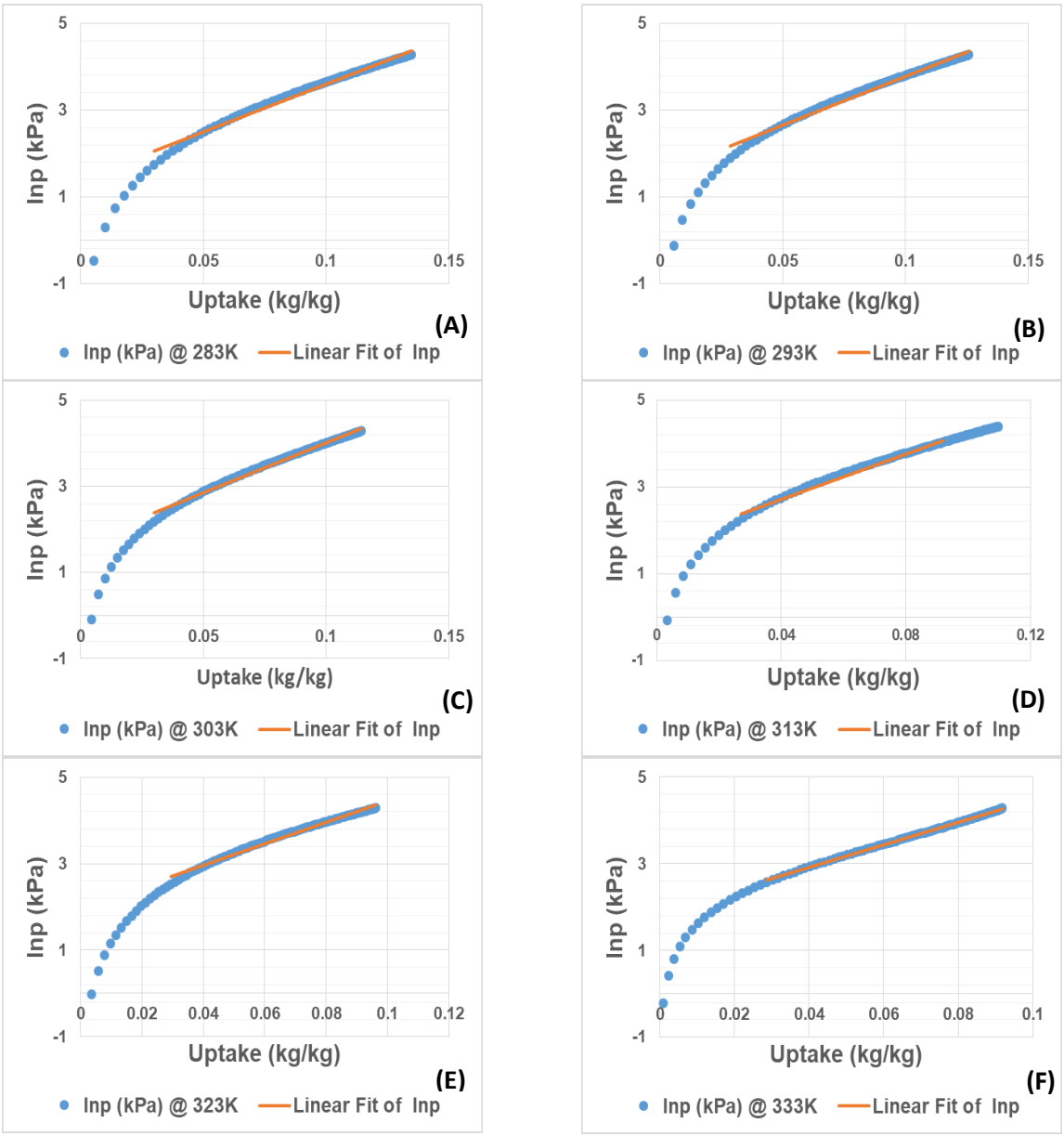


Figure 5.2: lnp against uptake for the adsorption isotherm on silica gel at 283 K – 333 K, with the linear fit at the estimated regions. The subfigure 5.2(A) represent the linear fit at temperature 283 K, subfigure 5.2 (B) represent the linear fit at temperature 293 K, subfigure 5.2 (C) represent the linear fit at temperature 303 K, subfigure 5.2 (D) represent the linear fit at temperature 313 K, subfigure 5.2 (E) represent the linear fit at temperature 323 K and subfigure 5.2 (F) represent the linear fit at temperature 333 K.

The pressures derived ($P_A$-$P_F$) at equal loadings are utilized to calculate $H_{ads}$ (m). The isosteric heat of adsorption determined through a graph of lnp vs 1/T to form isosteric adsorptions. That was derived from vapour uptake between six temperatures ($T_A$-$T_F$), and the vapour uptake vs. $P_{A-F}$ data triples from the linear regression graph (Figure 5.3). The gradient m of the linear regression with six data points at lnp $_{A-F}$ versus $1/T_{A-F}$, assuming equal loading vapour uptake, according to Eq. 5.4, provides $H_{ads}$ (m). For didactic purposes the graph lnp vs 1/T is shown in Figure 5.3 with 10 loadings-uptakes.

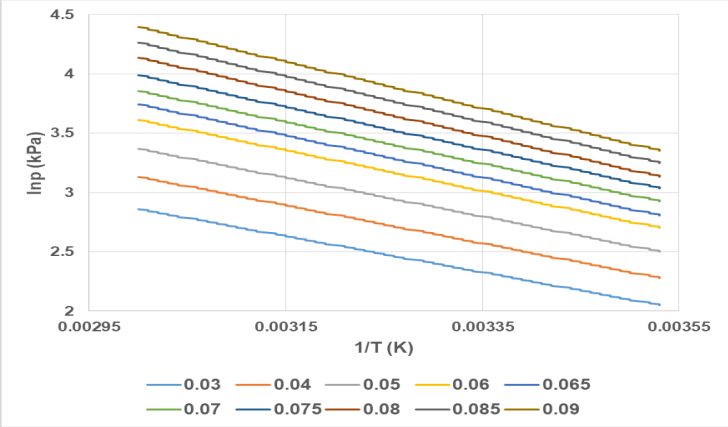


Figure 5. 3: Isosteric lnp against 1/T and the T represent the temperature from 283 K up to 333 K for 10 different uptake loadings.

The gradient in Figure 5.3 was used to get the values represented in Figure 5.4. In Figure 5.4, the isosteric enthalpy, $\Delta H_{ads}$, calculated from a Freundlich-Langmuir model and the linear regression fit of a graph lnp versus the vapour uptake plot in the range of 10 fractional vapour uptake loadings compared. For the isosteric enthalpy greater adsorption, both fit approaches produce identical findings; however, this is not the case in the low-uptake area. The lnp vs n plot approach greatly underrated $H_{ads}$(m). The gradient of all six linear regression fit in Figures 5.3 were almost same, resulting in a special situation of a fixed $H_{ads}$ that is unaffected by loading.

In Figure 5.4, $\Delta H_{ads}$ explains the degree of the adsorbate-adsorbent energy states. The value expected to alter with uptake in the process of adsorption. A strong degree among both the adsorbents and vapour uptake explains the high adsorption enthalpy value. At low pressure, pore spaces with the strongest affinity for the adsorbed molecules are commonly saturated. For extremely low loadings, these pore gaps were associated with higher (negative) $H_{ads}$ values, as seen in Figure 5.4. This shows that even though the methods followed were different, the values of the $\Delta H_{ads}$ found were in the same region.

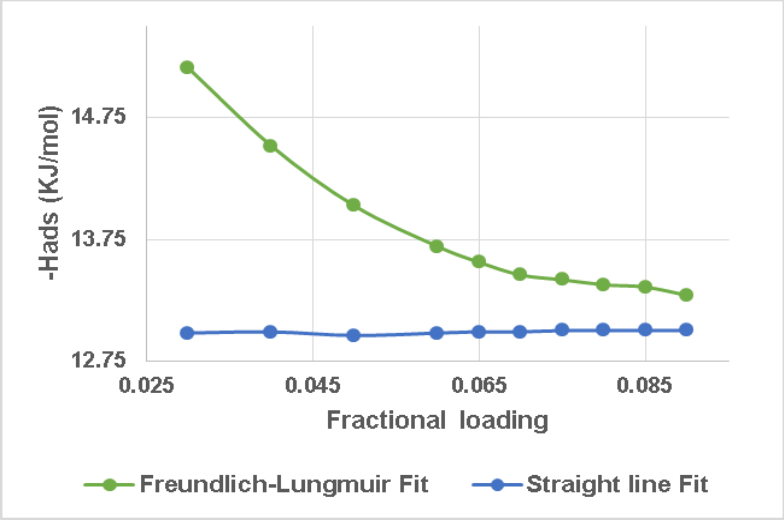


Figure 5. 4: Isosteric heat of adsorption found between vapour uptake and silica gel

The results of the proposed equations and origin software compared to the results of the approximation formulas are highly recommended in assessing gas. The results of the approximation Clausius-Clapeyron like equations (Equation 5.3) provide precise predictions for isosteric temperatures of adsorption with a slightly moderately difference from the one derived using the straight line. The approximate equations and software used have the benefit of simply requiring adsorption isotherm data rather than the rigorous equations, which require additional information, such as the heat of vaporization or the excess enthalpy of mixing.

The basic parameters of any adsorbate-adsorbent system are adsorption properties. Experimental isotherms for silica gel derived in this study, which used to develop an adsorption chiller. In comparison to other methods that require many factors to find the Isosteric heat, the present study found an improvement in accuracy for measured adsorption data. The observed isotherm data used to calculate the isosteric heat, which is helpful in deciding which adsorbent to utilize on a reactor bed to get the high intensity of engagements between both the adsorbate and the adsorbents.

## 5.4. Conclusion

The isosteric heat of adsorption $\Delta H_{ads}$ of an adsorbent-adsorbate system is an important thermodynamic quantity for the design of realistic gas separation and adsorption cooling systems. The purpose of this work was to compute the isosteric enthalpy of adsorption at equilibrium using the gradient shown in Figure 5.3. In this study, the characteristics and vapour uptake isotherms used to predict $\Delta H_{ads}$ behaviours, which are then adsorbate validated against computed

adsorption data. The experimental results were compared to the model data to demonstrate the applicability of the model equations.

The value of $\Delta H_{ads}$ utilized as a critical parameter in determining how much heat the absorbent because of vapour uptake emits. For both isotherms at six different temperatures, the same model was utilized. The Clausius–Clapeyron equation was used to compute the isosteric temperatures of adsorption. These figures were compared to the Langmuir model's enthalpy parameter (Figure 5.4). The straight line fit constant values demonstrate that the assumption of energy homogeneity made by the Langmuir model for the vapour is correct. The isosteric heat was found to be in the range of 13 KJ/mol to 15, 5 KJ/mol.

## 5.5. References


Abdulsalam, J., Mulopo, J., Bada, S.O. & Oboirien, B. 2020. Equilibria and Isosteric Heat of Adsorption of Methane on Activated Carbons Derived from South African Coal Discards. *ACS Omega*, 5(50): 32530–32539.

Babatunde, K.A., Negash, B.M., Jufar, S.R., Ahmed, T.Y. & Mojid, M.R. 2022. Adsorption of gases on heterogeneous shale surfaces: A review. *Journal of Petroleum Science and Engineering*, 208(PB): 109466. https://doi.org/10.1016/j.petrol.2021.109466.

Bakhtyari, A. & Mofarahi, M. 2019. A New Approach in Predicting Gas Adsorption Isotherms and Isosteric Heats Based on Two-Dimensional Equations of State. *Arabian Journal for Science and Engineering*, 44(6): 5513–5526. https://doi.org/10.1007/s13369-019-03838-2.

Bénard, P. & Chahine, R. 2007. Storage of hydrogen by physisorption on carbon and nanostructured materials. *Scripta Materialia*, 56(10): 803–808.

Builes, S., Sandler, S.I. & Xiong, R. 2013. Isosteric heats of gas and liquid adsorption. *Langmuir*, 29(33): 10416–10422.

Chakraborty, A., Saha, B.B., Koyama, S. & Ng, K.C. 2006. On the thermodynamic modeling of the isosteric heat of adsorption and comparison with experiments. *Applied Physics Letters*, 89(17): 2004–2007.

Gabelman, A. 2017. Adsorption basics: Part 2. *Chemical Engineering Progress*, 113(8): 1–6.

Gediz Ilis, G., Demir, H., Mobedi, M. & Baran Saha, B. 2019. A new adsorbent bed design: Optimization of geometric parameters and metal additive for the performance improvement. *Applied Thermal Engineering*, 162(July): 114270.

https://doi.org/10.1016/j.applthermaleng.2019.114270.

Giraldo, L., Rodriguez-Estupiñán, P. & Moreno-Piraján, J.C. 2019. Isosteric heat: Comparative study between Clausius-Clapeyron, CSK and adsorption calorimetry methods. *Processes*, 7(4).

Khanam, M., Jribi, S., Miyazaki, T., Saha, B.B. & Koyama, S. 2018. Numerical investigation of small-scale adsorption cooling system performance employing activated carbon-ethanol pair. *Energies*, 11(6).

Loh, W.S., Rahman, K.A., Chakraborty, A., Saha, B.B., Choo, Y.S., Khoo, B.C. & Ng, K.C. 2010. Improved isotherm data for adsorption of methane on activated carbons. *Journal of Chemical and Engineering Data*, 55(8): 2840–2847.

Mohammed, R.H., Mesalhy, O., Elsayed, M.L., Su, M. & Chow, L.C. 2018. Revisiting the adsorption equilibrium equations of silica-gel/water for adsorption cooling applications. *International Journal of Refrigeration*, 86: 40–47. https://doi.org/10.1016/j.ijrefrig.2017.10.038.

Ng, K.C., Thu, K., Chakraborty, A., Saha, B.B. & Chun, W.G. 2009. Solar-assisted dual-effect adsorption cycle for the production of cooling effect and potable water. *International Journal of Low-Carbon Technologies*, 4(2): 61–67.

Nuhnen, A. & Janiak, C. 2020. A practical guide to calculate the isosteric heat/enthalpy of adsorption: Via adsorption isotherms in metal-organic frameworks, MOFs. *Dalton Transactions*, 49(30): 10295–10307.

Olkis, C., Brandani, S. & Santori, G. 2019. Cycle and performance analysis of a small-scale adsorption heat transformer for desalination and cooling applications. *Chemical Engineering Journal*, 378(April): 122104. https://doi.org/10.1016/j.cej.2019.122104.

Rahimi, B. & Chua, H.T. 2017. *Low Grade Heat Driven Multi-Effect Distillation and Desalination*. 1st ed. Elsivier Inc.

Rezk, A. 2012. Theoretical and experimental investigation of silica gel/water adsorption refrigeration systems. *Doctor of Philosophy*, 1: 2017.

Rouquerol, F., Rouquerol, J., Sing, K.S.W., Llewellyn, P. & Maurin, G. 2014. *Adsorption by Powders and Porous Solids Principles, Methodology and Applications*. 2nd ed.

Shen, D., Bülow, M., Siperstein, F., Engelhard, M. & Myers, A.L. 2000. Comparison of experimental techniques for measuring isosteric heat of adsorption. *Adsorption*, 6(4): 275–286.

Tun, H. & Chen, C.C. 2021. Isosteric heat of adsorption from thermodynamic Langmuir isotherm. *Adsorption*, 27(6): 979–989. https://doi.org/10.1007/s10450-020-00296-3.

# Chapter 6: Conclusion and recommendations

The world in general is facing a water scarcity problem, due to climate change and population growth. Many researchers and academic institutions embarked in a study of improving water shortage. In literature, it has been found that the high percentage of water is in oceans. There are so many ideas brought forward in regard converting seawater into portable water, however the major setback is that most of them are costly to implement, and to sustain. Ng et al., (2009) and other scholars came up with a better idea of incorporating a thermal desalination with adsorption, the intentions were to lower the energy consumption.

With all the work that has been done and provided on the literature, it is not stated which adsorbent to be used on the adsorption desalination. There are a lot of adsorbents in the market with different parameters, it is therefore important to know which adsorbent is performing at best. Another question left unanswered on the literature is the condition at which they should be operated at. Therefore, this study is conducted to close that gap. A complete analysis of current adsorption techniques and their performance is conducted with the goal of developing a cost-effective solid vapour adsorbent for adsorption desalination.

This is accomplished by comparing the amount of vapour adsorbed by each adsorbent. Different types of adsorbents (silica gel, molecular sieve zeolite and activated alumna) were employed to optimize the adsorption cycle. Under certain conditions, the optimum cycle time for a specific adsorption cycle was calculated. The kinetics of adsorbent material response rate and adsorbent capacity were also determined. Due to the limited equipment to undertake this research, the small new lab-scale adsorption chiller is designed and built according to gravimetric method standards.

The importance of this new scaling adsorption chiller was to examine the performance of adsorbent material, the impact of cycle time, hot/cold child water temperature, adsorption isotherms, cycle performance (COP), as well as adsorption isosteric or heat of adsorption. The heat of adsorption represents the strength of interactions between the adsorbate and the solid adsorbent, whereas the isotherm shows the adsorption capacity. Adsorption of gases on solids is a common method for determining surface properties as well as separating and capturing gases and vapour.

According to the test made, zeolite absorbs moisture more effectively than silica gel or activated alumina. However, a major setback with that, a zeolite regenerates at a higher temperature whereas a silica gel can regenerate at low temperature. Which then makes the silica gel to be the suitable adsorbent for this study, because any adsorbent that regenerate at a high temperature

consume a lot of energy. Desorption temperatures for silica gel range from 55℃ to 140℃, activated alumina from 120℃ to 260℃, and molecular sieve zeolite from 175℃ to 370℃.

Despite its high adsorptive capacity, zeolite cannot be considered the best adsorbent because it requires more energy for desorption process. As a result, unlike a molecular sieve zeolite with a homogeneous structure, silica gel has a fair probability of becoming the best adsorbent since it can easily desorb the vapour if the temperature rises. This study further intends to propose experimental methods for measuring equilibrium states of gases adsorbed on solid materials' surfaces. It primarily focuses on adsorption-based gas separation methods and the use of graph to determine the isosteric heat as it known as a measure of the effectiveness of the adsorbate's bonds with the solid adsorbent.

The Clausius-Clapeyron technique is used to calculate the isosteric heat of adsorption from adsorption isotherms at six different temperatures, but all close to 10°C. Regarding the given experimental data, a full computational explanation of the Clausius-Clapeyron technique to determining $\Delta H_{ads}$ provided. Logarithmic-scale uptakes vs. pressure isotherm plots for the Freundlich and Langmuir graph in the low-pressure zone is used to assess and confirm the quality of the crucial and underlying isotherm. A data for the six temperatures were extrapolated using straight-line regression of Langmuir and Freundlich.

A programming coded on Origin software, these six adsorption isotherms used to compute the isosteric enthalpy ($\Delta H_{ads}$) and heat ($Q_{st}$) of adsorption using either the Clausius-Clapeyron technique or virial analysis. Isotherms used to predict $\Delta H_{ads}$ behaviours, which are then adsorbate validated against computed adsorption data. In Chapter 5, the experimental data were compared against the model data to demonstrate the applicability of the model equations. The main objective of incorporating thermal desalination with adsorption desalination was to save energy while producing potable water.

Therefore, the best adsorbent should be an adsorbent that is able to adsorb steam at a low temperature and regenerate it at a low temperature. In chapter three the adsorbents were tested via adsorption uptake, and the silica gel adsorbs 12% vapour higher than zeolite and 18.9% vapour to $Al_2O_3$ at equilibrium (1200 s). Through the results provided in this study, it can be concluded that the silica gel is a suitable adsorbent for adsorption chiller as it outperformed the other two adsorbents when compared using the adsorption chiller’s conditions. To respond to the missing information in adsorption kinetics in literature with the information collected on this research.

It can be stated that the cooling temperature needed to saturate the adsorbent in adsorption process is 10℃ and the evaporator temperature can be operated at 30℃ and the regenerated temperature is 70℃. The results found in this study further confirm that silica gel is the best adsorbent suitable for thermal desalination systems since it can regenerate the steam at the lowest temperature as compared to its corresponding adsorbents. It has been shown that it has an ability to adsorb more steam.

## Recommendations

The author would like to recommend this information:

- In future, for a system to produce more water, two or more adsorption chillers should be used.
- The adsorbents should be dried out on the oven before use
- In the design of adsorption chiller using a load cell, the load cell should be always kept under the insulator pad as the vapour can easily damage it.
- The adsorption chiller should be vacuumed or insulated during the adsorption process, to avoid condensation.
- The future recommendation study to improve this system; would be to check if the adsorbent perform better when the time cycle of adsorption process differs from the time cycle of desorption process as well as the pressure effect on vapour movement.

# Chapter 7: REFERENCE

## 7.1. REFERENCE LIST


Abdulsalam, J., Mulopo, J., Bada, S.O. & Oboirien, B. 2020. Equilibria and Isosteric Heat of Adsorption of Methane on Activated Carbons Derived from South African Coal Discards. *ACS Omega*, 5(50): 32530–32539.

Al-Jabari, M. 2016. Kinetic models for adsorption on mineral particles comparison between Langmuir kinetics and mass transfer. *Environmental Technology and Innovation*, 6: 27–37. http://dx.doi.org/10.1016/j.eti.2016.04.005.

Alnajdi, O., Wu, Y. & Calautit, J.K. 2020. Toward a Sustainable Decentralized Water Supply : Review of Adsorption Desorption Desalination ( ADD ) and Current Technologies : Saudi Arabia ( SA ). : 1–30.

Alsaman, A.S., Askalany, A.A., Harby, K. & Ahmed, M.S. 2017. Performance evaluation of a solar-driven adsorption desalination-cooling system. *Energy*, 128: 196–207. http://dx.doi.org/10.1016/j.energy.2017.04.010.

Ambarita, H. & Kawai, H. 2016. Experimental study on solar-powered adsorption refrigeration cycle with activated alumina and activated carbon as adsorbent. *Case Studies in Thermal Engineering*, 7: 36–46. http://dx.doi.org/10.1016/j.csite.2016.01.006.

Aristov, Y.I. 2012. Adsorptive transformation of heat: Principles of construction of adsorbents database. *Applied Thermal Engineering*, 42: 18–24.

Bakhtyari, A. & Mofarahi, M. 2019. A New Approach in Predicting Gas Adsorption Isotherms and Isosteric Heats Based on Two-Dimensional Equations of State. *Arabian Journal for Science and Engineering*, 44(6): 5513–5526. https://doi.org/10.1007/s13369-019-03838-2.

Barbosa, G.D., Bara, J.E., Weinman, S.T. & Turner, C.H. 2022. Molecular aspects of temperature swing solvent extraction for brine desalination using imidazole-based solvents. *Chemical Engineering Science*, 247: 116866. https://doi.org/10.1016/j.ces.2021.116866.

Bindu, B. 2019. Getting Started with EasyEDA an Online PCB Design Software | StudentCompanion.

Builes, S., Sandler, S.I. & Xiong, R. 2013. Isosteric heats of gas and liquid adsorption. *Langmuir*, 29(33): 10416–10422.

Bundschuh, J., Ghaffour, N., Mahmoudi, H., Goosen, M., Mushtaq, S. & Hoinkis, J. 2015. Low-

cost low-enthalpy geothermal heat for freshwater production: Innovative applications using thermal desalination processes. *Renewable and Sustainable Energy Reviews*, 43: 196–206. http://dx.doi.org/10.1016/j.rser.2014.10.102.

Cameron, N. 2019. *Arduino Applied:Comprehensive Projects for Everyday Electronics*.

Chakraborty, A., Saha, B.B., Koyama, S. & Ng, K.C. 2006. On the thermodynamic modeling of the isosteric heat of adsorption and comparison with experiments. *Applied Physics Letters*, 89(17): 2004–2007.

Chen, X., Boo, C. & Yip, N.Y. 2020. Transport and structural properties of osmotic membranes in high-salinity desalination using cascading osmotically mediated reverse osmosis. *Desalination*, 479(January): 114335. https://doi.org/10.1016/j.desal.2020.114335.

Chiou, C.T. 2002. *OF ORGANIC CONTAMINANTS IN ENVIRONMENTAL SYSTEMS PARTITION AND ADSORPTION OF ORGANIC CONTAMINANTS*. John Wiley & Sons, Inc.

Choi, O.K., Seo, J.H., Kim, G.S., Hendren, Z., Kim, G.D., Kim, D. & Lee, J.W. 2021. Non-membrane solvent extraction desalination (SED) technology using solubility-switchable amine. *Journal of Hazardous Materials*, 403(April 2020): 123636. https://doi.org/10.1016/j.jhazmat.2020.123636.

Condon, J.B. 2006a. Heat of Adsorption - an overview | ScienceDirect Topics. *Elsevier*. https://www.sciencedirect.com/topics/chemistry/heat-of-adsorption 22 October 2021.

Condon, J.B. 2020. *Measuring the physisorption isotherm*.

Condon, J.B. 2006b. *Surface Area and Porosity Determinations by Physisorption Measurements and Theory*. 1st ed. Elsevier B.V.

Distribution, W., Moisture, S. & Ice, G. 2020. What is the big deal? *SPC Water, Sanitation and Hygen: Water distribution*, 2: 2–3.

Gabelman, A. 2017. Adsorption basics: Part 2. *Chemical Engineering Progress*, 113(8): 1–6.

Gediz Ilis, G., Demir, H., Mobedi, M. & Baran Saha, B. 2019. A new adsorbent bed design: Optimization of geometric parameters and metal additive for the performance improvement. *Applied Thermal Engineering*, 162(July): 114270. https://doi.org/10.1016/j.applthermaleng.2019.114270.

Giraldo, L., Rodriguez-Estupiñán, P. & Moreno-Piraján, J.C. 2019. Isosteric heat: Comparative study between Clausius-Clapeyron, CSK and adsorption calorimetry methods. *Processes*, 7(4).

Grande, C.A. 2012. Advances in Pressure Swing Adsorption for Gas Separation. , 2012: 100–102.

Gude, V.G. 2018. Exergy Evaluation of Desalination Processes.

Guo, J., Tucker, Z.D., Wang, Y., Ashfeld, B.L. & Luo, T. 2021. Ionic liquid enables highly efficient low temperature desalination by directional solvent extraction. *Nature Communications*, 12(1): 1–7. http://dx.doi.org/10.1038/s41467-020-20706-y.

Halvorsen, H.-P. 2018. *Programming With Arduino*. 978-82-691106.

Israelachvili, J.N. 2011. *Intermolecular and surface forces*. 3rd ed. Elisvier.

Kaiser, R. 1970. *Carbon molecular sieve*.

Khalil, A., El-Agouz, E.S.A., El-Samadony, Y.A.F. & Sharaf, M.A. 2016. Experimental study of silica gel/water adsorption cooling system using a modified adsorption bed. *Science and Technology for the Built Environment*, 22(1): 41–49.

Khanam, M., Jribi, S., Miyazaki, T., Saha, B.B. & Koyama, S. 2018. Numerical investigation of small-scale adsorption cooling system performance employing activated carbon-ethanol pair. *Energies*, 11(6).

Li, A., Thu, K., Ismail, A. Bin, Shahzad, M.W. & Ng, K.C. 2016. Performance of adsorbent-embedded heat exchangers using binder-coating method. *International Journal of Heat and Mass Transfer*, 92: 149–157. http://dx.doi.org/10.1016/j.ijheatmasstransfer.2015.08.097.

Loh, W.S., Rahman, K.A., Chakraborty, A., Saha, B.B., Choo, Y.S., Khoo, B.C. & Ng, K.C. 2010. Improved isotherm data for adsorption of methane on activated carbons. *Journal of Chemical and Engineering Data*, 55(8): 2840–2847.

Mancosu, N., Snyder, R.L., Kyriakakis, G. & Spano, D. 2015. Water scarcity and future challenges for food production. *Water (Switzerland)*, 7(3): 975–992.

Mitra, S., Kumar, P., Srinivasan, K. & Dutta, P. 2015. Performance evaluation of a two-stage silica gel + water adsorption based cooling-cum-desalination system. *International Journal of Refrigeration*, 58: 186–198.

Mitra, S., Thu, K., Saha, B.B., Srinivasan, K. & Dutta, P. 2017. Modeling study of two-stage, multi-bed air cooled silica gel + water adsorption cooling cum desalination system. *Applied Thermal Engineering*, 114: 704–712. http://dx.doi.org/10.1016/j.applthermaleng.2016.12.011.

Mohammed, R.H., Mesalhy, O., Elsayed, M.L. & Chow, L.C. 2019. Assessment of numerical models in the evaluation of adsorption cooling system performance. *International Journal of Refrigeration*, 99: 166–175. https://doi.org/10.1016/j.ijrefrig.2018.12.017.

Mohammed, Ramy H., Mesalhy, O., Elsayed, M.L., Hou, S., Su, M. & Chow, L.C. 2018. Physical properties and adsorption kinetics of silica-gel/water for adsorption chillers. *Applied Thermal Engineering*, 137(March): 368–376. https://doi.org/10.1016/j.applthermaleng.2018.03.088.

Mohammed, Ramy H, Mesalhy, O., Elsayed, M.L., Su, M. & Chow, L.C. 2018. Revisiting the adsorption equilibrium equations of silica-gel/water for adsorption cooling applications. *International Journal of Refrigeration*, 86: 40–47. https://doi.org/10.1016/j.ijrefrig.2017.10.038.

Mondal, P. & George, S. 2015. A review on adsorbents used for defluoridation of drinking water. *Reviews in Environmental Science and Biotechnology*, 14(2): 195–210. http://dx.doi.org/10.1007/s11157-014-9356-0.

Moshoeshoe, M., Silas Nadiye-Tabbiruka, M. & Obuseng, V. 2017. A Review of the Chemistry, Structure, Properties and Applications of Zeolites. *American Journal of Materials Science*, 2017(5): 196–221. http://journal.sapub.org/materials.

Nasir, S.Z. 2020. Introduction to Proteus - The Engineering Projects. *TheEngineeringProjects*.

Ng, K.C., Burhan, M., Shahzad, M.W. & Ismail, A. Bin. 2017. A Universal Isotherm Model to Capture Adsorption Uptake and Energy Distribution of Porous Heterogeneous Surface. *Scientific Reports*, 7(1): 1–11. http://dx.doi.org/10.1038/s41598-017-11156-6.

Ng, K.C., Chua, H.T., Chung, C.Y., Loke, C.H., Kashiwagi, T., Akisawa, A. & Saha, B.B. 2001. Experimental investigation of the silica gel-water adsorption isotherm characteristics. *Applied Thermal Engineering*, 21: 1631–1642. www.elsevier.com/locate/apthermeng.

Ng, K.C., Thu, K., Chakraborty, A., Saha, B.B. & Chun, W.G. 2009. Solar-assisted dual-effect adsorption cycle for the production of cooling effect and potable water. *International*

*Journal of Low-Carbon Technologies*, 4(2): 61–67.

Ng, K.C., Thu, K., Kim, Y., Chakraborty, A. & Amy, G. 2013. Adsorption desalination: An emerging low-cost thermal desalination method. *Desalination*, 308: 161–179. http://dx.doi.org/10.1016/j.desal.2012.07.030.

Nuhnen, A. & Janiak, C. 2020. A practical guide to calculate the isosteric heat/enthalpy of adsorption: Via adsorption isotherms in metal-organic frameworks, MOFs. *Dalton Transactions*, 49(30): 10295–10307.

Olkis, C., Brandani, S. & Santori, G. 2019a. A small-scale adsorption desalinator. *Energy Procedia*, 158: 1425–1430. https://doi.org/10.1016/j.egypro.2019.01.345.

Olkis, C., Brandani, S. & Santori, G. 2019b. Cycle and performance analysis of a small-scale adsorption heat transformer for desalination and cooling applications. *Chemical Engineering Journal*, 378(April): 122104. https://doi.org/10.1016/j.cej.2019.122104.

Osman, S.M., Hasan, E.H., El-Hakeem, H.M., Rashad, R.M. & Kouta, F. 2013. Conceptual design of multi-capacity load cell. , 03002: 03002.

Qasem, N.A.A. & Zubair, S.M. 2019. Performance evaluation of a novel hybrid humidification-dehumidification (air-heated) system with an adsorption desalination system. *Desalination*, 461(March): 37–54. https://doi.org/10.1016/j.desal.2019.03.011.

Rahimi, B. & Chua, H.T. 2017. *Low Grade Heat Driven Multi-Effect Distillation and Desalination*. 1st ed. Elsivier Inc.

Raj, R. & Baiju, V. 2019. Thermodynamic analysis of a solar powered adsorption cooling and desalination system. *Energy Procedia*, 158: 885–891. https://doi.org/10.1016/j.egypro.2019.01.226.

Raluy, G., Serra, L. & Uche, J. 2006. Life cycle assessment of MSF, MED and RO desalination technologies. *Energy*, 31(13): 2361–2372.

Rautenbach, R., Linn, T. & Eilers, L. 2000. Treatment of severely contaminated waste water by a combination of RO, high-pressure RO and NF - Potential and limits of the process. *Journal of Membrane Science*, 174(2): 231–241.

Rezk, A. 2012. Theoretical and experimental investigation of silica gel/water adsorption refrigeration systems. *Doctor of Philosophy*, 1: 2017.

Riffel, D.B., Wittstadt, U., Schmidt, F.P., Núñez, T., Belo, F.A., Leite, A.P.F. & Ziegler, F. 2010. Transient modeling of an adsorber using finned-tube heat exchanger. *International Journal of Heat and Mass Transfer*, 53(7–8): 1473–1482. http://dx.doi.org/10.1016/j.ijheatmasstransfer.2009.12.001.

Rouquerol, F., Rouquerol, J., Sing, K.S.W., Llewellyn, P. & Maurin, G. 2014. *Adsorption by Powders and Porous Solids Principles, Methodology and Applications*. 2nd ed.

Sah, R.P., Choudhury, B. & Das, R.K. 2015. A review on adsorption cooling systems with silica gel and carbon as adsorbents. *Renewable and Sustainable Energy Reviews*, 45: 123–134. http://dx.doi.org/10.1016/j.rser.2015.01.039.

Santamaria, S., Sapienza, A., Frazzica, A., Freni, A., Girnik, I.S. & Aristov, Y.I. 2014. Water adsorption dynamics on representative pieces of real adsorbers for adsorptive chillers. *Applied Energy*, 134: 11–19.

Sapienza, A., Santamaria, S., Frazzica, A., Freni, A. & Aristov, Y.I. 2014. Dynamic study of adsorbers by a new gravimetric version of the Large Temperature Jump method. *Applied Energy*, 113: 1244–1251. http://dx.doi.org/10.1016/j.apenergy.2013.09.005.

Seol, S.H., Nagano, K. & Togawa, J. 2020. Modeling of adsorption heat pump system based on experimental estimation of heat and mass transfer coefficients. *Applied Thermal Engineering*, 171(February): 115089. https://doi.org/10.1016/j.applthermaleng.2020.115089.

Shen, C.H., Kee, T.S., Lee, B.C.T. & Albert, F.Y.C. 2017. Development and Implementation of Load Cell in Weight Measurement Application for Shear Force. *International Journal of Electronics and Electrical Engineering*, 5(3): 240–244.

Shen, D., Bülow, M., Siperstein, F., Engelhard, M. & Myers, A.L. 2000. Comparison of experimental techniques for measuring isosteric heat of adsorption. *Adsorption*, 6(4): 275–286.

Thu, K., Kim, Y.D., Shahzad, M.W., Saththasivam, J. & Ng, K.C. 2015. Performance investigation of an advanced multi-effect adsorption desalination (MEAD) cycle. *Applied Energy*, 159: 469–477. http://dx.doi.org/10.1016/j.apenergy.2015.09.035.

Thu, K., Yanagi, H., Saha, B.B. & Ng, K.C. 2013. Performance analysis of a low-temperature waste heat-driven adsorption desalination prototype. *International Journal of Heat and*

*Mass Transfer*, 65: 662–669. http://dx.doi.org/10.1016/j.ijheatmasstransfer.2013.06.053.

Tien, C. 2019. *Introduction to Adsorption, Basics, Analysis, and Applications*. Elsevier.

Tun, H. & Chen, C.C. 2021. Isosteric heat of adsorption from thermodynamic Langmuir isotherm. *Adsorption*, 27(6): 979–989. https://doi.org/10.1007/s10450-020-00296-3.

Volmer, R., Eckert, J., Füldner, G. & Schnabel, L. 2017. Evaporator development for adsorption heat transformation devices – Influencing factors on non-stationary evaporation with tube-fin heat exchangers at sub-atmospheric pressure. *Renewable Energy*, 110: 141–153. http://dx.doi.org/10.1016/j.renene.2016.08.030.

Vordos, N., Gkika, D.A. & Bandekas, D. V. 2020. Wheatstone Bridge and Bioengineering. *Journal of Engineering Science and Technology Review*, 13(5): 4–6.

Wang, D., Zhang, J., Yang, Q., Li, N. & Sumathy, K. 2014. Study of adsorption characteristics in silica gel-water adsorption refrigeration. *Applied Energy*, 113: 734–741.

Wang, R., Wang, L. & Wu, J. 2014. ADSORPTION REFRIGERATION TECHNOLOGY THEORY AND APPLICATION. *John Wiley & sons*: 526.

Wenten, I.G. & Khoiruddin. 2016. Reverse osmosis applications: Prospect and challenges. *Desalination*, 391: 112–125. http://dx.doi.org/10.1016/j.desal.2015.12.011.

Wibowo, E., Sutisna, Rokhmat, M., Murniati, R., Khairurrijal & Abdullah, M. 2017. Utilization of Natural Zeolite as Sorbent Material for Seawater Desalination. In *Procedia Engineering*. Elsevier Ltd: 8–13.

Worch, E. 2012. *Adsorption Technology in Water Treatment*.

Wu, J.W., Biggs, M.J. & Hu, E.J. 2014. Dynamic model for the optimisation of adsorption-based desalination processes. *Applied Thermal Engineering*, 66(1–2): 464–473. http://dx.doi.org/10.1016/j.applthermaleng.2014.02.045.

Wyma, B.D. 2020a. *Measuring Pilot Control Force in General Aviation Subtitle: Strain gauges and Load Cell*.

Wyma, B.D. 2020b. *Measuring Pilot Control Force in General Aviation Subtitle: Strain gauges and Load Cell*. Florida Institute of Technology.

Yan, S., Cao, Z., Guo, Z., Zheng, Z., Cao, A., Qi, Y., Leng, Q. & Zhao, W. 2018. Design and fabrication of full wheatstone- bridge-based angular GMR sensors. *Sensors (Switzerland)*,

18(6): 1–8.

Yang, R.T. 2003. *Adsrbents: Fundamentals and Applications*. 1st ed. http://elib.tu-darmstadt.de/tocs/95069577.pdf.

Youssef, P.G., Dakkama, H., Mahmoud, S.M. & AL-Dadah, R.K. 2017. Experimental investigation of adsorption water desalination/cooling system using CPO-27Ni MOF. *Desalination*, 404: 192–199.

Youssef, P.G., Mahmoud, S.M. & AL-Dadah, R.K. 2015. Performance analysis of four bed adsorption water desalination/refrigeration system, comparison of AQSOA-Z02 to silica-gel. *Desalination*, 375: 100–107.

# Appendix

## Appendix A

Experimental results of 5 different temperature isothermS Experimental data of vapour results adsorbed by silica gel in a gravimetric method

| Temperatute @ 10°C | | Temperatute @ 20°C | | Temperatute @ 30°C | | Temperatute @ 40°C | | Temperatute @ 50°C | | Temperatute @ 60°C | |
|---|---|---|---|---|---|---|---|---|---|---|---|
| Pressure (kPa) | Up-take (kg/kg) | Pressure (kPa) | Up-take (kg/kg) | Pressure (kPa) | Up-take (kg/kg) | Pressure (kPa) | Up-take (kg/kg) | Pressure (kPa) | Up-take (kg/kg) | Pressure (kPa) | Up-take (kg/kg) |
| 0,624 | 0,008 | 0,876 | 0,005 | 0,921 | 0,004 | 0,924 | 0,0035 | 0,969 | 0,003 | 0,9798 | 0,002 |
| 1,329 | 0,011 | 1,719 | 0,009 | 1,815 | 0,007 | 1,815 | 0,004 | 1,311 | 0,005 | 1,5965 | 0,004 |
| 2,8956 | 0,017 | 3,099 | 0,016 | 3,177 | 0,0125 | 3,21 | 0,011 | 2,655 | 0,01 | 3,2557 | 0,008 |
| 5,415 | 0,028 | 6,027 | 0,027 | 6,198 | 0,023 | 6,15 | 0,019 | 6,573 | 0,0175 | 6,433 | 0,015 |
| 8,61 | 0,0395 | 9,156 | 0,0365 | 8,82 | 0,0295 | 9,375 | 0,027 | 9,627 | 0,024 | 9,6104 | 0,021 |
| 12,036 | 0,05 | 12,303 | 0,045 | 12,537 | 0,0395 | 12,546 | 0,034 | 12,615 | 0,0295 | 12,7252 | 0,0265 |
| 14,232 | 0,056 | 15,543 | 0,053 | 15,669 | 0,0465 | 15,495 | 0,04 | 15,855 | 0,035 | 15,8841 | 0,0334 |
| 15,75 | 0,0595 | 19,551 | 0,0615 | 19,377 | 0,054 | 19,392 | 0,047 | 19,644 | 0,041 | 19,9252 | 0,0413 |
| 23,091 | 0,077 | 24,057 | 0,07 | 23,886 | 0,062 | 24,105 | 0,0545 | 24,09 | 0,0475 | 24,4957 | 0,049 |
| 28,737 | 0,0855 | 29,82 | 0,079 | 28,752 | 0,0695 | 28,863 | 0,0615 | 28,893 | 0,054 | 29,0973 | 0,057 |
| 33,543 | 0,093 | 34,467 | 0,0865 | 34,404 | 0,077 | 34,467 | 0,069 | 34,545 | 0,061 | 32,513 | 0,061 |
| 39,444 | 0,101 | 40,791 | 0,095 | 40,695 | 0,085 | 40,821 | 0,0765 | 41,01 | 0,0685 | 40,8052 | 0,072 |
| 45,861 | 0,109 | 46,989 | 0,1025 | 47,049 | 0,092 | 47,004 | 0,083 | 47,208 | 0,075 | 47,207 | 0,0775 |
| 52,467 | 0,1165 | 53,217 | 0,109 | 53,373 | 0,098 | 53,514 | 0,089 | 53,31 | 0,0805 | 53,4052 | 0,0825 |
| 58,884 | 0,123 | 59,586 | 0,115 | 59,556 | 0,104 | 60,324 | 0,095 | 60,135 | 0,0865 | 58,447 | 0,0865 |
| 65,472 | 0,129 | 65,973 | 0,1205 | 65,832 | 0,1095 | 66,288 | 0,1 | 68,04 | 0,092 | 65,6296 | 0,089 |
| 72,219 | 0,1345 | 72,204 | 0,1255 | 72,123 | 0,1145 | 72,531 | 0,105 | 72,375 | 0,096 | 72,2191 | 0,0896 |
| 72,408 | 0,1351 | 72,222 | 0,1261 | 72,312 | 0,1151 | 81,42 | 0,109 | 72,396 | 0,0966 | 72,2379 | 0,0902 |

Table A 1: Experimental data of vapour results adsorbed by silica gel in a gravimetric method

The table A2 shows the results on finding the isosteric heat of adsorption at the first three temperature

| Temperatute @ 10°C | | | | Temperatute @ 20°C | | | | Temperatute @ 30°C | | | |
|---|---|---|---|---|---|---|---|---|---|---|---|
| 0,28601 | 0,02914 | 0,79873 | | 0,25958 | 0,02486 | 0,8483 | | 0,22868 | 0,02115 | 0,90061 | |
| Pressure (kPa) | Up-take (kg/kg) | Calc Pressure | lnP | Pressure (kPa) | Up-take (kg/kg) | Calc Pressure | lnP | Pressure (kPa) | Up-take (kg/kg) | Calc Pressure | lnP |
| 0,624 | 0,00561 | 0,624517421 | -0,470776054 | 0,876 | 0,00564 | 0,875573605 | -0,132876058 | 0,921 | 0,0044 | 0,919917213 | -0,083471599 |
| 1,34909 | 0,01021 | 1,349379176 | 0,299644617 | 1,59667 | 0,00925 | 1,595544808 | 0,46721525 | 1,64212 | 0,00732 | 1,642564103 | 0,496258498 |
| 2,07418 | 0,01418 | 2,073071342 | 0,729031248 | 2,31733 | 0,01253 | 2,31761852 | 0,840540159 | 2,36324 | 0,01003 | 2,362371271 | 0,85966589 |
| 2,79927 | 0,01778 | 2,79819511 | 1,028974606 | 3,038 | 0,01557 | 3,03800543 | 1,111201191 | 3,08436 | 0,0126 | 3,083560924 | 1,126085073 |
| 3,52436 | 0,02111 | 3,523824694 | 1,259546961 | 3,75867 | 0,01843 | 3,758011341 | 1,323889919 | 3,80548 | 0,01505 | 3,803936624 | 1,336036484 |
| 4,24945 | 0,02422 | 4,247776221 | 1,446395604 | 4,47933 | 0,02115 | 4,479625592 | 1,49953947 | 4,52661 | 0,01741 | 4,527243963 | 1,510113358 |
| 4,97455 | 0,02716 | 4,972741767 | 1,603971351 | 5,2 | 0,02374 | 5,199668144 | 1,648594805 | 5,24773 | 0,01967 | 5,246568316 | 1,657574209 |
| 5,69964 | 0,02996 | 5,699795556 | 1,740430307 | 5,92067 | 0,02622 | 5,919110539 | 1,778186191 | 5,96885 | 0,02186 | 5,968428218 | 1,786483613 |
| 6,42473 | 0,03262 | 6,423748607 | 1,860001842 | 6,64133 | 0,02861 | 6,640287972 | 1,893155332 | 6,68997 | 0,02398 | 6,69058069 | 1,90070067 |
| 7,14982 | 0,03517 | 7,148478249 | 1,966899502 | 7,362 | 0,03091 | 7,360324426 | 1,996104011 | 7,41109 | 0,02603 | 7,410951334 | 2,002958816 |
| 7,87491 | 0,03762 | 7,873477393 | 2,063499819 | 8,08267 | 0,03313 | 8,079801062 | 2,089367251 | 8,13221 | 0,02802 | 8,131253593 | 2,095715105 |
| 8,6 | 0,03998 | 8,598840494 | 2,151627368 | 8,80333 | 0,03528 | 8,799845404 | 2,174734154 | 8,85333 | 0,02996 | 8,853695263 | 2,180834916 |
| 9,32509 | 0,04226 | 9,325207064 | 2,232721171 | 9,524 | 0,03737 | 9,522084297 | 2,253613764 | 9,57445 | 0,03184 | 9,57318696 | 2,258966166 |
| 10,05018 | 0,04446 | 10,05037 | 2,30760945 | 10,24467 | 0,03939 | 10,24138461 | 2,326436826 | 10,29558 | 0,03368 | 10,29620247 | 2,331775135 |
| 10,77527 | 0,04658 | 10,77216495 | 2,376965488 | 10,96533 | 0,04136 | 10,96337889 | 2,394560527 | 11,0167 | 0,03547 | 11,01780401 | 2,39951251 |
| 11,50036 | 0,04865 | 11,49915723 | 2,442273748 | 11,686 | 0,04327 | 11,68308866 | 2,458142383 | 11,73782 | 0,03721 | 11,73684207 | 2,462732789 |
| 12,22545 | 0,05065 | 12,22284895 | 2,503307065 | 12,40667 | 0,04513 | 12,40298054 | 2,51793681 | 12,45894 | 0,03892 | 12,46074177 | 2,522583044 |
| 12,95055 | 0,0526 | 12,94901095 | 2,561019411 | 13,12733 | 0,04695 | 13,12593652 | 2,57459016 | 13,18006 | 0,04058 | 13,18019739 | 2,578715506 |
| 13,67564 | 0,05449 | 13,67261541 | 2,615394957 | 13,848 | 0,04872 | 13,84699697 | 2,628068384 | 13,90118 | 0,04221 | 13,90303707 | 2,632107311 |
| 14,40073 | 0,05634 | 14,40017234 | 2,667240175 | 14,56867 | 0,05044 | 14,56502222 | 2,678622916 | 14,6223 | 0,0438 | 14,62413293 | 2,682673105 |
| 15,12582 | 0,05813 | 15,12266619 | 2,716194691 | 15,28933 | 0,05213 | 15,28752216 | 2,72703695 | 15,34342 | 0,04535 | 15,34263595 | 2,730635616 |
| 15,85091 | 0,05988 | 15,84701589 | 2,762981211 | 16,01 | 0,05377 | 16,00510198 | 2,772907545 | 16,06455 | 0,04687 | 16,0624771 | 2,776485937 |
| 16,576 | 0,06159 | 16,57237097 | 2,807736909 | 16,73067 | 0,05538 | 16,72566301 | 2,816944247 | 16,78567 | 0,04836 | 16,7830951 | 2,820372135 |
| 17,30109 | 0,06326 | 17,29787374 | 2,850583589 | 17,45133 | 0,05696 | 17,44864923 | 2,859262238 | 17,50679 | 0,04982 | 17,50392111 | 2,862424919 |
| 18,02618 | 0,06489 | 18,02265892 | 2,891629795 | 18,172 | 0,0585 | 18,16877101 | 2,899704242 | 18,22791 | 0,05126 | 18,22946744 | 2,903039375 |
| 18,75127 | 0,06649 | 18,75045326 | 2,931217926 | 18,89267 | 0,06001 | 18,88998335 | 2,9386318 | 18,94903 | 0,05266 | 18,94907134 | 2,941754925 |
| 19,47636 | 0,06804 | 19,47127791 | 2,968940452 | 19,61333 | 0,06148 | 19,60678081 | 2,975875466 | 19,67015 | 0,05403 | 19,66712669 | 2,978948546 |
| 20,20145 | 0,06957 | 20,19834808 | 3,005600823 | 20,334 | 0,06293 | 20,32832905 | 3,012015433 | 20,39127 | 0,05538 | 20,3884241 | 3,014967294 |
| 20,92655 | 0,07106 | 20,92156659 | 3,040780521 | 21,05467 | 0,06435 | 21,04920673 | 3,046862874 | 21,11239 | 0,05671 | 21,11265755 | 3,049872745 |
| 21,65164 | 0,07253 | 21,65004037 | 3,075007319 | 21,77533 | 0,06574 | 21,76881046 | 3,080478232 | 21,83352 | 0,05801 | 21,83391395 | 3,083464447 |
| 22,37673 | 0,07396 | 22,37324831 | 3,107865973 | 22,496 | 0,06711 | 22,49185667 | 3,113153318 | 22,55464 | 0,05928 | 22,55156283 | 3,115804368 |
| 23,10182 | 0,07537 | 23,10068758 | 3,139862383 | 23,21667 | 0,06845 | 23,21259869 | 3,144695178 | 23,27576 | 0,06054 | 23,27657571 | 3,14744752 |
| 23,82691 | 0,07674 | 23,82141348 | 3,170584902 | 23,93733 | 0,06976 | 23,93040839 | 3,175149968 | 23,99688 | 0,06177 | 23,99710555 | 3,177933221 |
| 24,552 | 0,0781 | 24,55072729 | 3,200741479 | 24,658 | 0,07105 | 24,65028063 | 3,204788285 | 24,718 | 0,06298 | 24,71850829 | 3,207552286 |
| 25,27709 | 0,07942 | 25,27205112 | 3,229699086 | 25,37867 | 0,07232 | 25,37187465 | 3,233641263 | 25,43912 | 0,06417 | 25,44042951 | 3,236339622 |
| 26,00218 | 0,08073 | 26,00128201 | 3,258145845 | 26,09933 | 0,07357 | 26,09484278 | 3,2617377 | 26,16024 | 0,06534 | 26,16250707 | 3,264327358 |
| 26,72727 | 0,082 | 26,72121464 | 3,285457806 | 26,82 | 0,07479 | 26,81289328 | 3,288882864 | 26,88136 | 0,06648 | 26,8780414 | 3,291309648 |

Table A 2: The results found in finding the slope to determine the heat of adsorption in between the adsorbents

## Appendix B

This section provides the values of affinity and maximal loading when simulated in Origin software

*Parameters*

| | | Value | Standard Error |
|---|---|---|---|
| Up-take | a | 0,28601 | 0,01574 |
| | b | 0,02914 | 8,69931E-4 |
| | c | 0,79873 | 0,01957 |
| | a | 0,22868 | 0,00783 |
| | b | 0,02115 | 3,88259E-4 |
| | c | 0,90061 | 0,01504 |
| | a | 0,28674 | 0,02198 |
| | b | 0,01355 | 6,07505E-4 |
| | c | 0,84462 | 0,01762 |

Reduced Chi-sqr = 2,65284622421E-7
COD(R^2) = 0,99977503870631
Iterations Performed = 16
Total Iterations in Session = 16
All datasets were fitted successfully.

*Statistics*

| | Up-take | | |
|---|---|---|---|
| Number of Points | 18 | 18 | 18 |
| Degrees of Freedom | 15 | 15 | 15 |
| Reduced Chi-Sqr | 8,18473E-7 | 2,96192E-7 | 2,65285E-7 |
| Residual Sum of Squares | 1,22771E-5 | 4,44288E-6 | 3,97927E-6 |
| Adj. R-Square | 0,99958 | 0,9998 | 0,99975 |
| Fit Status | Succeeded(100) | Succeeded(100) | Succeeded(100) |

Fit Status Code :
100 : Fit converged - tolerance criterion satisfied.

Table B 1: Uptake values of affinity constant and maximal loadings